Molecular characterization of the C-type lectin like domain family 16A (CLEC16A)

Subcellular localization and its role in endosomal distribution

Anna Maria Eriksson

Master thesis at the Department of Bioscience
Faculty of Mathematics and Natural Sciences

UNIVERSITY OF OSLO

December 2014

Subcellular localization and its role in endosomal distribution

Anna Maria Eriksson
Department of Bioscience
University of Oslo

December 2014

Molecular characterization of the C-type lectin like domain family 16A (CLEC16A)

Anna Maria Eriksson

http://www.duo.uio.no

Print: Reprosentralen, Universitetet i Oslo

Abstract

Multiple sclerosis (MS) is a common autoimmune, neurological disease. The cause of MS is unknown, however, the leading hypothesis is that it is developed in genetic predisposed individuals triggered by environmental factors. The genetics is complex, where it is thought that several susceptibility genes each exert a small effect. One of the genes that have been identified to be associated with MS is the *CLEC16A* gene, which contains several MS-associated single nucleotide polymorphisms. Gaining an understanding of the functions of the MS susceptibility genes can contribute to insights in the underlying mechanisms leading to MS development.

Earlier studies about the protein, C-type lectin like domain family 16A encoded by the *CLEC16A* gene, has shown that it plays a role in autophagy and endosomal maturation. Its role in immune cells is not determined. The subcellular localization of the protein seems to be different in different cell types and has not been studied in T cells before.

The aim of my project was to investigate the subcellular localization of CLEC16A in T cells and its role for endosomal distribution in T cells using confocal microscopy. Jurkat T cells were transfected with CLEC16A fused with a tag. To ensure that the tag did not influence the localization, both C-terminal and N-terminal tagged CLEC16A constructs were created. Confocal microscopy analyses showed that CLEC16A was partially co-localized with Rab4a, which is localized in rapid recycling-endosomes. To examine the role of CLEC16A in endosomal distribution, we analysed endosomal markers by confocal microscopy in Jurkat T cells transfected with CLEC16A small interfering RNA (siRNA) or a CLEC16A expression plasmid and compared with corresponding controls. The endosomes investigated were; Rab5-positive (early endosome), Rab4a-positive (rapid recycling endosome) and LAMP1-positive (lysosomal protein).

Our data indicate that CLEC16A knockdown causes an accumulation of Rab5-positive endosomes, a similar phenotype has been observed in Rab4-mutant cells. These findings indicate a possible function for CLEC16A in rapid recycling-dependent processes in T cells.

Acknowledgements

First and foremost I would like to thank my supervisor Tone Berge for excellent supervision with daily guidance and encouragement. Thank you for always being available, for both big and small questions, listening on my ideas and for trusting me to work as independently as I have.

Secondly I would like to thank Ingvild Sørum Leikfoss, both for all help in the lab and for all discussion and input during the work. I also want to thank Anja Bjølgerud for always taking time to answer my questions, helping me in the lab and in the writing process. I would also like to thank Ole Landsverk for all help with the confocal microscopy and input about the work.

Further I want to thank Professor Hanne Harbo for being such inspiring group leader, and for giving me the opportunity to be a part of the MS-research group. I also want to thank the rest of the group for sharing all positivity and knowledge in the MS-research field.

Next, I want to thank Ina for all motivation she has given me during the master degree. I greatly appreciate all sharing of frustrations and joys over a coffee during this time. Without you in the same group, it had not been the same experience! Further I also want to thank my fellow students, especially Margrete and Marie for always giving me inspiration and motivation.

I would also thank my family for always believing in me and always trying to understand what I have been doing. Finally I want to devote a special thank to Kjell for being there every day with support and love.

December 2014

Anna Eriksson

Table of content

1 Introduction

This thesis explores the role of a protein, encoded by a multiple sclerosis (MS)-associated gene, in T cells6. The introduction first gives a short description of the immune system and potential important processes for the protein studied, before a section describing MS and MS genetics. Finally, the introduction is more specific to the protein studied. In the whole thesis, T cells are in focus.

1.1 The Immune system

The immune system is the body‘s defence against foreign invaders and protects against diseases. A complex system of cells and molecules interact to extinguish the invaders. The innate immune system is the first line of defence after a pathogen has got past the physical barriers. It can discriminate between host cells and pathogens by recognition of patterns on the surface of the pathogen, and initiate an unspecific immune response as well as activating the adaptive immune response. The adaptive immune system is highly specific and acts as a second line of defence if the pathogens are able to get past the innate immune system. The adaptive immune system is characterized by specific recognition, mediated through cell-surface receptors on specific immune cells, B and T cells.

1.1.1 T cell activation

The major players in the adaptive immune system are T and B cells. T cells are divided in two types; helper T cells (CD4+), which is stimulating and activating other cells in both the innate and the adaptive immune system, and cytotoxic T cells (CD8+), which kills infected cells. CD4+ T cells are further divided in groups depending on their function and their cytokine production.

T cells are activated through interactions with the T cell receptor (TCR), if it is recognizing its specific antigen. The TCR forms a complex on the cell surface, composed of the TCR, CD3 and the ζ chain. For the activation to take place, the naïve T cell requires two signals (figure 1.1) (1). Binding between a professional antigen-presenting cell´s (APC) major histocompatibility complex (MHC)-peptide complex and a naïve T cell´s TCR with a co-receptor (CD4 or CD8) generates the first signal. The second signal is generated from the

binding of co-stimulatory receptor B7, which is induced by pathogens and only expressed on professional APCs, to its ligand CD28 on the Naïve T cell (2).

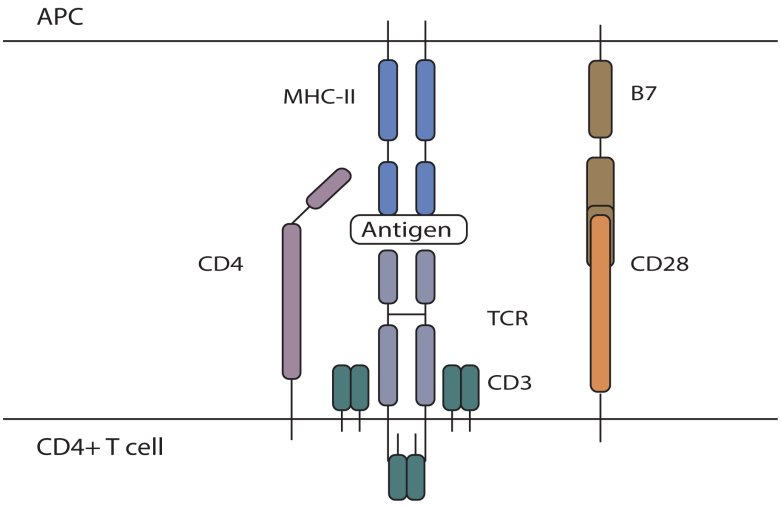

Figure 1.1. The T cell receptor (TCR) complex during T cell activation (here illustrated for a CD4+ T cell). The TCR interacts with a major histocompatibility complex (MHC) molecule with a specific antigen bound. The complex is expressed on the cell surface at antigen-presenting cells (APC). In addition the co-receptor (CD4 or CD8) interacts with the MHC molecule (class II for CD4 and class I for CD8). This interaction give one signal to the cell, but to become activated the T cell needs and additionally signal from interactions between CD28 on the T cell and B7 on the APC.

Upon T cell activation, CD3 and ζ chain are responsible for signalling further into the interior of the cell. CD3 has a tail on the cytosolic side of the membrane, containing immunoreceptor tyrosine-based activation motifs (ITAMs). ITAMs associate with tyrosine kinases that become activated upon receptor clustering, and phosphorylate the ITAM motifs. The phosphorylated tyrosines serve as docking- and activation sites for enzymes and other signalling-molecules, which can start an intracellular signalling cascade, resulting in alterations in gene expression (3).

Endsomal pathway

There are many cellular processes that use the endosomal pathway, including immunological processes, for instance antigen presentation by APCs, T cell activation and signalling (4). For cellular functions, endosomal pathways are of special importance during endocytosis, when extracellular material is internalized through invaginations of the plasma membrane. The transport into the interior of the cell proceeds through membrane enclosed vesicles called endosomes. GTPases and its effectors are some of the proteins that define the membranes of the endosomes e.g. the GTPase Rab5, which is localized at early endosomes, Rab4 at rapid recycling endosomes, Rab7 at late endosomes and Rab11 at slow recycling endosomes

(figure 1.2). Endocytosed material, like a receptor and its cargo, is first transported to early endosomes, where the cargo is sorted. From early endosomes, the cargo and receptor can be sent to degradation in lysosomes or the receptor can be rapidly recycled back to the plasma membrane in Rab4-positive endosomes. The receptors can also be sorted to Rab11-positive endosomes and be recycled back to the membrane through slow recycling (figure 1.2) (5-7). These mechanisms can regulate a signalling process by sending receptors to lysosomes for degradation to decrease a signal, or by recycle the receptors to the plasma membrane to prolong a signal (6, 8).

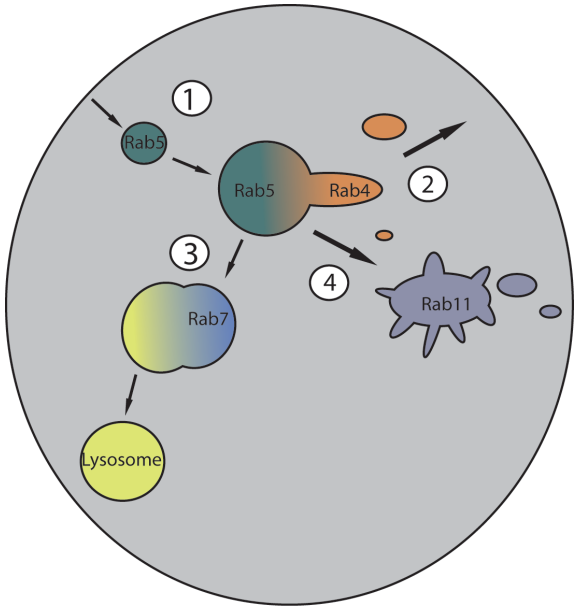

Figure 1.2. A simplified overview of Rab4-, Rab5-, Rab7- and Rab-11 endosomes and their transport routes for cargo from the plasma membrane. Rab5 (green) is located in early endosomes, Rab4 (orange) in rapid recycling endosomes, Rab7 (blue) in late endosomes and Rab11 (violet) in slow recycling endosomes. **(1)** Internalized material from endocytosis are transported from the plasma membrane and routed into early endosomes (Rab5), where they e.g. can be **(2)** recycled back to the plasma membrane by Rab4-recyclings endosomes, **(3)** be sent to late endosomes, which will fuse with lysosome and degrade the content or **(4)** they can be sent to Rab11-recycling endosomes which recycle the cargo back to the plasma membrane in a slow route.

Endocytic vesicles leaving early endosomes after sorting, mature into late endosomes by acidifying the environment (lowering the pH) (9). Late endosomes mature into lysosomes by further acidification or by fusing with existing lysosomes (10).

Recycling endosomes

For Rab4 GTPases there are two known isoforms (called Rab4a and Rab4b), both are localized in the same compartment and seem to have the same function; recycling receptors back from early endosome to the plasma membrane through rapid recycling (11). They have been indicated to be involved in MHC class II antigen presenting on B cells, since the presentation is blocked in Rab4-mutant cells (12). In addition they have been indicated to recycle tyrosine kinases, integrins (13), TCRs (during T cell activation) among others (14). Rab11 is responsible for the slow recycling pathway between recycling endosomes and plasma membrane. Cellular functions where Rab11 have been implicated are autophagy and cytokinesis among others (13).

Endosomal role in T cell activation

Interactions between MHC and TCR during T cell activation form an immunological synapse when clustering together with co-receptors and co-stimulatory signals (figure 1.3) (15). When T cell activation is initiated, the Golgi apparatus and recycling-endosomes are polarized close to the immunological synapse (16). TCRs are recycled to the immunological synapse on the plasma membrane, using both rapid recycling (Rab4-positive) and slow recycling (Rab11-positive) (14, 17, 18). The TCR recycling during T cell activation has been demonstrated to enhance the amount of TCR molecules delivered to the immunological synapse (16). In addition, the endosomal pathway has been shown to be important in signalling, since signalling complexes are built by delivery from endosomal compartment rather than movement in the plasma membrane (19). The endosomal pathway is recycling TCRs even in resting T cells (before activation), the constitutively recycled TCRs are a process that regulates the T cells ability to be activated (20).

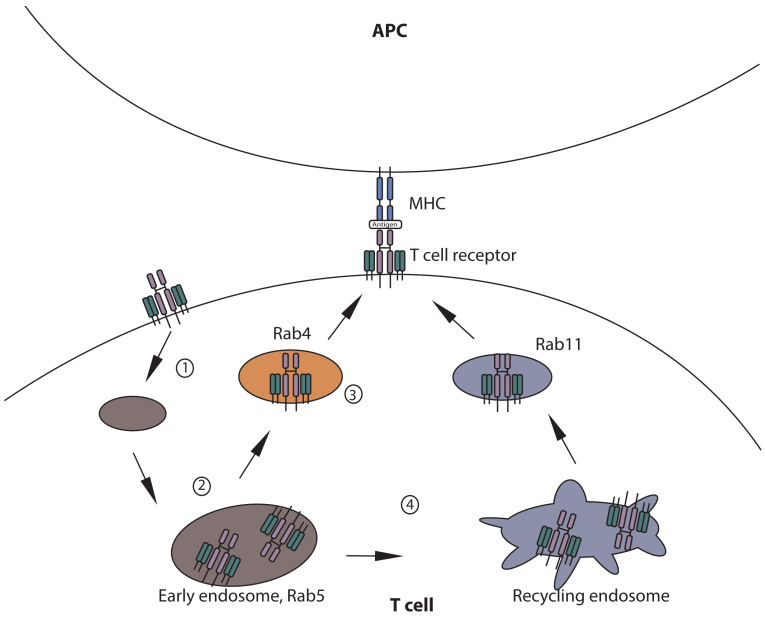

Figure 1.3. A simplified overview of the endosomal pathways involved during T cells activation. When a T cell is activated, the contact between the T cell receptor (TCR) and major histocompatibility complex (MHC) is creating an immunological synapse. The cells polarize recycling endosomes and Golgi (not seen) in the direction of the immunological synapse to rapidly transport more TCRs and other components to this area. **(1)** TCRs expressed on the cell surface are **(2)** sorted into Rab5-positive early endosomes. From there, TCR can be **(3)** rapidly recycled to the cell surface where the immunological synapse is being formed, by Rab4 positive endosomes. Or it can be transported to the polarized **(4)** recycling endosomes and be slowly recycled to the immunological synapse by Rab11-endosomes.

Endosomal pathways in MHC class II antigen presentation

MHC molecules are presenting antigens to the T cells. MHC class I molecules present antigens for CD8+ T cells and MHC class II molecules present antigens for CD4+ T cells. The MHC molecules differ in the antigen source and antigen processing. In addition they differ in cell type presenting them. MHC class I is expressed on nearly all cells, meanwhile MHC class II is only expressed on professional APCs.

The MHC class II is using the endosomal pathways for the antigen processing and loading. The antigens presented by MHC class II originate from extracellular environment by uptake through endocytosis. *MHC class II transactivator* (*CIITA*) is regulating gene expression of MHC class II molecules. When promoting expression, the two transmembrane chains (α and β), building the MHC class II molecule, are assembled in endoplasmic reticulum (ER), where they also associate with the invariant chain (figure 1.4). The invariant chain is protecting the binding cleft of the MHC class II and prevents binding of peptides until reaching the right compartment. The complex is transported to MHC class II compartment (MIIC), a late

endosome. In MIIC the invariant chain is cleaved, but the part binding to the MHC cleft (named Class II-associated invariant chain peptide (CLIP)) is left still binding. The internalized proteins are hydrolysed in the endosomal system and in MIIC the hydrolysed peptides meet the MHC class II molecules. CLIP is exchanged with a peptide with specificity for the binding cleft. The loaded MHC molecule is transported from MIIC to the plasma membrane for the presentation of antigens to CD4+ T cells (reviewed in (21)). Upon arrival at the plasma membrane it is possible for the complex to be rapidly recycled through the early endosome, where antigen exchange can be performed, or they can be sorted for degradation in lysosomes (22) (figure 1.4).

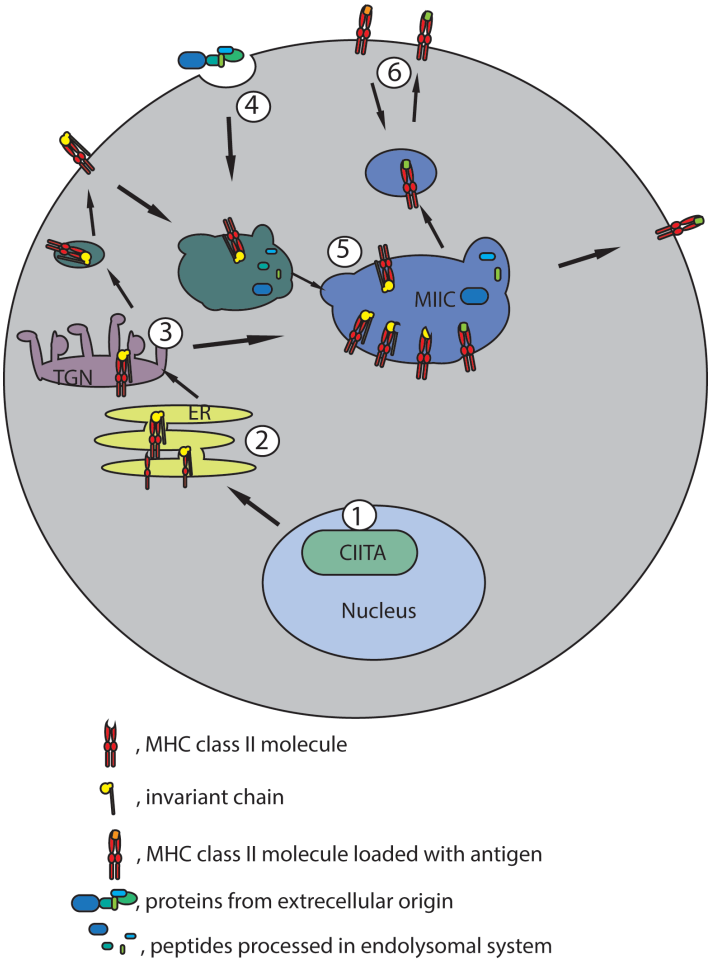

Figure 1.4. Overview of MHC class II presentation. (1) CIITA is promoting expression of MHC class II. (**2)** MHC class II chains are associated in ER, where invariant chain is binding to the binding cleft of the complex. (**3)** The complex is transported to Golgi, and from trans golgi network (TGN) the complex is sorted to MHC class II compartment (MIIC), and in some cases with a detour to the plasma membrane and early endosomes. In MIIC the invariant chain on MHC class II is trimmed to CLIP, only binding in binding cleft. (**4)** Extracellular proteins are endocytosed and hydrolysed in endosomal pathway. (**5)** The hydrolysed peptides are transported to MIIC where they compete on being exchanged with CLIP on MHC class II binding cleft. (**6)** The antigen loaded MHC class II complexes are transported to the plasma membrane from MIIC. From the plasma membrane the MHC class II can be recycled back and forth.

1.1.2 Autophagy

Autophagy is a process where the cytosolic content (proteins or entire organelles) is being degraded. It is a vital process happening constantly to obtain homeostasis in the cells (23). This process is critical for the cells during starvation, growth, activation and proliferation. Autophagy has also been implicated in many diseases such as; neurodegenerative diseases (24, 25) and autoimmune diseases, like Crohn´s disease (26, 27) and diabetes (28).

Autophagy pass through four phases; nucleation, elongation, fusion and degradation. In nucleation, a double membrane (phagophore) is formed and in elongation the membrane is engulfing a part of cytosolic content or an organelle. When the membrane closes around the cargo it forms an autophagosome. The cargo is degraded when the autophagosome is fused with a lysosome (reviewed in (29)).

Autophagy has been implicated to have a role in several immunological processes. For the innate immune system, autophagy can be induced by several pattern recognition receptors, where autophagy is facilitating several processes including phagocytosis and cytokine production (30-33). Autophagy is implicated to have a role for T cell development and T cell selection (34). In addition it is suggested to be required for cell-survival for B cell development (35).

Autophagy in T cell activation and signalling

T cells are known for having a high rate of continuous autophagy and for expressing genes linked to autophagy (34, 36, 37). In human CD4+ and CD8+ T cells, the level of autophagy is kept constantly low until TCR stimulation, where the level of autophagy have been shown to increase (38, 39). In addition, autophagy levels are high in cortical thymic epithelial cells, indicating autophagy to be important for T cell development and T cell selection (23, 40). T cells seem to develop normally in thymic tissue in studies using mouse models where autophagy is being blocked (34, 41-43). However, for mature T cells, autophagy-deficiency has a larger effect, it is giving rise to a reduction in the number of T cells and an increased level of apoptosis. In addition, the T cells do not proliferate efficiently after T cell activation in cells where autophagy is blocked (34, 43). All the effects mentioned originate probably from the cells inability to regulate organelle turnover. The quality control of organelles is lacking. In T cells lacking the autophagy machinery, there are an increased number of

mitochondria, which are giving high amounts of reactive oxygen species, resulting in increased cell death (37, 41). In addition, inability to regulate ER turnover in autophagy would result in failure in calcium influx upon T cell stimulation (37).

1.2 Multiple Sclerosis (MS)

A critical task for the immune system is to discriminate self-derived components from non-self derived components. If the immune response in an organism is turned against its own cells or tissue, autoimmunity develops.

Multiple Sclerosis (MS) is characterized as an autoimmune, neurological disease, where an inflammation in the central nervous system (CNS) results in demyelination of the myelin sheaths. Myelin sheaths insulates nerve fibers and demyelination is causing impaired conducting of the impulses in these nerve fibers (44). The prevalence of MS in Norway is 203 per 100 000 inhabitants, which is among the highest reported worldwide (45). The disease typically appears in young adults and females are affected more than twice as often as males (46).

1.2.1 Immunopathogenesis of MS

The trigger of MS is not known. CD4+ T cells have for a long time been thought to be the major player in MS pathogenesis, a hypothesis that originated from animal models where an MS-like disease (experimental autoimmune encephalomyelitis (EAE)) is induced by myelin-reactive T cells (47-50). The activation of the T cells is thought to occur in lymphoid tissue before crossing the blood brain barrier (51, 52). However, both CD4+ and CD8+ T cells have been found in MS lesions, where CD4+ T cells predominate in acute lesions and CD8+ T cells are more frequently present in chronic lesions (reviewed in(3)).

1.2.2 MS genetics

The cause of MS is unknown. However, both environmental factors, such as smoking, low levels of vitamin D and Epstein Barr virus (53), and genetic factors have shown to be associated with the disease. The hypothesis is that environmental factors together with multiple genes, where each factor exert a relatively small effect, play a role in disease development (review (54)). A better understanding of the cause of MS can be achieved by

characterizing the role of the MS associated genes and the function of the proteins they encode.

The human leukocyte antigen (HLA) gene region was the first gene region that was shown to be associated with MS (55). It is the *HLA-DRB1*15:01* allele that is exerting the biggest known genetic risk for MS (odds ratio =3.1) (56). The first genome-wide association study (GWAS) performed, did confirm the HLA-gene region on chromosome 6, for MS susceptibility. In addition, it identified the first non-HLA genes to be associated with MS susceptibility (57). The newest GWAS identified 57 MS susceptibility loci, where 29 of these loci were novel (56). The majority of the identified genes are involved in immunological processes (58). In 2013, another 48 MS susceptibility genes were identified using the ImmunoChip genotyping array (59).

Already in the first GWAS from 2007, one of the identified single nucleotide polymorphisms (SNP) with a suggestive association with MS was located in the *C-type lectin-like domain family 16A* (*CLEC16A*) gene (57). Studies (GWAS and ImmunoChip genotyping array) performed afterwards have replicated that *CLEC16A* is a susceptibility gene for MS (reviewed in (60)).

16p13 chromosomal region and the *CLEC16A* gene

CLEC16A is located at the chromosome region 16p13 in a gene-complex including the following genes: *MHC class II transactivator* (*CIITA), dexamethasone-induced (DEXI), CLEC16A* and *Suppressor of cytokine signalling 1 (SOCS1)* (figure 1.5 A) (reviewed in (60)). Of these genes both *CIITA* and *SOCS1* are identified to be immune regulatory genes (61, 62). The protein expressed by *CIITA* is a master regulator of MHC class II expression (61). As described above (in section 1.1.2), MHC class II is only expressed in professional APCs. However, studies have shown that some other cells can be induced (by interferon gamma (IFNγ) or other stimuli) to express the MHC class II molecules (63-66). The SOCS1 protein is encoded from another immune-regulatory gene, which suppresses cytokine signalling (62). The function of the protein encoded by the *DEXI* gene is unknown. Since, several SNPs in this region are associated with autoimmunity and *CLEC16A* (and *DEXI*) are located in a gene region where several other immune regulatory genes are located, the functions of these proteins are of interest to identify.

The *CLEC16A* gene contains 238 kb and is composed of 24 exons[1]. In addition to MS, the *CLEC16A* gene has been shown to be associated with several other autoimmune diseases, including, type I diabetes, and Addison´s disease among others (reviewed in (60)), see also figure 1.5 B.

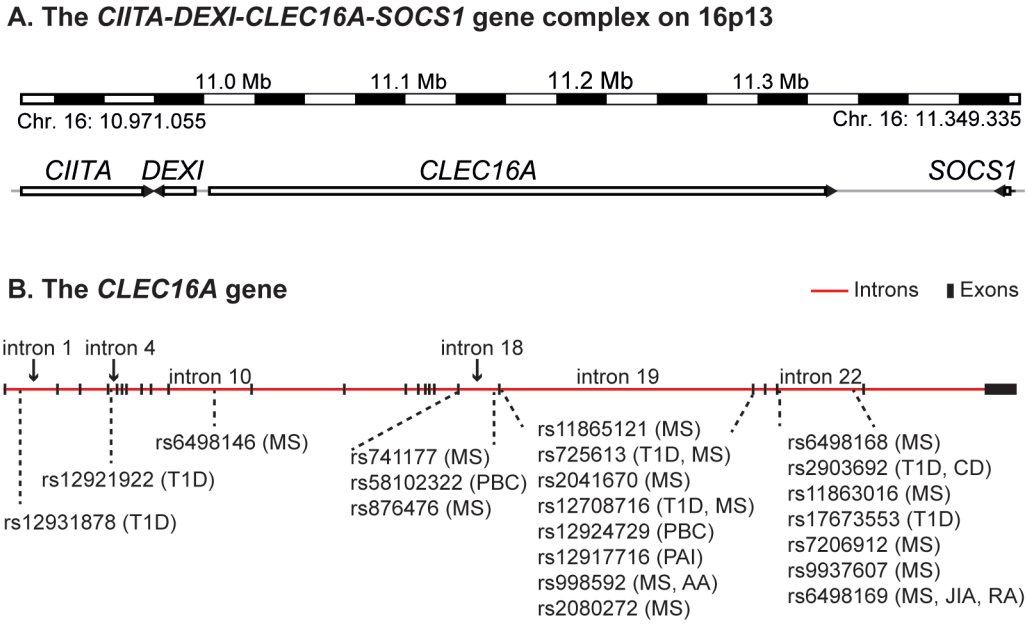

Figure 1.5. Overview of the *CIITA-DEXI-CLEC16A-SOCS1* gene complex and autoimmune associated SNPs on the *CLEC16A* gene. A) The *CIITA-DEXI-CLEC16A-SOCS1* gene complex with chromosomal location 16p13. **B)** The *CLEC16A* gene has several SNPs associated with autoimmune diseases, e.g multiple sclerosis (MS), type I diabetes (TID), crohn´s disease (CD), primary adrenal insuffienciey (Addisons disease, PAI), primary biliary cirrhosis (PBC), rheumatoid arthritis (RA), juvenile idiopathic arthritis (JIA) and alopecia areata (AA). The figure is adapted from (60).

1.3 C-type lectin like domain, family 16A protein-CLEC16A

The full-length *CLEC16A* gene encodes a protein of 1053 amino acids. Three different splice variants of the CLEC16A is known so far, where two are long (24 exons, Q2KHT3-1 and 21 exons, Q2KHT3-2; figure 1.7 A) and one is short (4 exons, Q2KHT3-3; figure 1.7 A).

[1] (http://genome-euro.ucsc.edu/cgi-bin/hgTracks?db=hg19&position=chr16%3A11038345-11276046&hgsid=200280572_IZYpmXFAuV4iILaECojM9K4T4W5w).

1.3.1 CLEC16A expression in immune cells

CLEC16A is expressed in different immune cells. The highest expression levels are found in monocytes (CD14hi, CD16+ cells), however it is also expressed in CD19+ B cells, CD4+ and CD8+ T cells and CD56+ NK cells (Figure 1.6 A). When analysing CD4+ T cells, no difference in CLEC16A expression was observed between MS cases and controls. However, when sorting the samples for genotype, an increase of CLEC16A expression was found in samples homozygous for the risk allele (see fig 1.6 B) (Leikfoss, Keshari, Berge, unpublished data).

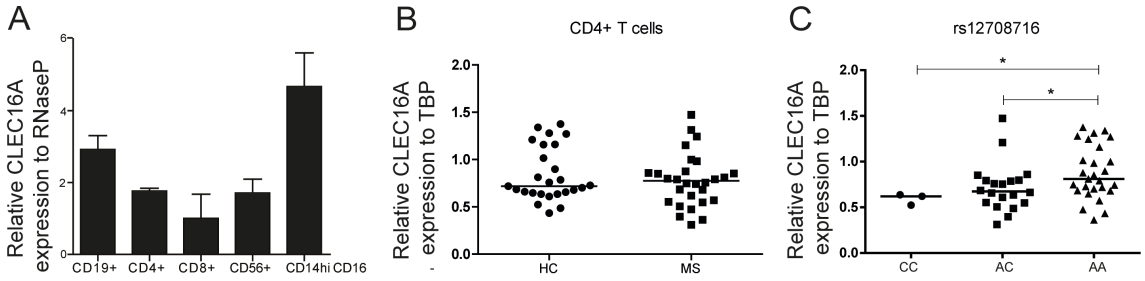

Figure 1.6. MS-risk genotype is correlated with increased CLEC16A expression. Relative expression of CLEC16A is normalized to **A)** *RNaseP* for primary immune cells (N=3) and **B** and **C)** TATA-box binding protein (*TPB*) for CD4+ T cells isolated from 28 MS patients (MS) and 26 healthy controls (HC). In C the samples are sorted for the CLEC16A SNP, rs12708716 (risk allele=A) (Leikfoss, Keshari, Berge, unpublished data).

1.3.2 Structural domains of the CLEC16A protein

As the name CLEC16A suggests, it contains a C-type lectin-like domain (CTLD). CTLD is involved in recognition of carbohydrates on the cell-surface (67). However, the CTLD domain of CLEC16A is only 23 amino acids long (reviewed in(60)), and it is unlikely that it will fold to the proper CTLD domain, which is normally composed of approximately 150 amino acids (67). CLEC16A also contains a potential ITAM motif, an FPL domain, which is a conserved uncharacterized domain, and it is predicted to contain a transmembrane (TM) region (figure 1.7 A). In addition, bioinformatic analyses performed by Torbjørn Rognes at the Bioinformatics Core Facility at the University of Oslo, indicates an un-ordered structure in the C-terminus. The predicted TM and ITAM motifs share some conserved amino acids between *Homo sapiens*, *Rattus norwegius* and *Drosophila melanogaster* (figure 1.7 B) indicating that the regions are important for the protein. However, the CTLD is conserved between *Homo sapiens* and *Rattus norwegius* but not further to *Drosophila melanogaster*.

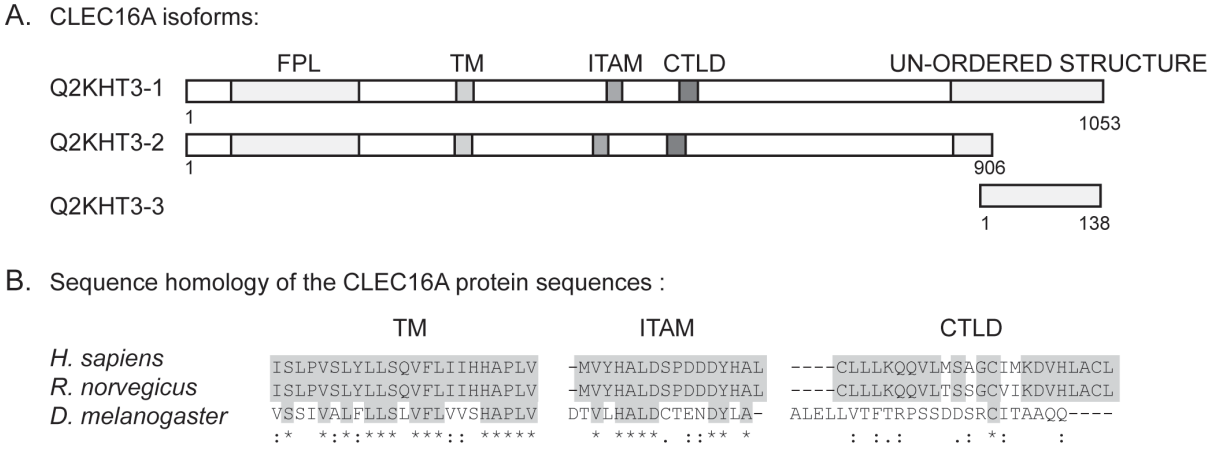

Figure 1.7. Overview of the CLEC16A isoforms with predicted domains and sequence homology of the protein sequence of CLEC16A. A) The predicted domains; FPL, trans membrane (TM), immunoreceptor tyrosine-based activation motif (ITAM) and C-type lectin-like domain (CTLD) shown in the different splice variants encoded by the *CLEC16A* gene. In addition, the predicted un-ordered structure is shown. **B)** Shows homology between the CLEC16A amino acid sequences between *Homo sapiens*, *Rattus norwegius* and *Drosophila melanogaster.* Figure adapted from (60).

1.3.3 The subcellular localization of CLEC16A

The few studies existing about the function of the CLEC16A protein show different subcellular locations of CLEC16A in different cell-types (68, 69). The same applies for Ema, CLEC16A´s orthologue in *Drosophila melanogaster* (70, 71). However, both CLEC16A and Ema are detected in the membrane fraction, when a subcellular fractionation is performed (68, 71). A report has shown that Ema is an integral membrane protein. In cellular fractionation of garland cells from *Drosophila Melanogaster,* Ema is obtained in the membrane fraction, and not extracted by high salt concentrations (71). In another report, human CLEC16A was shown to be a membrane-associated protein. In cellular fractionation of overexpressed CLEC16A in pancreatic β cells (cell-line Min6 β), CLEC16A is present both in cytosolic and membrane fractions. When treated with alkaline carbonate, which disrupt protein-protein interactions, meanwhile keeping lipid-protein interactions, the localization of the protein is changed to only be in cytosolic fraction. This indicates that CLEC16A is associated with the membrane through protein interactions rather than lipid interactions (68).

Expression of Ema-green fluorescent protein (GFP) (fused to the N terminal of Ema) in garland cells from *Drosophila melanogaster* has shown that Ema is localized in late endosomes (71). Meanwhile, the same Ema-GFP has been shown to localize in the Golgi apparatus in fat body cells, salivary gland cells, muscle cells and epithelial cells, all from

Drosophila Melanogaster (70). Expression analyses of CLEC16A-TurboGFP (tGFP, fused to the N-terminal of human CLEC16A) in a human erythroleukemia cell-line (K562 cells) showed that CLEC16A (isoform 1) is localized in rough ER. In the same study, the result was not reproducible when using a C-terminally tGFP-tagged CLEC16A, this fusion protein did not co-localize with any of the markers they tested (69). Another study using Min6 β cells shows that CLEC16A (isoform 2) with a FLAG-tag is localized in the lysosomal-associated membrane protein 1 (LAMP1)-positive lysosomal compartment (68). The different subcellular localizations for CLEC16A can be in due to different localization in different cell-types but it can also be that different CLEC16A isoforms localize to different compartments.

1.4 The function of CLEC16A

Studies about the function of the proteins, CLEC16A and Ema, have shown that they are involved in endosomal trafficking and maturation as well as autophagy (68, 70, 71). In this section the potential involvement of CLEC16A in endosomal trafficking, autophagy and T cell activation is described.

1.4.1 CLEC16A in endosomal trafficking and maturation

Ema has shown to be involved in endosomal maturation and endosomal trafficking in *Drosophila melanogaster*. In Ema mutant cells, accumulation of large endosomal intermediates occur, membrane trafficking is disrupted and failure of proper lysosomal degradation is observed. The latter is due to lack of conversion from late endosomes to lysosomes. Interestingly, when expressing human CLEC16A in Ema mutant cells, the endosomal phenotypes were rescued. This indicates a similar function for the human counterpart of Ema (71). In a study using transient transfection of CLEC16A-siRNA in Min β cells, late Rab7-positive endosomes were accumulated, indicating that late endosomes are not converted into lysosomes (68).

1.4.2 CLEC16A in autophagy

In both Ema mutant fat body cells (from *Drosophila Melanogaster*) and CLEC16A loss-of-function fibroblasts, there are defects in autophagy (68, 70). In Ema mutant fat body cells, smaller autophagosomes are formed in the early steps of autophagy. Ema seems to be required for recruitment of Golgi elements to the autophagosomes, resulting in smaller size of

the autophagosomes in absence of Ema (70). Human CLEC16A has been implicated in autophagy of mitochondria, a process called mitophagy. Studies in fibroblasts with CLEC16A-loss-of-function showed increased mitophagy with impaired fusion between autophagosomes and lysosomes, resulting in accumulated autophagosomes containing damaged mitochondria (68).

1.4.3 CLEC16A in T cell activation

The role of CLEC16A in T cell activation has been investigated for B cells (Lymphoblastoid cell line, LCL) where CLEC16A was knocked down. Here, they show that there are no differences in the B cell activation markers; CD80, CD86, CD40 and HLA-DR for CLEC16A knocked down cells compared to controls, indicating that CLEC16A does not influence the ability of the B cells to activate T cells. In addition, the study confirmed this by finding that there were no differences in T cell proliferation when CD4+ T cells are co-culture with the CLEC16A knocked down B cells (69). In contrast, when CLEC16A was knocked down in monocyte derived dendritic cells there has been detected a decrease of HLA-II on the cell surface, compared to controls. These results indicate that CLEC16A is involved in the expression of HLA-II on the cells surface of APCs. If the effect also influence the T cell activation has not yet been tested (Marvin Luijn, personal communication). In an unpublished study from our lab, the effect of CLEC16A expression for the cell surface expression of activation markers (CD25 and CD69) and cytokine secretion (interleukin 2) have been measured after T cell activation. Preliminary results indicate that CLEC16A does not influence the T cell`s ability to be activated. However, phorbol 12-myristate 13-acetate (PMA) and ionomycin were used to induce the activation, and the involvement of CLEC16A via activation through the TCR has not been evaluated (unpublished, Leikfoss et al).

1.5 Aims of study

The cause of MS is unknown, but it is thought to involve complex interactions between several genes together with environmental factors, where each factor exerts a small effect. There have been several genome-wide association studies that have identified MS susceptibility genes. One of the identified genes is *CLEC16A*, which contains several MS-associated SNPs. To understand the cellular mechanisms underlying the disease development, the proteins encoded by the MS susceptibility genes should be mapped.

There have been some studies about the function of CLEC16A and Ema (orthologue in *Drosophila melanogaster*) earlier, which have shown that the protein is involved in endosomal trafficking and autophagy. Subcellular localization studies have shown that CLEC16A is located in rough ER (erythroleukemia cell-line) and in lysosomes (pancreatic β cells). Studies of Ema have shown that it is localized in early endosome and Golgi (in two different cell types). The subcellular localization of CLEC16A seems to differ between cell-types. The function and subcellular localization has not been studied in T cells before.

The aims for this thesis are:

- To evaluate the subcellular localization of CLEC16A in T cells.
- Study the role of CLEC16A in endosomal distribution in T cells.

The main approach to reach the aims in this thesis is confocal microscopy. These analyses have been complemented by cellular fractionation assays.

2 Methods

The main goals for this thesis were to investigate the subcellular localization of CLEC16A and to examine the possible role of CLEC16A in endosomal distribution. The methods performed to reach the goals are described in this section. All materials, equipment, recipes and primer sequences are listed in appendix.

2.1 Sub-cloning

Sub-cloning was performed to generate plasmids with recombinant deoxyribonucleic acid (DNA) encoding N- and C-terminally GFP-tagged CLEC16A. In addition, by removing CLEC16A-MYC-DDK from pCMV6-CLEC16A-MYC-DDK an empty plasmid was created (generation of all plasmids, are described in section 3.1). The created plasmids were transformed into bacteria to be amplified. To express the encoded protein in mammalian cells, the plasmids were purified from bacteria and transfected into mammalian cells. A flowchart describing the order of the sub-cloning procedure can be seen in figure 2.1.

In this thesis, the *Escherichia coli (E.Coli*) XL1.Blue bacterial strain was used in all bacterial work. The solutions (prior to addition of antibiotics) (recipe is found in appendix 3) and equipment used in this work were autoclaved at 121°C for 20 minutes prior to use.

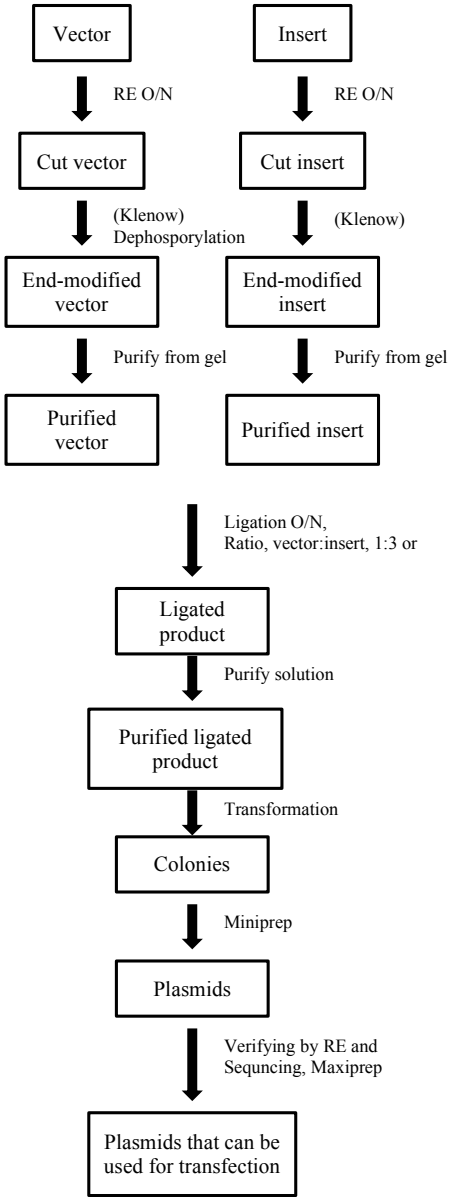

Figure 2.1. Overview over the order and steps followed in the sub-cloning. The steps were followed in indicated order to generate the plasmids with DNA-constructs described above, and to enable them for transfections into mammalian cells. RE= restriction enzyme digestion, O/N =over night. Vector is the destination plasmid and insert is the DNA-fragment to be inserted into to the vector. All insert- and vector fragments were not Klenow treated.

2.1.1 DNA plasmids

DNA plasmids are circular DNA-molecules. Plasmids are separated from chromosomal DNA in the cell and are replicated independently. They are common in bacteria and can be used as molecular tools, like vector for recombinant DNA. Sub-cloning is a technique used to move a gene/gene segment (insert) from one vector/plasmid (parent vector) to another (destination vector).

This section describes the cloning vectors used in the process of sub-cloning and these are also listed in materials (in appendix 2). All vectors in this thesis contain the specific elements that are required for the vector to be replicated and amplified when transformed into bacteria. They are also so-called expression vectors as they contain elements required for the inserted gene of interest to be expressed when transfected into mammalian cells.

pEGFP-N3

pEGFP-N3 (Clontech) contains the gene encoding GFP located downstream the multiple cloning sites (MCS). The location of the GFP gene makes it suitable for cloning a gene-fragment in fusion with GFP. The cloned gene-fragment then encodes a protein with GFP fused on the C-terminal side of the protein of interest.

In this thesis, the vector was used for generation of C-terminally GFP tagged CLEC16A. It was also used as a marker of transfection efficiency measured by flow cytometry (described in section 2.2.4).

pCMV6-CLEC16A-MYC-DDK

pCMV6-CLEC16A-MYC-DDK (Origene) is a pCMV6-entry vector containing complementary DNA (cDNA) of CLEC16A-isoform 1 fused with a MYC-DDK encoding tag on the C-terminal side of CLEC16A.

In this thesis, the vector was used to generate both C- and N-terminal GFP tagged CLEC16A. It was also used in functional assay to study the subcellular localization of CLEC16A and in endosomal distribution studies.

pEGFP-C1-SUMO

pEGFP-C1-SUMO was kindly provided by Odd Gabrielsen´s group and is a vector with pEGFP-C1 as backbone with a Small Ubiquitin-like Modifier 1 (SUMO1) insert (described in (72)). pEGFP-C1 is a vector suitable to fuse cDNA of the gene of interest with GFP, generating an N-terminal GFP tagged version of the protein encoded by the gene of interest.

In this thesis, cDNA of SUMO1 was replaced with cDNA of CLEC16A, generating an N-terminal GFP tag on CLEC16A.

2.1.2 Polymerase chain reaction - PCR

Polymerase chain reaction (PCR) is a technique for amplifying a specific part of a DNA sequence. The components needed to run a PCR are; two different gene specific primers (one forward primer and one reverse primer), a mix with the four types of nucleotides, a heat insensitive DNA polymerase and a suitable buffer. The forward primer together with the reverse primer defines the part of the DNA sequence to be amplified. The primers anneal to complementary DNA sequences whereas the DNA polymerase binds to the primers and incorporate the nucleotides given by the parent DNA strand. One cycle of PCR can be divided into three stages. The different stages are defined by specific temperature and duration. The stages in PCR are;

1. Denaturation, where the DNA strands separate from each other.
2. Annealing, the primers anneal to complementary sequences on each strand. Low annealing-temperature might give unspecific binding, and high annealing temperature may give rise to no binding. Recommended annealing temperature is 5-10°C below the melting temperature of the primer. The melting temperature of a primer depends on the sequence and also the length of the primer.
3. Elongation, both strands are being elongated by DNA polymerase.

The cycle is repeated for about 20-30 times.

Procedure:
Primers (final concentration 0,4 µM), deoxynucleotide (dNTP) (final concentration 0,4 µM), 10x Pfu DNA Polymerase reaction buffer (final concentration 1x) and template (10 ng) were mixed. Autoclaved Milli-Q (MQ)-water was added to a final reaction volume of 20 µl. Finally, Pfu Turbo DNA Polymerase (2.5U) was added to the reaction. The reaction was placed in a PCR cycle machine with the PCR program:

1 cycle:	Denaturation	95°C for 2 minutes
30 cycles:	Denaturation	95°C for 30 seconds
	Annealing	55°C for 30 seconds
	Elongation	72°C for 1 minute
1 cycle:	Elongation	72°C for 7 minutes

The primer sequences can be found in appendix 4.

2.1.3 Agarose gel electrophorese

In agarose gel electrophoresis, different DNA fragments are separated according to their sizes. Since DNA is negatively charged, it will migrate to the positive pole when being in an electric field. Agarose in the gel disrupts the migration, and makes the bigger fragments migrate slower and thereby be more delayed in the gel. This creates a separation where the small fragments migrate further then the large fragments. A good separation depends on the sizes of the fragments to be separated and the concentration of agarose in the gel, which contributes to the agarose network. To visualize DNA, ethidium bromide is added in the agarose gel. It intercalates with double stranded nucleotides and makes the DNA visible as bands in ultraviolet light (UV-light). Prior to loading, the samples are mixed with loading buffer containing glycerol, which makes the samples sink to the bottom of the wells.
To know the sizes of the bands, a molecular weight standard with fragments with known sizes is used.

Procedure:
In this thesis, 1% agarose gels were used. Agarose powder (final concentration of 1%) was mixed with Tris-acetate-EDTA (TAE) buffer (1x) and the reaction mix was heated until the agarose had melted completely. When the solution had cooled down to approximately 50°C, ethidium bromide was added (final concentration of 0,5 µg/ml). The gel solution was poured into a gel-casting tray and a comb was inserted into right place to make the wells. When the gel had solidified, the comb was removed and TAE (1x) buffer was added until covering the gel. Before the samples were loaded into the wells, a 6x loading dye (final 1x) was added to the samples. The gel was run at 80V, 240mA for 40 minutes, and finally the DNA fragments were visualized in UV-light in a gel doc (GeneGenius Gel Light Imaging System, Syngene).

2.1.4 Restriction enzyme digestion

A restriction enzyme binds to a specific DNA sequence and cleaves the phosphodiesterbond holding the nucleotides together. Different restriction enzymes recognize different DNA sequences and generates either a blunt end or a cohesive end at the position for cleave. A cohesive end is created when one strand is left with unpaired nucleotides. Dependent on

which strand the unpaired nucleotides are positioned, the cohesive ends can be with a 5´- or a 3´overhang.

In this thesis restriction enzymes were used to digest DNA fragments to get complementary ends before ligation. It was also used to verify plasmids after maxiprep or miniprep (described in section 2.1.12).

Procedure:
10x FastDigest buffer (final 1x), DNA (1 µg) and MQ-water (up to 20 µl) were mixed and FastDigest restriction enzyme(s) of interest was added (1U). The mix was incubated in 37°C for one hour, if the DNA fragments not were subject for further use, otherwise, the solution was incubated in 37°C overnight. The reaction was terminated by adding loading buffer or by heating the samples to the temperature required for inactivation of the enzyme (specified by the manufacturer).

2.1.5 Blunting

Blunting is a process that converts cohesive ends to blunt ends. Nucleotides are incorporated in overhangs by a polymerase.

In this thesis a Klenow fragment was used as polymerase. A Klenow fragment is a DNA polymerase, which has lost its 5´→3´ exonuclease activity. Meaning that it can fill a 5´overhang, but it cannot remove it.

Procedure:
Nucleotides (to a final concentration of 0,5 µM) and Klenow fragment (3U) was added to the inactivated restriction enzyme solution (final volume 20 µl). The reaction mix was incubated at 37°C for 20 minutes, and then the Klenow fragment was heat-inactivated at 75°C for 10 minutes.

2.1.6 Dephosphorylation of DNA

After restriction enzyme digestion (described in section 2.1.4) and blunting (described in section 2.1.5), the DNA is left with a free phosphate group on each strand. The phosphate group can be used to create a phosphodiesterbond and join two DNA fragments together by ligation (described in section 2.1.9).

To prevent an already digested plasmid to re-ligate in the ligation process, the phosphate groups on the vectors are removed by a phosphatase prior to ligation. The fragment is then free to be joined to the insert of interest, which provides the phosphatase groups.

Procedure:
FastAP Thermosensitive Alkaline Phosphatase (Thermo Scientific) (1U) was added to the reaction mixture after inactivation of the restriction enzymes or the Klenow fragment. This was incubated at 37°C for 10 minutes before the phosphatase was inactivated at 80°C for 5 minutes.

2.1.7 Purification of DNA from gel or solution

Isolation of one DNA fragment from a mix containing several fragments is carried out by running an agarose gel (described in section 2.1.3), collecting the fragment of interest from the agarose and purifying the DNA from the components in the gel. The piece of gel containing the fragment of interest is cut out from the gel while visualizing the DNA in UV-light. The DNA is purified from the gel by a spin-system kit from Promega (Wizard® SV Gel and PCR clean-up system). The kit contains a binding buffer that is used to make the DNA less soluble and more prone to bind to a silica membrane provided by the kit. With the DNA bound to the membrane, other components can easily be washed away by centrifugation. The DNA is eluted and collected from the membrane in a low-salt buffer, which makes the DNA soluble and loses the capacity to bind to the silica membrane. The same kit can be used to purify DNA from solution.

In this thesis DNA purification from gel was used after restriction enzyme digestion to purify DNA fragments prior to ligation. DNA purification from solution was used after PCR reaction and before transformation to remove components used in ligation, like PEG and ligase.

Procedure:

The protocol recommended from Promega (The Wizard SV Gel and PCR Clean-Up System kit) was followed.

2.1.8 Measurement of DNA concentration by Nanodrop

Concentration and purity of nucleic acids can be determined by measuring absorbance at different wavelengths. By measuring absorbance at 260 nm, the concentration of DNA and ribonucleic acid (RNA) can be determined, as the nucleic acids absorb light in this wavelength. Proteins absorb light at 280 nm and organic compounds absorb light at 230 nm. The ratio between 260/230 and 260/280 shows the purity of a nucleic acid solution, since it is the amount of proteins and organic compounds present in ratio of nuclei acids.

The DNA concentration was measured before ligation (described in section 2.1.9) to get the right ratio of insert and vector. It was also measured after maxiprep and miniprep (described in section 2.1.12) to determine the DNA/RNA concentration prior to further work.

Procedure:

The nucleic acids solution (2 µl) was applied on a micro volume UV-Vis spectrophotometer (Nanodrop 2000 c spectrophometer, Thermo Scientific). Before measurements the spectrophotometer was calibrated with the solution the nucleic acid was solved in. The NanoDrop ND-2000 software calculated the concentration and ratios of the sample.

2.1.9 Ligation

Ligation is a process where two DNA fragments are joined together by an enzyme, ligase. The fragments are joined by a phosphodiester bond between a 3´ hydroxylgroup and a 5´ phosphoryl group.

The right molar ratio between insert and vector is critical to get a successful ligation.

The ratio (R) of insert/vector can be calculated by;

$$\frac{\text{ng of insert/bp of insert}}{\text{ng of vector/bp of vector}} = \text{R}$$

The ligase used in the ligation requires right physiological conditions to work properly, which is obtained through a buffer containing the components needed, like adenosine triphosphateadenosine triphosphate. A transient connection between nucleotides in cohesive ends will increase the possibility for the ligase to connect the nucleotides together. Blunt ends do not get a transient connection, but some difference in the environment can help to get a successful ligation. PEG is a crowding agent that reduces the solvent available for the fragments and the ligase, which increases the possibility for the fragments to align and being ligated together by the ligase. By using a higher amount of ligase the possibility for the aligned fragments to be joined together can be further increased.

Procedure:
The molar ratio used was 1:3 or 1:6 (vector:insert), with 70 ng vector. Amount insert was calculated by the equation above.

Blunt end ligation:
Vector and insert were mixed with 10x T4 DNA ligase buffer (final concentration 1x), 50 % PEG 4000 solution (final concentration 5%) and MQ-water (to get a 20 µl reaction). T4 DNA ligase was added (5 U), and the reaction was incubated at 16°C overnight. The T4 DNA ligase was not inactivated, since inactivation in the presence of PEG could inhibit the electrotransformation (section 2.1.11) that is following ligation.

Sticky end ligation:
Vector and insert were mixed with 10x T4 DNA ligase buffer (final concentration 1x) and MQ-water (to get a 20 µl reaction). T4 DNA ligase was added (1 U) and the reaction was incubated at 16°C for one hour. The T4 DNA ligase was inactivated at 70°C for 5 minutes. The ligation mix was not purified before transformation.

2.1.10 Production of Electrocompetent E.Coli XL1.Blue.

Prior to electrotransformation the bacteria need to gain the ability for uptake of exogenous DNA, called to achieve competence. To gain competence, the bacteria are grown in lysogeny broth (LB) medium to an optical density (OD) of OD600nm=0,94. Afterwards the bacteria are washed several times to remove all traces of LB medium as components from the medium

can cause an electric flow through the solution and reduce the viability of the bacteria upon electroporation.

Competent bacteria are used to amplify a plasmid of interest. Antibiotic resistance is used to sort between bacteria with or without the plasmid of interest. The plasmids are carrying an antibiotic resistance gene and only the bacteria that have taken up the plasmid will survive in a medium with the specific antibiotic. Since it is critical that the competent bacteria do not carry an antibiotic resistance without the plasmid of interest, the bacteria are examined for antibiotic resistance prior to the production of competent bacteria.

Procedure:
Prior to the production, the bacteria were tested for growth on LB-plates containing kanamycin, ampicillin or no antibiotics.
Only colonies that did not grow in medium containing kanamycin or ampicillin were chosen to proceed.

On day 1; one colony was inoculated in LB medium (20 mL/litre final culture) (recipe in appendix 3), called "pre-culture" and incubated over-night in 37°C while shaking at 200-250 rpm. On day 2; the pre-culture was inoculated in pre-warmed LB medium (1 litre/20mL pre-culture) and grown in 37°C while shaking at 200-250 rpm. Every 10 minutes, the optical density (OD) at 600 nm was measured. When OD reached 0,94, the culture was placed on ice-bath for 15 minutes. The bacteria were harvested by centrifugation, 4000 x g at 4^{o}C for 5 minutes, and the bacterial pellet were washed twice with cold water (200mL/litre culture) and once with cold 10% glycerine (50 mL/litre culture) (recipe in appendix 3). Finally, the bacteria were resuspended in glycerol-yeast extract-tryptone (GYT) medium (4mL/litre culture) (recipe in appendix 3), aliquoted into tubes on an ethanol/dry-ice bath and stored at -80°C.

2.1.11 Electrotransformation of *E.Coli* XL1-blue cells

Transformation is a process in which bacteria take up genetic material from the environment with high efficiency. In electrotransformation, the genetic material is introduced with help of an electric field/pulse. Purification of DNA (described in section 2.1.7) is necessary prior to

electro-transformation if the plasmid has been created by blunt-end ligation in due to the presence of PEG that interferes with electrotransformation.

Procedure:
Cuvettes were put on ice and Super Optimal broth with Catabolite repression (SOC) medium (recipe in appendix 3) was pre-warmed to 37°C. The competent bacteria were thawed on ice. Plasmid solution (1 µl with the concentration 1ng/µl to 50 µl bacteria) or ligation solution (1-2 µl to 50 µl bacteria) were mixed with electro-competent bacteria and transferred to 2 mm-cuvettes. The cuvettes were pulsed at 900V/(mm gap on the cuvette) (ECM 399 electroporation system BTX®, Harvard apparatus), and pre-warmed SOC medium (500µl/50µl bacteria) was added immediately after the pulse. The bacteria mix were transferred to Eppendorf tubes and incubated in a shaker at 37°C, 225 rpm for one hour. The bacteria mix were transferred to LB agar plates (150 µl/plate) (recipe in appendix 3) with appropriate antibiotics (kanamycin 25 µg/ml or ampicillin 50 µg/ml) and incubated at 37°C overnight. The rest of the transformed bacteria were kept in the fridge until the day after. If no colonies appeared on the plates, the rest of the bacteria (kept overnight in the fridge) were transferred to a new LB agar plate, as described above.

2.1.12 Isolation of plasmid DNA

Plasmid DNA was isolated from bacterial cultures as miniprep (QIAprep Spin Miniprep Kit, Qiagen) or maxiprep (EndoFree Plasmid Maxi Kit, Qiagen).

Plasmid purification by miniprep

The QIAprep Spin Miniprep kit from Qiagen is based on a spin-system. A buffer containing chaotropic salts distrupt the hydrogen bond between water and nucleic acids, which makes the nucleic acids less soluble and more prone to binding to a silica membrane. Proteins and other components that do not bind to the silica membrane during these conditions are removed during several washing steps. To elute the nucleic acids, a buffer with low salt concentration is used to make the nucleic acids soluble. Miniprep is used when a low amount of the plasmid is needed.

In this thesis miniprep was used to verify clones after electrotransformation (described in section 2.1.11).

Procedure:

After transformation, one colony was transferred to LB medium (3-5mL) with appropriate antibiotics (25 µg/ml of kanamycin or 50 µg/ml of ampicillin) and grown for 16-18 h at 37°C in 225 rpm. Cells were harvested by centrifugation at 6800 xg for 3 minutes at room temperature (RT) and miniprep was performed according to the manufacturers recommendations in the kit protocol from Qiagen.

Plasmid purification by maxiprep

Maxiprep can be performed to get a higher yield of plasmids than possible from miniprep. The maxiprep kit from Qiagen is designed to isolate DNA plasmids from 200 mL LB medium culture grown overnight in Erlenmeyer bottles. The purification is based on an anion exchange resin with high affinity for plasmids. The negative phosphate groups on the DNA bind to the positive groups on the surface of the resin. To make the DNA bind to the resin, a buffer with low salt concentrations is used in the binding step. Buffer with medium salt concentration is used to wash away proteins, RNA and other components. The DNA is eluted in a buffer with high salt concentrations, the positive groups at the resin make stronger bonds with the salt and the DNA is eluted. To remove the salt in the elution buffer, DNA is precipitated with isopropanol and the DNA pellet is washed in 70% ethanol prior to resuspension in Tris-EDTA (TE) buffer (400 µl).

Procedure:

After transformation, one colony was transferred to LB medium (200 mL) with appropriate antibiotics (with 25 µg/mL of kanamycin and 50 µg/mL of ampicillin) and grown for 16-18 h at 37°C for 225 rpm. The bacteria were harvested in 6000 xg for 15 minutes in 4°C. The maxiprep was performed as recommended in the protocol from the manufacturers.

2.1.13 Sequencing

DNA sequencing is a technique used to determine the exact order of nucleotides in a DNA molecule.

Sequencing was performed after generation of new vectors to verify the sequences in the transition between the vector and the insert.

Procedure:

A company called GATC Biotech (http://www.gatc-biotech.com/en/index.html) performed the sequencing. Samples were prepared for sequencing by mixing template-solution (5 µl in concentration; 80-100 ng/µl) with primer (5 µl of 5 pmol/µl) in Eppendorf tubes (primer sequences can be found in appendix 4). The tubes were marked with barcodes and sent to GATC Biotech. The results were analysed in the sequencing program Geneious (http://www.geneious.com/).

2.2 Mammalian cell work

A T-cell line was used in this thesis to perform subcellular localization and functional studies of CLEC16A. The main tool for the cell work in this study is transfection, which in this thesis is used either to overexpress a protein of interest by introduction of exogenous DNA (DNA plasmids) or knock down expression of the gene of interest, i.e. CLEC16A by introducing CLEC16A specific siRNA.

The T cell line used was Jurkat TAg T cell line. Other group members have shown that the Jurkat T cell line expresses endogenous CLEC16A and that it can be knocked down when transfected by CLEC16A specific siRNA. In addition it is a cell-line suitable for transfection.

Jurkat TAg T cell line

The Jurkat TAg cell line is a derivative of the human T-cell leukemia Jurkat E6.1 cell line (www.atcc.com) stably transfected with the SV40 large T antigen (73). This T cell line is derived from peripheral blood from a human male with acute T cell leukaemia. It is rapidly growing and is suitable for transfection.

2.2.1 Cell cultivation

Jurkat TAg cells were cultivated in Roswell Park Memorial Institute (RPMI) 1640 medium with fetal bovine serum (FBS, 10%) as serum supplement, penicillin/streptomycin (1%) to prevent bacterial growth, sodium pyruvate (1%) as energy source, non-essential amino acids (1%) and β-mercaptoethanol (0,05mM) as a reducing agent to prevent toxic oxygen radicals to be produced.

The cells were cultivated at a concentration of 0,3 x 10^6 cells/ml - 2 x 10^6 cells/ml at 37°C in 5% CO_2. Fresh media were added three times a week and the concentration did never exceed 2.5 million cells/ml. Stocks of the cells were stored in liquid nitrogen and new cells were thawed every third month.

2.2.2 Cell count

The cells were counted prior to all cell-experiments and when given fresh media. An automated cell counter (TC20™ Automated Cell Counter, Bio-Rad) was used to count both live and dead cells.

Procedure:
Resuspended cell suspension was transferred to a chamber slide (Counting Slides dual chamber for cell count, Bio-Rad) (10 µl/slide). To count both live and dead cells the resuspended cell suspension was mixed with trypan blue (1:1) before it was transferred to the slide (10µl/slide). The chamber slide was inserted into the cell counter, which calculated the amount of cells (and percentage of dead cells if trypan blue was used).

2.2.3 Transfection of Jurkat T cells

Transfection is a common technique used to introduce exogenous DNA into mammalian cells. Transfection can also be used to knock down the expression of cell-endogenous genes by transfecting with a target-specific siRNA.

Jurkat T cells are transfected by electroporation where a short intense pulse of an electric field is applied to the cells to increase the permeability of the cell membrane enabling external genetic material to pass.

Procedure:
The cells were counted and harvested (15 x10^6 cells/transfection) at 300 x g for 8 minutes at RT. The cells were washed twice with RPMI medium and resuspended in transfection medium (400 µl/transfection) (RPMI with 5% FBS, 1% non-essential-amino acids, 1% sodium pyruvate and 0,05mM β-mercaptoethanol). The cells were mixed with the DNA/RNA of interest (the amount of DNA/RNA was empirically determined for each plasmid/siRNA). The cell/DNA or cell/RNA mix was transferred to cuvettes (4mm) and incubated at RT for 15

minutes. The cuvettes were pulsed once with the current settings: 240V, 25ms. After the pulse, the cells were incubated at RT for 15 minutes. The cells were transferred to T-75 flasks with pre-heated (37°C) transfection medium (10ml/transfection) and incubated for 24 or 48 hours at 37°C in 5% CO_2. If the cells were cultivated for 48 hours, fresh medium was added after 24 hours to achieve a cell concentration of 0,9 x 10^6 cell/ml.

2.2.4 Flow cytometry

Flow cytometry is a technology used to analyse the physical and chemical characteristics of particles in a fluid as it passes through a laser. It is routinely used for analysing expression of cell surface and intracellular molecules. Different detectors are placed to catch light scatter or emitted light from fluorescently labelled cells. In the light beam, forward scatter (FSC) and side scatter (SSC) are measured. FSC correlates with the diameter of the cells whereas SSC correlates with the density of the particle, i.e. the granularity of the cells.

Pulsed cells (with no plasmid) were used to define single and living cells by gating as described in figure 2.2. In addition pulsed cells were used as a negative control for GFP. The following gating was performed: single cells were gated in a Forward Scatter (FSC) Areal/FSC Height plot (figure 2.2 A) and living cells were gated in a FSC areal/side scatter (SSC) areal plot (figure 2.2 B).

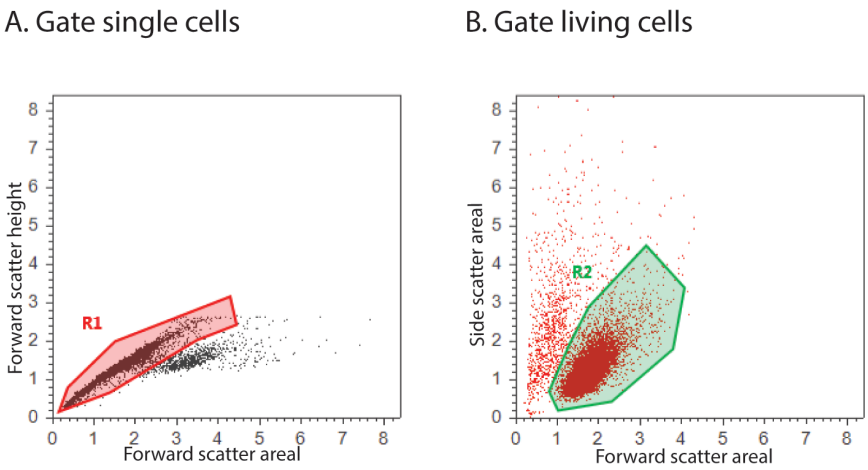

Figure 2.2. Overview of cell gating in flow cytometry measurements. A) Single cells are gated in a forward scatter areal (FSC(A))/forward scatter height (FSC(H)) plot. **B)** The plot displays the single cells (R1) and R2 defines the living cells gated in FSC (A)/side scatter areal (SSC(A)) plot.

To estimate the transfection efficiency of an experiment, one extra sample was added when transfection was performed. Cells were transfected with a plasmid expressing GFP (pEGFP-

N3). Flow cytometry was used to analyse the percentage of GFP-positive (GFP+) cells after transfection. The percentage of GFP+ cells was determined in a population of single and living cells. The percentage was used as a measurement between transfections performed at different times.

Procedure:
Cells directly from suspension were analysed on flow cytometry (Attune acoustic focusing cytometer, Applied Biosystem by Life Technologies) (solutions used are listed in materials in appendix 2). 10 000 cells were analysed by flow cytometry for each transfection performed.

2.2.5 Cell lysis

Radioimmunoprecipitation assay buffer (RIPA) (Pierce RIPA buffer, Bio-Rad) was used to make whole cell lysates. It contains Sodium dodecyl sulphate (SDS) that destroys the cell membrane, and it has a salt concentration that favours osmosis, meaning that the fluid in the cells are moving out to the extracellular environment. These properties together will lead to cell lysis. This procedure is performed to release the cell content and collect the proteins for further analysis, for instance for Western blotting.

Procedure:
The cells were counted and harvested by centrifugation at 300 x g for 8 minutes at RT. The cells were washed twice with phosphate buffered saline (PBS). All PBS was removed from cell pellet. The cells were either lysed directly or the pellet was stored at -20°C and lysed at a later time point.

Protease inhibitor cocktail (PIC) was added to the RIPA buffer and the mix was added to the cell pellet (20 µl/million cells). The tube was vortexed until the pellet had been completely resuspended in the buffer. The tube was put on a rotator machine at 4°C for 1 hour and then centrifuged at 12 000 x g at 4°C for 15 minutes. The supernatant was transferred to a new ice-cold tube and stored at -80°C.

2.3 Protein work

When transfecting Jurkat T cells with a plasmid, the proteins encoded by DNA on the plasmids will be expressed in Jurkat T cells. In this thesis the proteins that are expressed is

analysed by Western blot analysis or by imaging technics (described in section 2.4). The subcellular localization is examined by either collecting proteins from different cellular fractions and detected them by Western blot analyse, or by visualize the cells by imaging. In this section, compartmental protein extracting and detecting on Sodium dodecyl sulphate polyacrylamide gel electrophoresis (SDS PAGE) and Western blot analysis are described.

2.3.1 Compartmental protein extracting

By using buffers to change the environment for cell content, proteins located in different compartments in the cell can be separated and collected. A kit form Millipore (Compartmental Protein Extraction kit) sequentially extracts proteins from the nucleus, cytosol, membrane and cytoskeleton. After the extraction, the different fractions are analysed on a Western blot with organelle-specific antibodies to show the purity of each fraction. With pure fractions it is possible to identify the fraction a protein of interest is located in.

This procedure was used for Jurkat T cells transfected with GFP/DDK-tagged CLEC16A-plasmids to identify the fraction the overexpressed protein was localized in. Additionally, it was used in untransfected Jurkat T cells to identify the fraction for endogenous CLEC16A.

Procedure:

The protocol provided by the manufacturer (Millipore) was followed, with these extra steps;

- The needle used in disrupting the cell membrane was with gauge 30 (26.5-29 were recommended in the protocol)
- The incubation step with nuclear lysis buffer was repeated with a double amount of buffer the second time.

2.3.2 Bradford assay for protein concentration determination

The same input of proteins should be applied on a gel when analysing proteins on SDS PAGE (section 2.3.3) and Western blot analysis (section 2.3.4). The protein concentration can be determined by performing Bradford assay. Coomassie blue, used in Bradford assay, is a dye that has different forms that is giving different colours to the solution. When proteins bind the form changes, hence the colour changes in the solution dependent on the protein concentration, which can be detected by measure OD at 595 nm in a spectrophotometer. Higher protein concentrations give rise to a stronger blue colour and a higher absorbance.

Procedure:

Coomasssie blue dye (1 ml, Quick start Bradford 1X Dye reagent, Bio-Rad) was mixed with either bovine serum albumin (BSA, Bio-Rad) (0.5 µl, 1 µl, 2 µl, 4 µl or 8 µl of 2 mg/ml) or the samples with unknown concentration (2 µl). All samples were prepared in duplicates. The samples were vortexed before incubated for 15 minutes at RT. The absorbance was measured at 595 nm (Ultraspec 2100 pro, Amersham Bioscience).

2.3.3 SDS PAGE

SDS PAGE separates proteins according to their mobility in polyacrylamid gels. SDS denatures and linearizes proteins and gives them an evenly distributed negative charge in a charge-to-mass ratio. This makes the separation only dependent on the molecular mass of the proteins. When an electrical field is applied, the proteins will migrate towards the positive pole due to its negative charge. The smaller proteins will migrate further than the bigger ones since they are less impaired by the polyacrylamide in the gel.

The percentage of polyacrylamide can vary between gels. High percentage of polyacrylamide will give more inhibition for the migrating proteins and will give a better separation of small proteins. In contrast, low percentage of polyacrylamide will give less inhibition and a better separation of larger proteins. In gradient gels the percentage will vary throughout the gel with low percentage nearest the negative pole and high percentage at the positive pole. Gradient gels can be used to get a good separation of both small and large proteins at the same time. A protein marker, with proteins of known sizes, is used to determine the size of the proteins of interest.

In this thesis SDS PAGE was performed to separate proteins after cell lysis (section 2.2.5) or cellular fractionation (section 2.3.1). To detect the protein(s) of interest, Western blotting was performed after SDS PAGE.

Procedure:

Precast gels (Bio-Rad); gradient 4-12%, 10% or 7,5% polyacrylamid gels were used. The gel was placed into the electrode assembly (Criterion™ cell, Bio-Rad) and the inner chamber was filled with running buffer (1x, recipe see appendix 3) until the wells were completely covered by buffer. The lower chamber was filled with the same buffer until the buffer covered the bottom of the gel. Loading dye with SDS (recipe, see appendix 3) was applied to the samples and incubated for 5 minutes at 95°C. The samples and the molecular standard were applied to the wells. The gel was running at 150 V and maximum milli-Ampere (mAmp) for 15 minutes followed by 200 V and maximum mAmp for approximately 45 minutes.

2.3.4 Western blotting

Western blotting is a technique that uses antibodies to detect specific proteins in a sample. After SDS PAGE (section 2.3.3), the separated proteins are transferred to a polyvinylidene fluoride (PVDF) membrane by electroblotting. The proteins are moving in an electric field towards the positive pole. They are pulled from the gel into the membrane where they bind through non-specific hydrophobic interactions. After the electro-transfer, the membrane is blocked with a protein-rich solution to inhibit un-specific binding of antibody to the membrane. The membrane is then incubated with a primary antibody specific against the target protein. This is followed by incubation with a secondary antibody, recognizing the species-specific part of the primary antibody. The secondary antibody is also linked to an enzyme, horseradish peroxidase (HRP), which catalyses the oxidation of a chemiluminescent substrate. The product of the reaction emits light, where the amount of light corresponds to the amount of HRP present, hence the amount of protein of interest present. The light can be strengthened in a process called enhanced chemiluminescence (ECL), which amplifies the signal by 1000-fold and makes it detectable. To detect the light signal, a film is placed over the membrane and the light emitted from the HRP-bound secondary antibody is captured on the film. The signals on the film are visualized and fixed by developing the film.
After use, the membrane is wrapped in plastic and stored at 4°C and can be stripped, i.e. removing both primary and secondary antibodies with a stripping blot buffer, enabling reprobing of the membrane with new antibodies.

Procedures:

Transfer from gel to membrane

After SDS PAGE, the gel was washed in distilled water (dH_2O) and put in cold transfer buffer (recipe in appendix 3). The PVDF membrane (Immun-Blot® PVDF membrane, Bio-Rad) was activated in methanol for 15-30 seconds, washed with dH_2O and put in cold transfer buffer. Two extra thick filters were soaked in cold transfer buffer. One filter was placed in the blotting apparatus with the membrane on the top. The gel was placed on top of the membrane and lastly the second filter was placed on top of the gel. Air bubbles were pressed out from each layer, and the lid from the blotting apparatus was placed on top of the assembly. The blot was run at 1 $mAmp/cm^3$, 50 V for one and a half hour (Amersham ECL Semi-Dry Blotters TE 77 PWR, Amersham Bioscience).

Antibody detection of protein of interest

The membrane was blocked with 4% skimmed milk/Tris-Buffered Saline with Tween 20 (TBS/T) (recipe in appendix 3) at RT for one hour. Primary antibody was diluted in 4% skimmed milk/TBS/T (according to the manufacturer, the exact dilution was determined empirically for each antibody) and incubated with the membrane over night at 4°C on a shaker. The membrane was washed 3x20 minutes at RT with TBS/T (recipe in appendix 3) before incubation with secondary antibody. Secondary antibody was diluted (according to manufacturer) in 4% skimmed milk/TBS/T and incubated with the membrane for one hour at RT. The membrane was washed 3x20 minutes in TBS/T. Super-signal solutions (ratio 1:1, SuperSignal ® West pica Chemiluminescent substrate, Thermo Scientific) were applied drop wise over the membrane to completely cover the membrane. The membrane was incubated for 5 minutes with the super-signal solution and placed in a developer cassette. A film was incubated in the cassette with the membrane and was developed using Curix 60 from AGFA HealthCare.

Stripping of PVDF membrane

The membrane was reactivated in methanol for 15 seconds, rinsed in dH_2O and washed once in TBS/T. The membrane was boiled in the microwave own for a few seconds with 10x SDS running buffer. The membrane was washed 3x20 minutes with TBS/T, and stripping buffer (Restore Western Blot Stripping Buffer, Thermo Scientific) was added to the membrane. It was incubated for 15 minutes at RT and then washed 3x20 minutes with TBS/T. The

membrane was then blocked for one hour in 4% skimmed milk and incubated with a new antibody as described above ("Antibody detection of protein of interest").

2.4 Imaging

The subcellular localization of CLEC16A and its function in endosomal distribution were investigated by the imaging techniques, confocal microscopy and Image Stream. In this thesis the proteins are visualized by being fused with a fluorescent molecule (as GFP or mCherry) or by being targeted by antibodies, which are coupled with a fluorescent molecule (immunostaining described in section 2.4.1), prior to confocal microscopy and Image Stream. This section describes these imaging techniques, in addition the method for visualizing proteins prior to imaging is described.

2.4.1 Immunostaining of cells

In immunostaining, a primary antibody is used to target a specific protein in the cell. Secondary antibody is used to target the primary antibody and is commonly coupled with a fluorescence molecule enabling visualization of the signals in for example a fluorescence microscope. In the current thesis, paraformalaldehyd (PFA) was used to fix the cells, to preserve the cell structure. Saponin was used to permeabilize the cells, to make it possible to target intracellular proteins. Saponin is a gentle detergent that makes small pores in the cells without destroying the membrane. To preserve the permeability, saponin needs to be applied in every step after the permeabilization.

In this thesis, immunostaining was used in co-localization studies, by targeting the DDK tag on CLEC16A, and to visualize the organelle markers LAMP1 and TGN46. In addition, it was used in endosomal distribution studies to target lysosomes by the marker LAMP1. The samples were visualized by confocal microscopy or Image Stream analyses (the latter was performed by Ingvild Sørum Leikfoss, PhD student in the lab).

Procedure:

Jurkat Tag cells (1,5 millions for confocal microscopy, 4 millions for Image Stream) were stained in their culture medium with Hoechst (1 mg/ml in a dilution of 1:1000) for 20 minutes in 37°C, 5% CO_2, then harvested by centrifugation, 300 xg for 8 minutes at RT. The cells were washed once with RPMI medium.

Preparation of samples for confocal microscopy:

The cells were resuspended in 75 µl RPMI/millions cells. The cells were applied on slides coated with poly-L-lysine (Polysine™ microscope slides, VWR). The cells on the slides were incubated for 10 minutes in RT to make the cells attach to the slides. The medium was removed and 3% PFA in PBS (200 µl) was applied on the cells. The cells were fixed for maximum 10 minutes at RT. The PFA was removed, and the cells were washed twice with PBS/2%FBS (200 µl). The cells were then permeabilized with PBS/0,05% Saponin/0,25% BSA (200 µl) for 5 minutes. After removal of the saponin-solution, the cells were washed twice with PBS/0,05% Saponin/2%FBS (200 µl) and blocked with PBS/0,05%Saponin/0,25% BSA (200 µl) for 20 minutes at RT. The blocking solution was removed and the cells were incubated with primary antibody (concentration of the antibodies was empirically determined for each antibody guided by the manufacturers recommendations) diluted in PBS/0,05% Saponin/0,25% BSA (100 µl) for one hour. The antibody solution was removed and the cells were washed three times with PBS/0,05% Saponin/0,25%BSA (200 µl). Further the cells were incubated with secondary antibody diluted (after manufacturers recommendations) in PBS/0,05% Saponin/0,25% BSA (100 µl) for one hour in RT. The cells were washed three times and left to nearly dry before mounting media (35 µl) were applied on top of the cells. A coverglass (Cover glass thickness no 1, VWR) was put over the mounting media (SlowFade® Gold antifade reagent) and nail polish was used to seal the edges.

Preparation of samples for Image Stream analyses

The cells were resuspended in 2% PFA in PBS (200 µl), transferred to a cone shaped 96 well plate and fixed for maximum 10 minutes at RT. The PFA was removed, and the cells were washed twice with PBS/2% FBS (200 µl). The cells were permeabilized with PBS/0,05% Saponin/0,25% BSA (200 µl) for 5 minutes. The saponin solution was removed, and the cells were washed twice with PBS/0,05% Saponin/2% FCS (200 µl) and blocked with PBS/0,05% Saponin/0,25% BSA (200 µl) for 20 minutes in RT. The medium was removed, and the cells were incubated with primary antibody diluted (the concentration of antibodies was empirically determined for each antibody prior to the immunostaining of cells) in PBS/0,05% Saponin/0,25% BSA (200 µl) for one hour. The antibody solution was removed and the cells were washed three times with PBS/0,05% Saponin/0,25% BSA (200 µl) before they were incubated with secondary antibody diluted (after manufacturers recommendations) in

PBS/0,05% Saponin/0,25% BSA (200 µl) for one hour in RT. The cells were washed three times in PBS/0,05% Saponin/0,25% BSA (200 µl) before they were resuspended in PBS with 0,05% sodium azide (120 µl).

2.4.2 Confocal scanning laser microscopy

Confocal microscopy is a technique used to achieve high-resolution optical images with depth-selectivity. The main difference between confocal microscopy and common fluorescent microscopy is the ability to remove out-of-focus light. The result is that light above and beneath the focus plane is removed through a pinhole (74).
Confocal microscopy enables specific cell structures and proteins (dependent on target for antibody) to be detected and transformed into high-resolution images.
High-energy lasers excite the fluorescent molecules at different wavelengths. Since fluorescent molecules excites at a specific wavelength, it is possible to label various targets in the same cell with different fluorochromes and use different lasers to excite these molecules. With excitation means that electrons "jump" to a higher energy state, and when falling back to ground state they emit light that can be detected. The energy difference between these states determines the wavelength of the emitted light. Different detectors are recording the emitted light from the various excited fluorochromes. The signals from the different detectors can then be gathered and transformed into an image.

Procedure:
The samples were obtained from transfected Jurkat T cells with the plasmid(s) of interest after 24 h or 48 h cultivation. If the samples not were subject for immunostaining (section 2.4.1), the protocol for immunostaining was followed to the step with fixation of cells with PFA. After fixation, the cells were nearly dried on the poly-L-lysine coated glass-slide before mounting medium (SlowFade® Gold antifade reagent) was applied (35 µl). A cover glass was put on top and the edges were sealed with nail polish. The samples were stored at 4°C.

Two confocal microscopes were used in this thesis, one located at core facility on Gaustad and the other one at the Imaging Platform at the department of Bioscience. Both microscopes were the same model, Olympus FV1000/BX61. The objectives used were PLAPO 60X (NA 1,40) or UPLSAPO 60X (NA1,35), both oil based. The images were obtained in size 1024x1024 pixels. For each sample, hundreds of cells were analysed and 5-10 images were

taken for each sample for more accurate analyses. The analyses of the endosomal distribution were performed without knowing which group the samples belonged in (overexpression, knock-down or controls).

2.4.3 Image Stream

Image stream is an instrument combining flow cytometry and fluorescence microscopy analyses. In image stream, a large amount of cells is analysed and the instrument software can be used to provide statistical analyses on these cells. The cells are analysed on fluorescence features.

Procedure:
The samples were obtained from transfected Jurkat T cells with the plasmid(s) of interest after 24 h or 48 h cultivation. If the samples not were subjected for immunostaining (2.4.1), the protocol for immunostaining was followed to the step with fixation of cells. After fixation, the cells were resuspended in PBS with natrium azide (0,05%) and stored at 4°C.

PhD student Ingvild Sørum Leikfoss ran the samples on the Image Stream and did the data analysis using IDEAS software.

3 Results

The main purpose for this thesis was to find the subcellular localization of CLEC16A in Jurkat T cells and further to evaluate the possible function of CLEC16A in endosomal distribution in the same cells.

The number experiments performed in each case is stated in the figure legend. Both the result from subcellular localization and endosomal distribution will be verified and quantified by Image Stream analyses to ensure that the observed pattern not is specific to only the subpopulation studied by confocal microscopy.

3.1 Plasmid construction

In order to perform the necessary experiments to study CLEC16A localization and function in Jurkat T cells, a toolbox with different CLEC16A expression plasmids was required. The sub-cloning of the plasmids needed is described in this section. However, the plasmids available in the laboratory are not described (only listed in materials in appendix 2).

The N- and C-terminal side of a protein can have different roles of importance for the function and localization, possible leading to different outcome of the localization when a tag is added on the C-terminal in contrast to the N-terminal side of a protein. To visualize the subcellular localization of CLEC16A by confocal microscopy, plasmids expressing GFP-tagged CLEC16A were constructed. Since GFP is a relatively large protein (approximately 27 kDa), there was a possibility that the localization of CLEC16A could be altered when it was fused to the GFP-protein. Since the importance of N- or C-terminal side of CLEC16A not was determined, two plasmids were constructed, one with GFP at the C-terminus of CLEC16A and one with GFP at the N-terminus of CLEC16A. The different gene construct will be referred to as CLEC16A-GFP_C and GFP_N-CLEC16A, respectively.

To generate a control plasmid for pCMV6-CLEC16A-MYC-DDK (available in the laboratory, see materials in appendix 2) an empty vector containing all elements except CLEC16A-MYC-DDK cDNA was generated, i.e. pCMV6-empty.

3.1.1 Sub-cloning of GFP-tagged CLEC16A

To create the GFP-tagged CLEC16A constructs, we used the following plasmids: pCMV6-CLEC16A-MYC-DDK, pEGFP-N3 and pEGFP-C1. All strategies ensured the right reading frame of the inserted cDNA, and we tried to minimize the length of the linker between GFP and CLEC16A.

To generate pCMV6-CLEC16A-GFP$_C$ two strategies were first created. GFP was amplified by PCR from pEGFP-N3 by primer combination 1 (strategy 1) or combination 2 (strategy 2) (primer sequences in appendix 4).

Generation of plasmid expressing CLEC16A-GFPc

Strategy 1: Forward primer for PCR of GFP from pEGFP-N3 contains a new *Not*I site upstream of the GFP gene and the reverse primer includes the stop codon from GFP in the vector. After PCR amplification of GFP, the PCR product was digested with *Not*I and ligated into the *Not*I/*Pme*I sites of pCMV6-CLEC16A-MYC-DDK, replacing MYC-DDK with GFP (figure 3.1 A).

Strategy 2: For PCR of GFP from pEGFP-N3, the same forward primer as in combination 1 and a reverse primer that anneals to pEGFP-N3 downstream of the GFP stop codon covering a vector sequence with a *Not*I site were used. After PCR amplification of GFP, the PCR product was digested with *Not*I and ligated into the *Not*I site of pCMV6-CLEC16A-MYC-DDK (figure 3.1 B).

However, none of these two strategies did work in practice to generate a plasmid containing cDNA for CLEC16A-GFP$_C$ and two new strategies were created, strategy 3 and 4. They were performed in parallel to each other to generate C-terminally GFP-tagged CLEC16A.

Strategy 3: To generate pCMV6-CLEC16A-GFPc: pEGFP-N3 was digested with *Not*I and *Sma*I to cut GFP out of the vector. This fragment was blunted and inserted into a blunted *Not*I site in pCMV6-CLEC16A-MYC-DDK (figure 3.2 A), replacing MYC-DDK with GFP.

Strategy 4: To generate pEGFP-N3-CLEC16A: pCMV6-CLEC16A-MYC-DDK was digested with *EcoR*I and *Not*I to cut out CLEC16A. The fragment was blunted and inserted into *Sma*I site of pEGFP-N3 (figure 3.2 B).

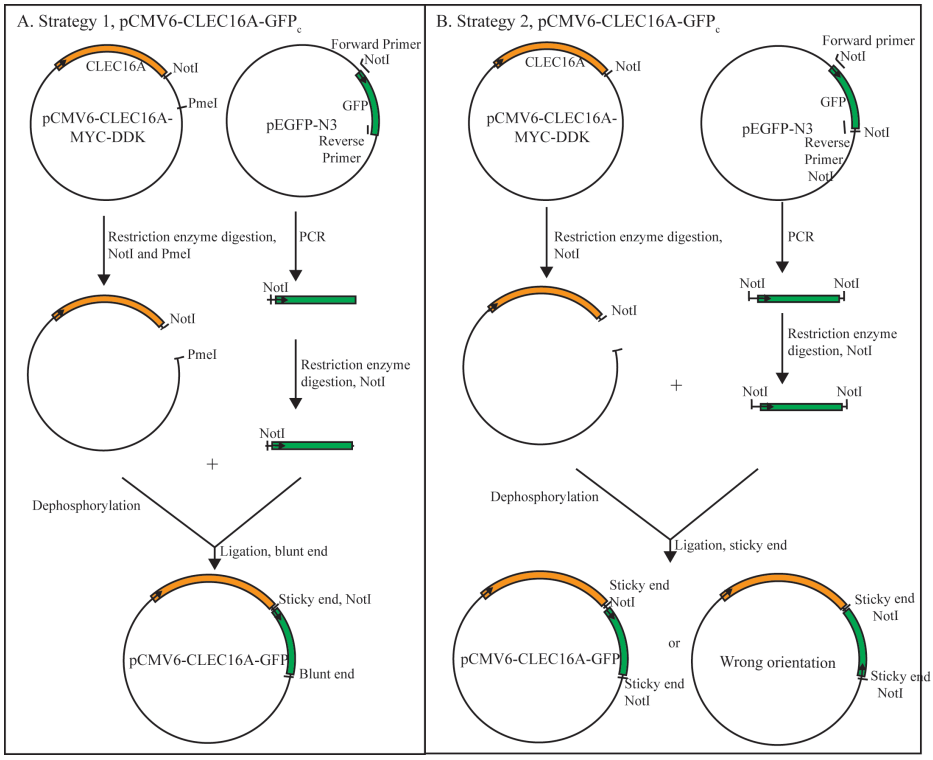

Figure 3.1 Generation of pCMV6-CLEC16A-GFP$_C$ - schematic overview of strategy 1 and 2. Strategy **(A)** 1 and **(B)** 2 were tested to generate pCMV6-CLEC16A-GFP$_c$. The CLEC16A cDNA is illustrated in orange and the GFP cDNA in green. The procedures and restriction enzymes used are indicated in the figure. The sequence of the primers distinguishes the two strategies as indicated in the result section above. The primer sequences are found in appendix 4.

Both strategy 3 and 4 gave rise to colonies containing a construct with GFP in the right orientation. From earlier work by other group members, pCMV6-CLEC16A-MYC-DDK has not been able to be used for transfection in Raji B cells. Additionally, we have observed that bacteria transformed with pCMV6-CLEC16A-GFP grow very slowly, making it difficult to isolate DNA from these cultures with sufficient concentrations needed for further use in transfection. Therefore, the construct from strategy 4 was chosen for further work and the plasmid is referred to as CLEC16A-GFP$_C$ in the rest of the thesis.

Generation of plasmid expressing CLEC16A-GFP$_N$

To generate GFP$_N$-CLEC16A (strategy 5): CLEC16A was obtained in same manner as described in strategy 4. The blunted fragment was inserted into *Sma*I and blunted *Xba*I in

pEGFP-C1-SUMO, to replace SUMO with CLEC16A (figure 3.2 C). A construct containing the right orientation of CLEC16A was obtained and the plasmid is referred to as GFP_N-CLEC16A in the rest of the thesis.

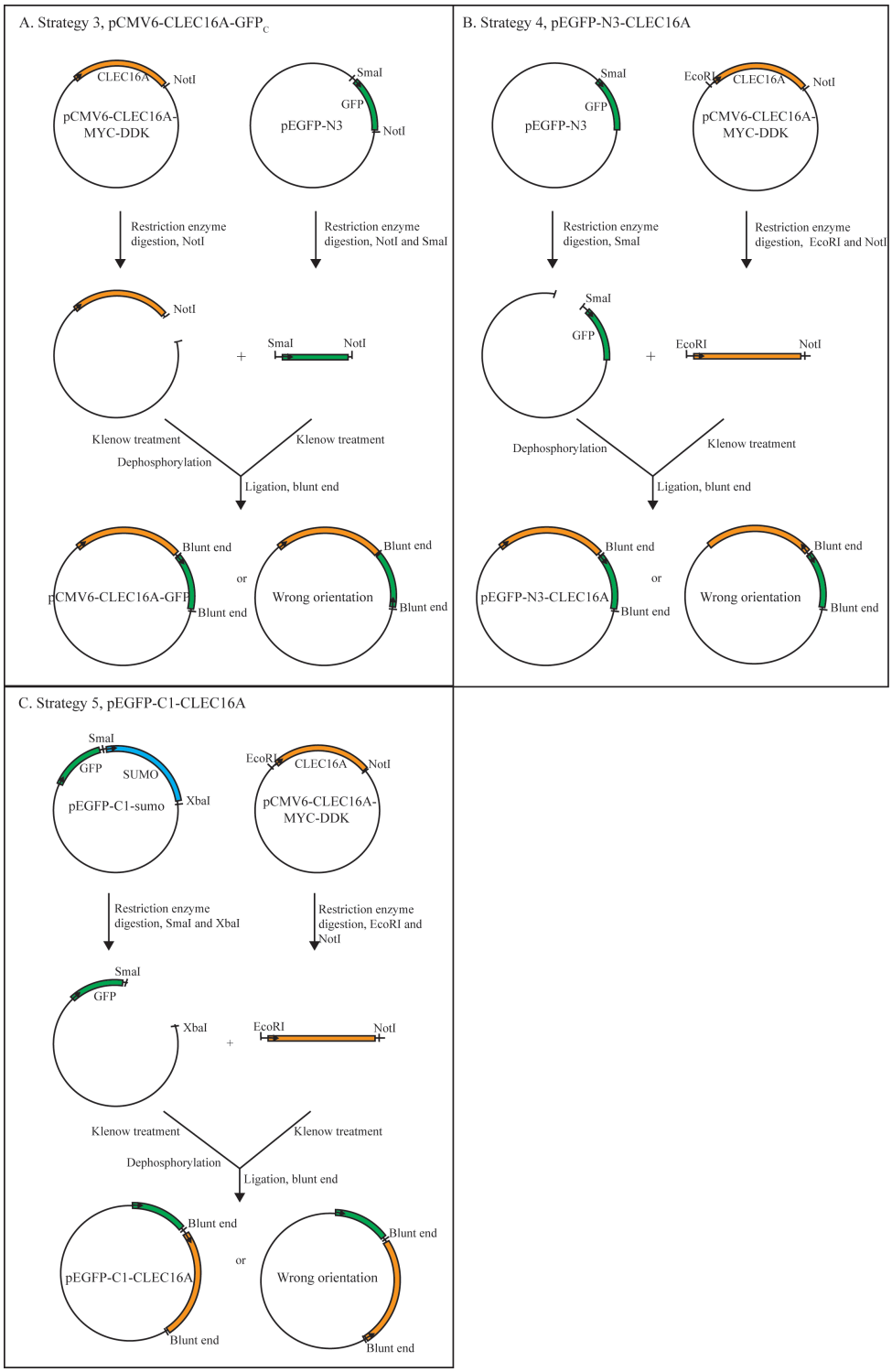

Figure 3.2. Generation of pCMV6-CLEC16A-GFP_C, pEGFP-N3-CLEC16A and pEGFP-C1-CLEC16A: Strategy **(A)** 3 and **(B)** 4 were developed for generating plasmids encoding CLEC16A-GFP_C and **(C)** strategy 5 was developed for generating plasmids encoding GFP_N-CLEC16A. The

CLEC16A cDNA is illustrated in orange, the GFP cDNA in green and the SUMO cDNA in blue. Procedures, restriction enzymes and plasmids used are indicated in figure.

All GFP-tagged CLEC16A plasmids obtained from sub-cloning were verified by restriction enzyme digestion and sequencing.

3.1.2 Cloning of pCMV6-empty

The restriction enzymes *BamH*I and *Pme*I removed CLEC16A-MYC-DDK from pCMV-CLEC16A-MYC-DDK. The vector backbone was re-ligated to generate pCMV6-empty (figure 3.3).

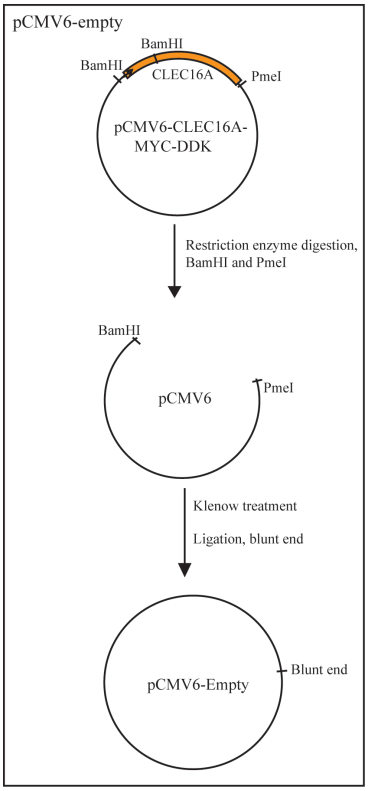

Figure 3.3. Schematic overview of the strategy to generate pCMV6-empty. The CLEC16A cDNA is illustrated in orange. The procedures, plasmid and restriction enzymes used to generate pCMV6-empty are indicated in the figure.

The pCMV6-empty plasmid was verified by restriction enzyme digestion and sequencing.

3.1.3 Expression of CLEC16A constructs in Jurkat T cells

After the plasmid had been verified on DNA level, it also needed to be verified at protein level. The plasmids were transfected into Jurkat T cells and the cells were harvested and lysed. The protein concentration in the whole cell lysate was measured by Bradford assay and

the same amount of protein from all samples to be compared, was applied on an SDS polyacrylamide gel. The fused proteins were analysed using Western blotting with antibodies against GFP or DDK.

Expression of CLEC16A fused with GFP

Before investigating the expression on the GFP-tagged CLEC16A, the optimal amount of plasmids for transfection into Jurkat T cells was determined by testing a range between 1-20 µg. Optimal amount was defined as when the overexpressed protein easily could be detected. Flow cytometry analyses were performed 24 h and 48 h after transfection of GFP-tagged proteins to identify the amount plasmids and time for harvesting, for optimal expression (data not shown). The optimal amount of plasmid was 5 µg for CLEC16A-GFP_C and 3 µg for GFP_N-CLEC16A. For both plasmids it were optimal for the cells to be harvested 48 hours after transfection.

Further, the proteins were confirmed to express the fused protein in the right size by Western blot analyses. Jurkat T cells were transfected with plasmids encoding GFP-tagged CLEC16A or GFP (positive control). The lysates were treated as described above, but to ensure a distinct band on the positive control, a smaller amount of proteins were applied from the lysate from GFP-transfected cells compared with the lysates from non-transfected Jurkat T cells and Jurkat T cells expressing GFP_N-CLEC16A and CLEC16A-GFP_C (figure 3.4).

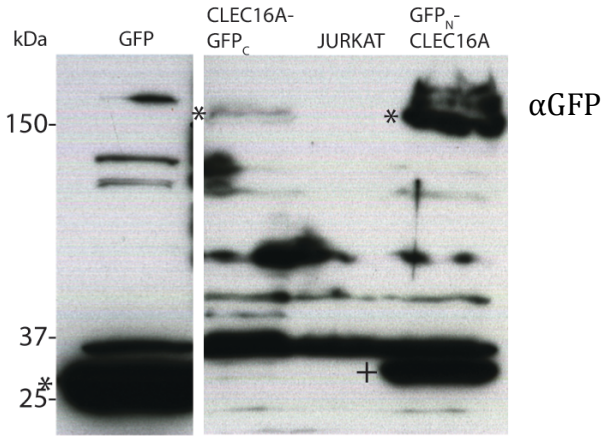

Figure 3.4. Expression of GFP-tagged CLEC16A in Jurkat T cells. Jurkat T cells were transfected with CLEC16A-GFP_C, GFP_N-CLEC16A or GFP. Transfected cells were harvested and lysed, and 20 µg of total proteins were used for the sample with GFP and 150 µg of total proteins were used for the other samples (the order of samples are indicated in figure). For detection, anti-GFP and HRP-conjugated secondary antibody was used. Expected bands are at approximately150 kDa for GFP-tagged CLEC16A and 27 kDa for GFP alone, bands of interest are marked by asterisks (*). An unidentified band in the lane with GFP_N-CLEC16A is marked by plus sign (+).

Both CLEC16A-constructs with GFP-tag were expressed at the expected size (150 kDa). The expected band for GFP (slightly above 25 kDa) can be seen for the positive control. In addition, an extra band was seen for GFP_N-CLEC16A (marked by +), where the protein size seemed to correspond to the size of GFP alone or to a protein migrating slightly slower. It could also be seen that GFP_N-CLEC16A were highly expressed compared to the CLEC16A-GFP_C. The expression of GFP-proteins was also measured by flow cytometry (figure 3.5).

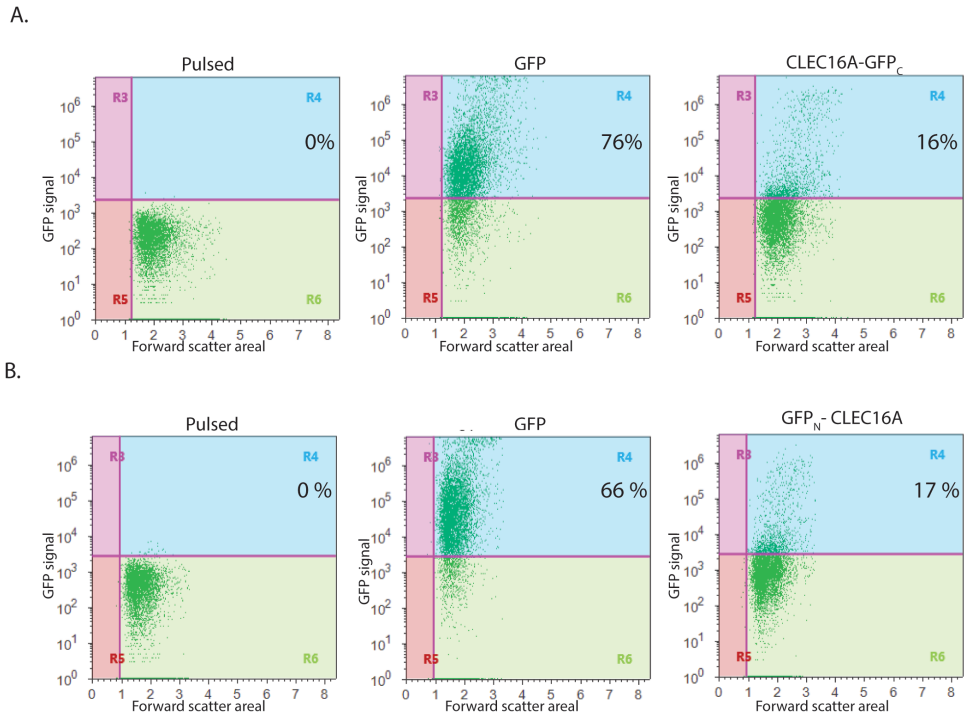

Figure 3.5. Flow cytometry measurement of CLEC16A-GFP_C and GFP_N-CLEC16A expression in transfected Jurkat T cells. Flow cytometry measurements of the expression of **(A)** CLEC16A-GFP_C and **(B)** GFP_N-CLEC16A. In addition, GFP in pEGFP-N3 (used as measurement for transfection efficiency) is shown for each experiment. Data shown are from single, living cells gated as described in section 2.2.4. Number in upper right corner of each plot corresponds to the percentage of GFP positive cells. Pulsed cells were used as a negative control.

In contrast to the Western blot analyses, flow cytometry measurements were showing almost the same expression levels for GFP_N-CLEC16A and CLEC16A-GFP_C. However, the transfection efficiency (see measurements for GFP in figure 3.5) was higher for GFP_N-CLEC16A, but not high enough to explain the difference obtained by Western blot analysis. Other flow measurements (figure 3.14) have shown slightly higher expression for N-terminally GFP-tagged CLEC16A.

Expression of CLEC16A-MYC-DDK

Other lab members had earlier determined the optimal amount of CLEC16A-MYC-DDK to be transfected into Jurkat T cells for optimal expression, i.e. 3 µg in the transfection and cells were harvested 48 hours after transfection.

To confirm the expression of CLEC16A-MYC-DDK in Jurkat T cells, the cells were transfected with either the empty plasmid (pCMV6-empty) or pCMV6-CLEC16A-MYC-DDK (further called CLEC16A-MYC-DDK in this thesis). The expression of CLEC16A-MYC-DDK was analysed with Western blotting, using an antibody against the DDK-tag, where the pCMV6-empty was used as a negative control (figure 3.6). The membrane was reprobed with anti-Glyceraldehyde 3-phosphate dehydrogenase (GAPDH) to control the protein loading (figure 3.6).

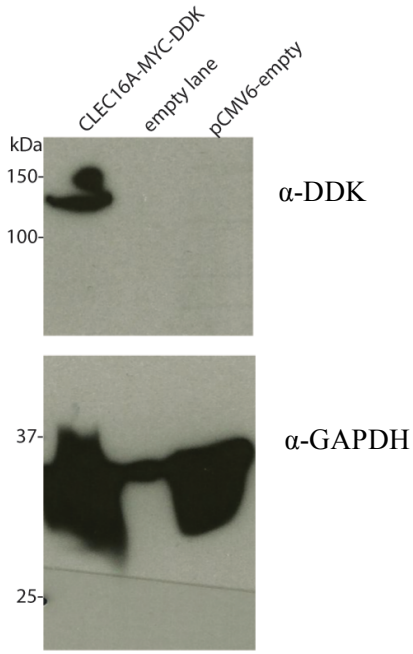

Figure 3.6. Expression of CLEC16A-MYC-DDK. Jurkat T cells were transfected with CLEC16A-MYC-DDK or pCMV6-empty. Transfected cells were harvested and lysed. 80 µg of total protein lysate were applied (the order of samples as indicated in figure). The membrane was probed with antibody against DDK-tag and HRP-conjugated secondary antibody, and stripped and reprobed with antibody against GAPDH and HRP-conjugated secondary antibody. The expected bands were at 125 kDa for CLEC16A-MYC-DDK and 35 kDa for GAPDH.

The expected size of CLEC16A-MYC-DDK (125 kDa) was confirmed (upper part of figure 3.6), this band was not present in the lysate from pCMV6-empty transfected cells despite that equal amounts of protein were loaded on gel (lower part of figure 3.6).

3.2 Localization of CLEC16A

Earlier published data have shown different subcellular localizations of CLEC16A in different cell types. CLEC16A has been shown to localize at lysosomes in pancreatic β cells (Min β cells) (68) and at ER in a human erythroleukemia cell-line (K562 cells) (69). Publications for the CLEC16A orthologue in *Drosophila*, Ema, have shown localization for Ema at Golgi in fat body cells of *Drosophila Melanogaster* (70) and at late endosomes in garland cells of *Drosophila Melanogaster* (71) (more details in section1.3.3). This thesis investigated the localization of CLEC16A in Jurkat T cells. The subcellular localization has not been studied earlier in immune cells.

3.2.1 CLEC16A-DDK and CLEC16A-GFP$_C$

One limitation using overexpression of tagged proteins for subcellular localization studies is that the tag can affect the protein so that it does not behave as endogenous proteins. To get an indication if the GFP tag was interfering with the localization of CLEC16A, CLEC16A-GFP$_C$ was co-transfected with CLEC16A-MYC-DDK. Since the DDK tag is considerable smaller, we expected that tag to give less distraction regarding the localization of CLEC16A than the GFP tag. The cells were harvested and immunostained with anti-DDK before the cells were analysed by confocal microscopy (figure 3.7).

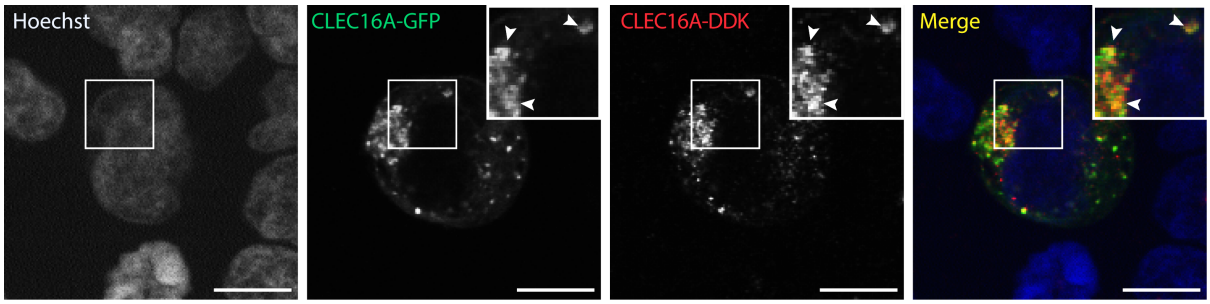

Figure 3.7. CLEC16A-GFP$_C$ was partially co-localized with CLEC16A-MYC-DDK. Jurkat T cells transfected with CLEC16A-GFP$_C$ and CLEC16A-MYC-DDK were stained with Hoechst, mounted on poly-L-lysine coated glass-slides, fixed and permeabilized before immunostaining with anti-DDK and Alexa555-conjugated secondary antibody. The cells were analysed by confocal microscopy. Indicated area is enlarged with arrowheads pointing at strong signals in the same place on all images. In the merged image, Hoechst is indicated in blue, CLEC16A-GFP$_C$ in green, CLEC16A-MYC-DDK in red and co-localized parts in yellow. One representative cell is shown from 3 experiments. Scale bars are 10 µm.

The confocal images (figure 3.7) showed partly co-localization between the C-terminally tagged-CLEC16A proteins.

3.2.2 CLEC16A-DDK and GFP_N-CLEC16A

To further examine the subcellular localization of CLEC16A, an N-terminally GFP-tagged CLEC16A was created (described in section 3.1). Since CLEC16A-GFP_C and CLEC16A-MYC-DDK not were completely co-localized, the localization of GFP_N-CLEC16A was further compared with CLEC16A-MYC-DDK. Jurkat T cells were transfected with plasmids encoding these proteins and the cells were harvested and immunostained with anti-DDK before they were analysed by confocal microscopy (figure 3.8).

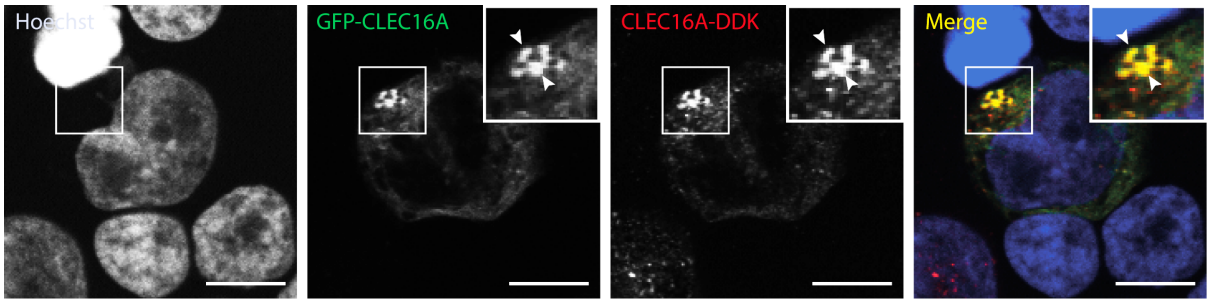

Figure 3.8. GFP_N-CLEC16A was co-localized with CLEC16A-MYC-DDK. Jurkat T cells were transfected with GFP_N-CLEC16A and CLEC16A-MYC-DDK. The cells were stained with Hoechst, mounted on poly-L-lysine coated glass-slides, fixed and permeabilized before immunostaining with anti-DDK and Alexa555-conjugated secondary antibody. The cells were analysed by confocal microscopy. Indicated area is enlarged with arrowheads pointing at strong signals in the same place on all images. In the merged image, Hoechst is indicated in blue, GFP_N-CLEC16A in green, CLEC16A-MYC-DDK in red, and co-localized parts in yellow. One representative cell is shown from one experiment. Scale bars are 10 µm.

In contrast to CLEC16A-GFP_C, the confocal microscopy analysis showed co-localization between GFP_N-CLEC16A and CLEC16A-MYC-DDK. This indicates that both of tagged CLEC16A proteins were in the same localization.

When comparing the pattern left by the GFP signals in GFP_N-CLEC16A and CLEC16A-GFP_C, some differences were detected, but both have distinct signals in small puncta (see arrowheads for the GFP signal in figure 3.7 and 3.8). These punctas were of interest to identify, and since both CLEC16A and Ema earlier have been shown to localize in endosomes (68, 71), the intracellular markers chosen for the identification, represents the endosomal pathway (for details about endosomal pathway, see section 1.2.2). The main

difference detected in the two GFP signals was a diffuse signal throughout the cell that was observed in GFP_N-CLEC16A, but not in CLEC16A-GFP_C.

3.2.3 Endogenous CLEC16A staining

Since the localizations of the tagged CLEC16A proteins were different, endogenous staining was tested to find the subcellular localization.

To get the most accurate results, endogenous staining of the protein of interest is preferred compared to transient overexpressing of the protein by transfection. The lack of specific antibodies is the biggest challenge for endogenous staining. To test the specificity of two antibodies against CLEC16A, Jurkat T cells transfected with CLEC16A-GFP_C, control siRNA or CLEC16A-specifc siRNA, were immunostained with anti-CLEC16A from Millipore (Figure 3.9) and anti-CLEC16A from abcam (data not shown). The purpose of transfecting the cells with CLEC16A-GFP_C prior to immunostaining was to examine whether GFP and anti-CLEC16A signals were co-localized (figure 3.9 A). The cells transfected with control siRNA (figure 3.9 B), or CLEC16A-specific siRNA (figure 3.9 C) were immunostained to examine if the anti-CLEC16A signals were reduced in CLEC16A-siRNA treated cells compared to control cells.

There was co-localization of the GFP signal and the CLEC16A-antibody signal (figure 3.9 A), indicating that the CLEC16A antibody binds to overexpressed CLEC16A. However, for the CLEC16A-siRNA and control-siRNA treated cells (figure 3.9 B and C) there was a reduction in CLEC16A-antibody signals for CLEC16A-siRNA treated cells in the first experiment, but in the second experiment there was a reduction for the signal in control-siRNA cells. In the third experiment no difference could be seen. This indicates that the anti-CLEC16A signals were unspecific binding or background from the high voltage settings used. In addition, the signals were seen all over the cell, also in the nucleus, and not in a distinct pattern.

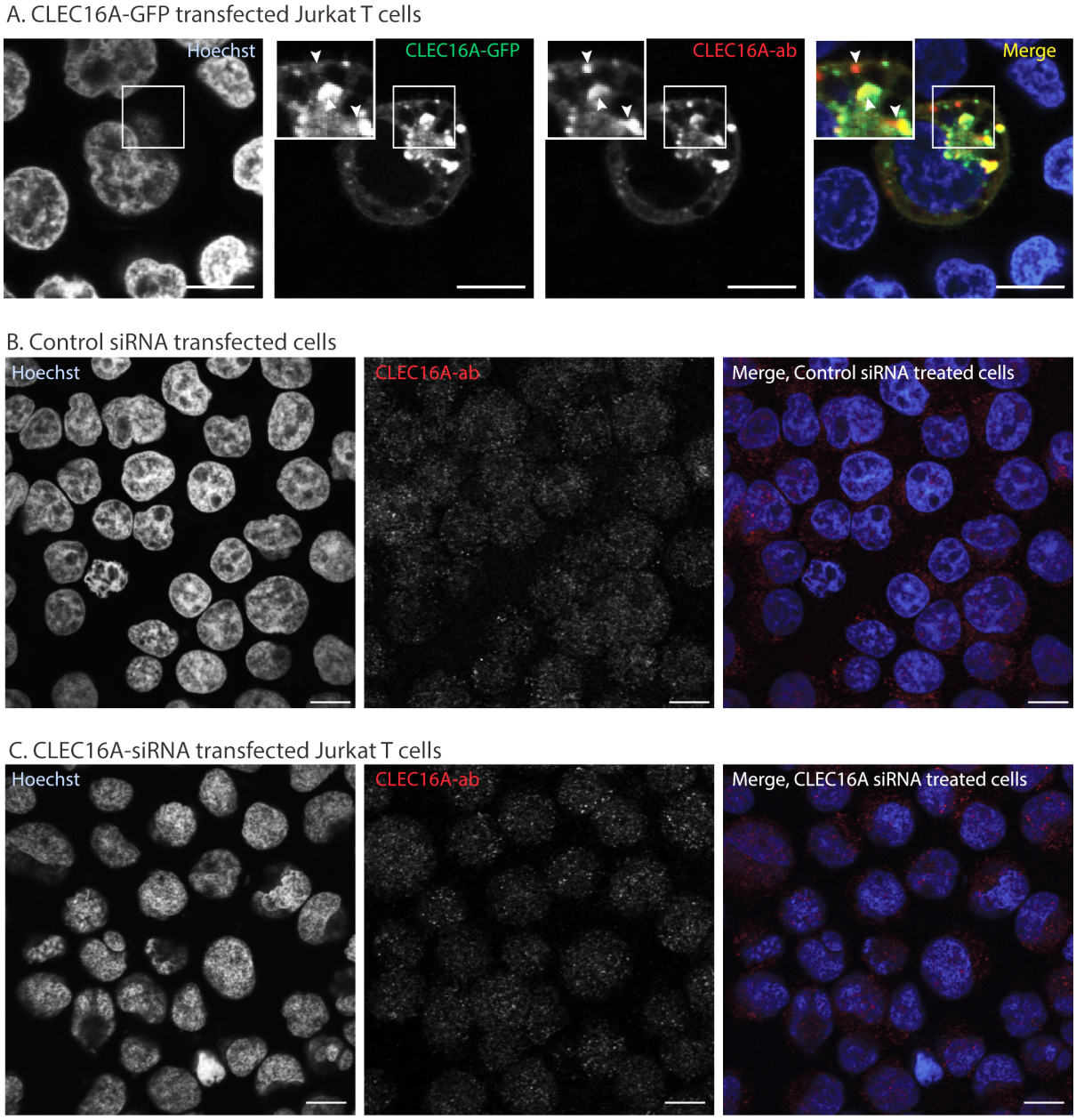

Figure 3.9. CLEC16A antibody does not bind specifically to endogenous CLEC16A. Jurkat T cells transfected with **(A)** CLEC16A-GFP_C were stained with Hoechst, mounted on poly-L-lysine coated glass-slides, fixed and permeabilized before immunostaining with anti-CLEC16A (Millipore) and Alexa647-conjugated secondary antibody. Indicated area is enlarged with arrowheads pointing at strong signals in the same place on all images. In the merged image, Hoechst is indicated in blue, CLEC16A-GFP_C in green, CLEC16A-antibody (Millipore) signals in red and co-localized parts in yellow. One representative cell is shown from one experiment. Jurkat T cells transfected with **(B)** control siRNA and **(C)** CLEC16A-specific siRNA were immunostained as described for (A). A representative section from three independent experiments is shown. In the merged image Hoechst is indicated in blue and CLEC16A-antibody (Millipore) signals in red. All scale bars are 10 µm.

To exclude that the varying result from the staining with the CLEC16A-antibody was due to lack of proper CLEC16A-knockdown after transfection with CLEC16A-specific siRNA, the

knocked down was confirmed. The transfected cells were harvested and lysed for further analysis on Western blot with CLEC16A-antibody (figure 3.10).

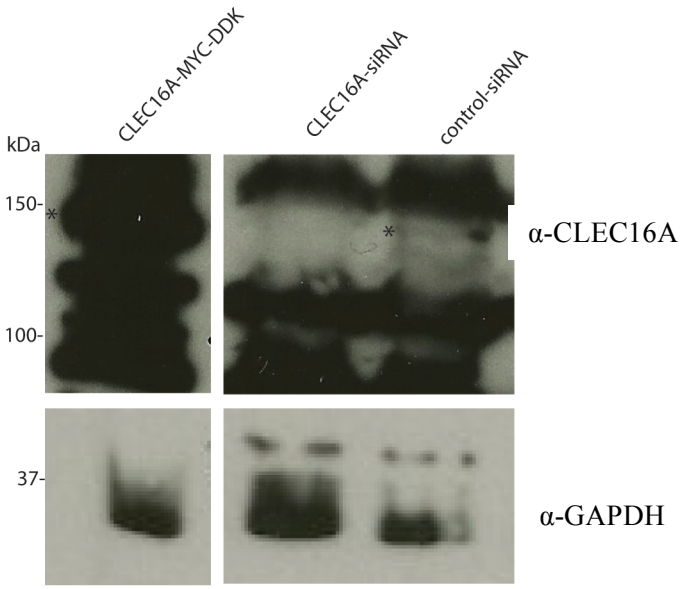

Figure 3.10. CLEC16A was knocked down at protein level in Jurkat T cells transfected with CLEC16A-specific siRNA. Jurkat T cells transfected with CLEC16A-MYC-DDK, CLEC16A-siRNA, or control-siRNA were harvested and lysed. Protein concentrations were measured prior to Western blot analysis, where 120 µg of total proteins were used. **(A)** The membrane was probed with anti-CLEC16A (millipore) and HRP-conjugated secondary antibody and **(B)** reprobed with anti-GAPDH and HRP-conjugated secondary antibody. The band was expected at 125 kDa, and is marked by asterisks (*).

Western blot analysis confirmed knockdown of CLEC16A expression at the protein level after transfection with CLEC16A-specific siRNA compared with cells transfected with control siRNA (see upper part of figure 3.10). Even though the bands were weak, the results fit with the procedure established in the lab, which confirms knockdown of CLEC16A in Jurkat T cells at both protein and messenger RNA (mRNA) level 48 hours after transfection. Additionally, the loading control indicated more total proteins in the CLEC16A-siRNA samples compared to control-siRNA (see lower part of figure 3.10)

3.2.4 Cellular Fractionation

Since endogenous staining not could be performed, cellular fractionations were executed on Jurkat T cells transfected with the different tagged CLEC16A proteins and on untreated Jurkat T cells. It was performed to examine if the GFP/DDK-tagged CLEC16A proteins were located in the same fraction(s) as endogenous CLEC16A.

In the fractionation kit (Compartmental Protein Extraction kit, Millipore) four fractions were collected, i.e. cytosolic-, nuclear-, membrane- and cytoskeleton fraction. Untreated Jurkat T cells were used to optimize the procedure. The purity was examined in each fraction with antibodies against housekeeping proteins with specific localization (cytosol: GAPDH, nuclear: lamin B1, membrane: epidermal growth factor receptor (EGFR), cytoskeleton: vimentin). When performing the protocol according to the manufacturers' recommendations, the nuclear proteins were detected in all fractions when being analysed by Western blot with anti-lamin B1 (nuclear protein). In addition, the membrane fraction seemed to have a very low amount of proteins on Bradford assay. The antibody that was used to detect membrane proteins (anti-EGFR) showed a signal in the positive control, but not in any of the other fractions (data not shown).

The method was optimized with focus on the nuclear fraction. The diameter of the needle used to free the nucleus from the rest of the cell was reduced, and the step where the cells were incubated with nuclear lysis buffer was repeated with double amount of nuclear lysis buffer the second time. The result after optimization can be seen in figure 3.11.

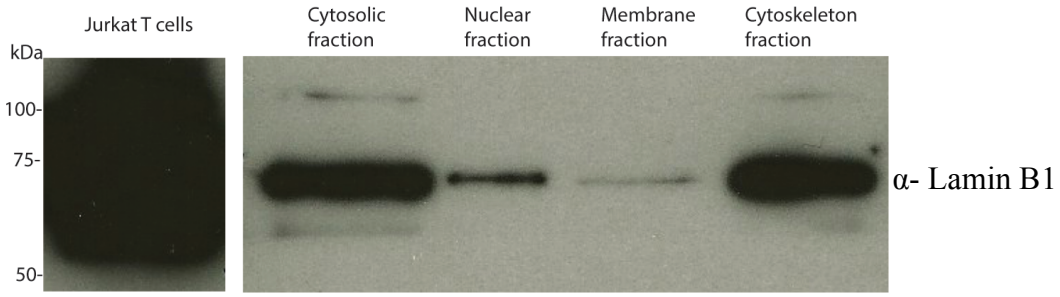

Figure 3.11. Nuclear proteins (lamin B1) were detected in all fractions. Expression of a nuclear protein (lamin B1) in extracted fractions from Jurkat T cells after optimizing the method for cellular fractionation, described above. The protein concentrations were measured, and 1,9 µg total proteins were used in Western blot analysis (the fractions are indicated in figure). Lamin B1 was detected with anti-lamin B1 and HRP-conjugated secondary antibody.

The nuclear proteins were still found in all fractions after optimization, and since the confocal microscopy images (see figure 3.7, 3.8) indicated that CLEC16A (or at least GFP/DDK-tagged CLEC16A) was not likely to be in the nucleus, we decided to discard this fraction. Furthermore, optimization for the membrane fraction was not performed, due to time limit.

Fractionations were performed in Jurkat T cells transfected with plasmids expressing GFP_N-CLEC16A, CLEC16A-GFP_C and CLEC16A-MYC-DDK. In addition, untreated Jurkat T cells were included enabling us to study the localization of endogenously expressed CLEC16A. Prior to fractionation, flow cytometry was performed to confirm protein expression of GFP-tagged CLEC16A proteins. Also, the efficiency of the transfection was measured (figure 3.14).

The concentrations of the proteins in the extracted fractions were measured by Bradford assay. Some of the samples had values that were too low to be determined. Previously (during optimization) we have applied the same amount of proteins on the SDS polyacrylamide gel for the analyses, but since the concentration for some fractions was undetermined, lysate from the same cell count was used instead. For each fraction, duplicates were applied on the gel, where one of the duplicates was used to examine the purity of the fractions with antibodies against housekeeping proteins (figure 3.12) and the other was used to detect the GFP/DDK tagged CLEC16A-protien or endogenous CLEC16A (figure 3.13).

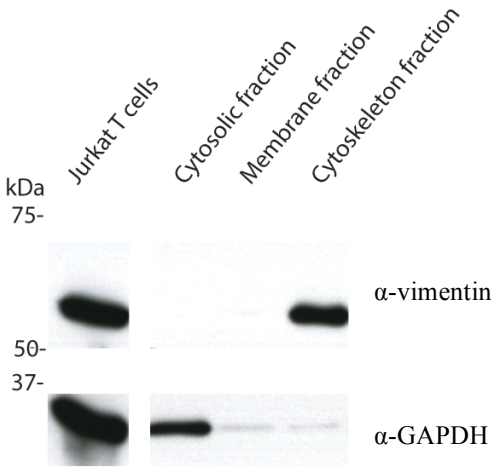

Figure 3.12. Analyses of cell fraction purity. Cellular fractions from 0,4 million cells were analysed on Western blot. Anti-GAPDH (and HRP-conjugated secondary antibody) and anti-vimentin (and HRP-conjugated secondary antibody) were used as subcellular markers for cytosol and cytoskeleton fractions, respectively. The expected band for GAPDH and vimentin are 35 kDa and 54 kDa. One representative membrane out of four is shown.

Unfortunately, when the purity of the fractions was examined, we could not detect the membrane proteins (used anti-EGFR) in any of the fractions except for in the total lysate (data not shown). However, vimentin was observed only in cytosolic fraction, as expected,

and GAPDH was observed mostly in cytosolic fraction, with small amounts expressed in the membrane and the cytoskeleton fraction (figure 3.12).

When investigating in which fraction the GFP/DDK-tagged CLEC16A were located, only GFP_N-CLEC16A and CLEC16A-MYC-DDK were detected on Western blot at the expected size. Both were detected in the cytoskeleton fraction (figure 3.13 A and 3.13 B).

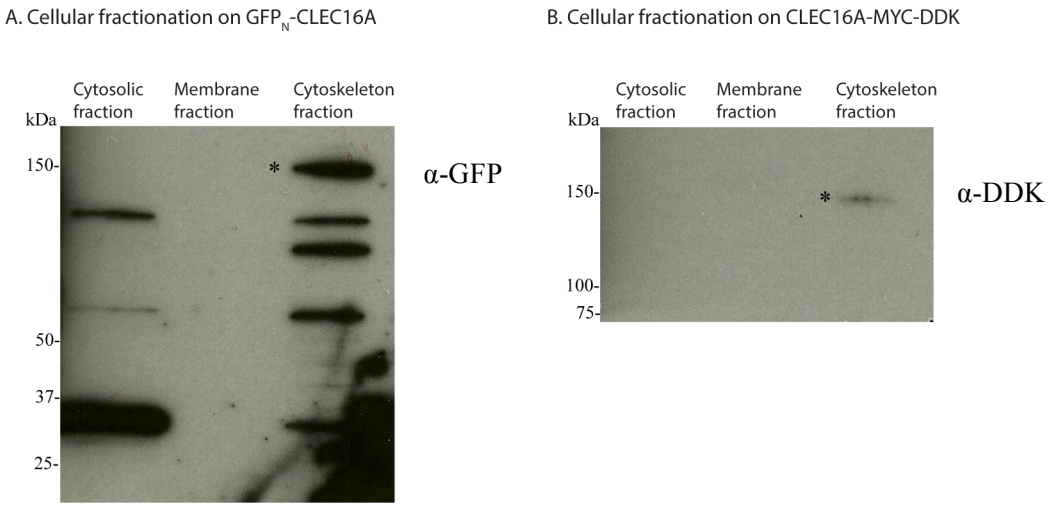

Figure 3.13. CLEC16A-MYC-DDK and GFP_N-CLEC16A were detected in the cytoskeleton fraction. The localization of GFP_N-CLEC16A and CLEC16A-MYC-DDK after performing subcellular fractionation on transfected Jurkat T cells. Fractions indicated corresponding to 0,4 million cells analysed on Western blot. **(A)** anti-GFP (and HRP-conjugated secondary antibody) or **(B)** anti-DDK (and HRP-conjugated secondary antibody) were used to detect GFP_N-CLEC16A and CLEC16A-MYC-DDK, respectively. The expected band for GFP_N-CLEC16A and CLEC16A-MYC-DDK are 150 kDa and 130 kDa. Bands of interest are indicated by asterisks (*).

The flow cytometry measurements performed prior to the cellular fractionations showed expression of CLEC16A-GFP_C (figure 3.14). However, it showed higher expression of GFP_N-CLEC16A than CLEC16A-GFP_C, despite that the transfection efficiency was higher for the latter. CLEC16A-GFP_C could not be detected when the fractions were analysed on Western blot. It has earlier shown to be difficult to detect in Western blot analysis with GFP-antibody, even though flow cytometry measurements have showed that the protein was present (figure 3.5).

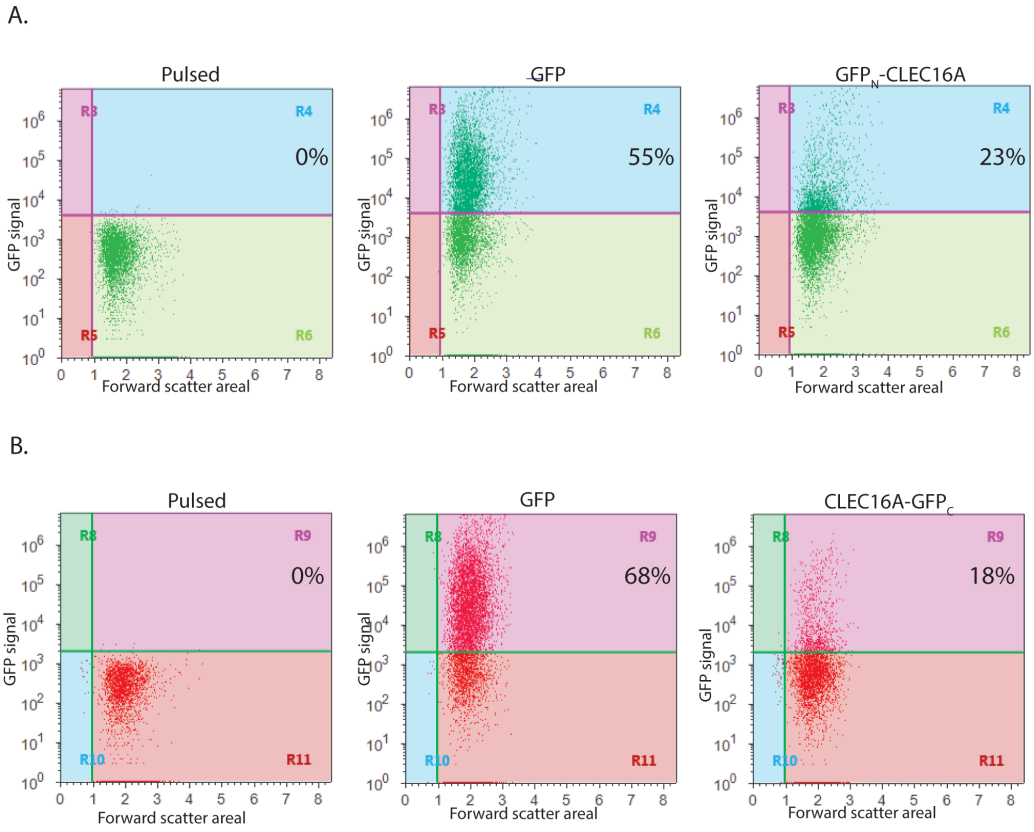

Figure 3.14. Expression of GFP_N-CLEC16A and CLEC16A-GFP_C prior to cellular fractionation of Jurkat T cells transfected with GFP-tagged CLEC16A plasmids. Flow cytometry measurements of the expression of **(A)** GFP_N-CLEC16A and **(B)** CLEC16A-GFP_C. In addition, GFP in pEGFP-N3 (used as measurement for transfection efficiency) is shown for each experiment. Data shown are from single, living cells gated as described in section 2.2.4. Number in upper right corner of each plot corresponds to the percentage of GFP positive cells. Pulsed cells were used as a negative control.

To summarize the cellular fractionation: Cytoskeleton proteins were only located in the cytoskeleton fraction and cytosolic proteins were mostly located in the cytosolic fraction, but with small amounts in both the membrane fraction and the cytoskeleton fraction (figure 3.12). Membrane proteins could not be detected. GFP_N-CLEC16A and CLEC16A-MYC-DDK were localized in the cytoskeleton fraction (figure 3.13), which can mean that they were localized in either the membrane fraction or the cytoskeleton fraction. Endogenous CLEC16A and CLEC16A-GFP_C could not be detected.

3.2.5 The intracellular localization of the tagged CLEC16A proteins

The subcellular localization was further examined with the tagged CLEC16A-proteins. We analysed whether DDK/GFP-tagged CLEC16A was co-localized with the following organelles (with indicated organelle marker); early endosomes (Rab5), late endosomes

(Rab7), recycling endosomes (Rab4a), trans-golgi network (TGN46) and lysosomes (LAMP1), in confocal microscopy. Rab molecules were visualized by transfection of plasmids expressing Rab molecule fused with a fluorescent molecule. Rab5 and Rab4a were fused with mCherry and Rab7 was fused with GFP. To detect lysosomes and trans-golgi network, cells were stained with antibodies for LAMP1 and TGN46, respectively.

Intracellular localization for CLEC16A-MYC-DDK

Jurkat T cells transfected with CLEC16A-MYC-DDK were either co-transfected with the different Rab-constructs (Rab4a-mCherry, Rab5-mCherry, Rab7-GFP) and immunostained with anti-DDK, or immunostained with anti-DDK and anti-TGN46 or anti-DDK and anti-LAMP1. The different samples were analysed by confocal microscopy (see figure 3.15)

CLEC16A-MYC-DDK was partially co-localized with recycling-(Rab4a) endosomes (middle row, Figure 3.15). Additionally it was partially co-localized with early-(Rab5) endosomes in the perinuclear area (row number two, figure 3.15). No co-localization was observed with Rab7, TGN46 or LAMP1.

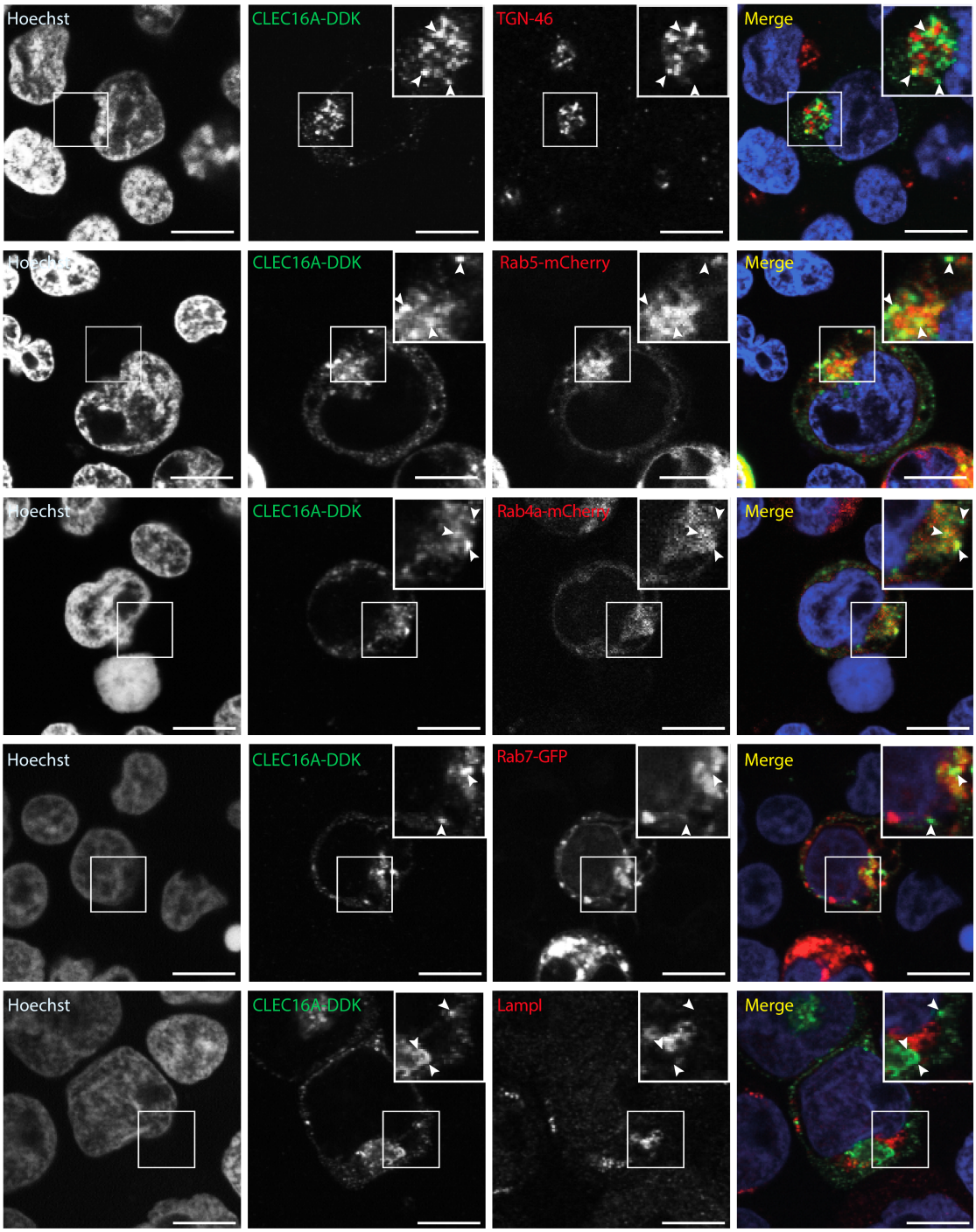

Figure 3.15. CLEC16A-MYC-DDK was partially co-localized with Rab4a and Rab5. Jurkat T cells transfected with CLEC16A-MYC-DDK and the Rab-construct indicated in figure. The cells were stained with Hoechst, mounted on poly-L-lysine coated glass slides, fixed and permeabilized before immunostaining with anti-DDK and Alexa647-conjugated secondary antibody or Alexa555-conjugated secondary antibody (only for Rab7-GFP). Jurkat T cells overexpressing only CLEC16A-MYC-DDK were treated as above, but immunostained with anti-DDK and Alexa555-conjugated secondary antibody in addition to anti-TGN46 or anti-LAMP1 and Alexa647-conjugated secondary antibody. The samples were analysed by confocal microscopy. Indicated areas are enlarged with arrowheads pointing at strong signals at the same place in all images. In the merged image; Hoechst is indicated in blue, CLEC16A-MYC-DDK in green, the organelle marker indicated in red and co-localized parts in yellow. Scale bars are 10 µm. One representative cell is shown from one experiment

for the cellular markers TGN46 and Rab7, two independent experiments for the cellular markers Rab5 and LAMP1 and three independent experiments for the cellular marker Rab4a.

Intracellular localization of CLEC16A-GFP$_C$

Jurkat T cells transfected with CLEC16A-GFP$_C$ were either co-transfected with Rab-constructs (Rab4a and Rab5) or immunostained with anti-TGN46 or anti-LAMP1. The different samples were analysed on confocal microscopy (see figure 3.16). The late endosomal-marker Rab7 was fused with GFP and could not be analysed with GFP-tagged CLEC16A.

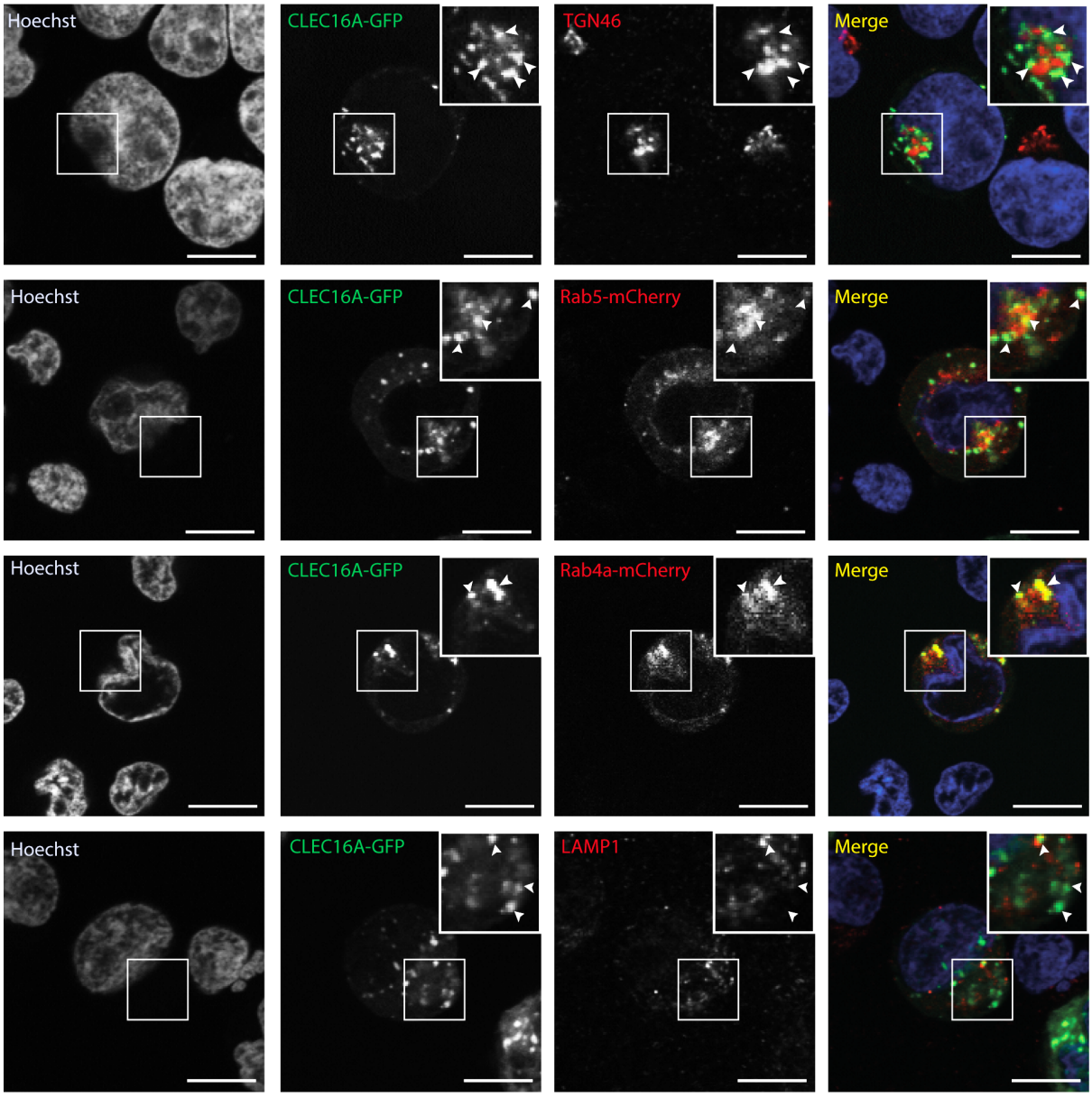

Figure 3.16. CLEC16A-GFP$_C$ showed co-localization with Rab4a and partial co-localization with Rab5. Jurkat T cells transfected with CLEC16A-GFP$_C$ and the Rab-constructs indicated in the figure, were stained with Hoechst, mounted on poly-L-lysine coated glass slides and fixed. Jurkat T

cells expressing only CLEC16A-GFP_C were treated as above but also permeabilized and immunostained with anti-TGN46 or anti-LAMP1 and Alexa647-conjugated secondary antibody. The samples were analysed by confocal microscopy. Indicated areas are enlarged with arrowheads pointing at the strong signals at the same place in all the images. In the merged image; Hoechst is indicated in blue, CLEC16A-GFP_C in green, the organelle marker is indicated in red and co-localized parts in yellow. Scale bars are10 μm. One representative cell is shown from one experiment for the cellular marker TGN46, two independent experiments for the cellular markers LAMP1 and Rab5, and three experiments with the cellular marker Rab4a.

Based on the confocal analysis of CLEC16A-GFP_C with the different organelle markers, CLEC16A-GFP_C showed co-localization with Rab4a-endosomes (row three, figure 3.16). In addition, CLEC16A-GFP_C seemed, like CLEC16A-MYC-DDK, to be partially co-localized with Rab5-endosomes in the perinucleuar area (row two, figure 3.16). No co-localization with TGN46 or LAMP1 was obtained.

Intracellular localization for GFP_N-CLEC16A

Jurkat T cells transfected with GFP_N-CLEC16A were either co-transfected with Rab-constructs (Rab4a and Rab5) or immunostained with anti-TGN46 or anti-LAMP1. The different samples were analysed by confocal microscopy (figure 3.17). As for CLEC16A-GFP_C, the late endosomal marker Rab7 could not be examined since it is fused with GFP.

Based on the confocal analyses for GFP_N-CLEC16A with the different organelle markers, GFP_N-CLEC16A was partially co-localized in Rab4a-positive endosomes (row three, figure 3.17). No co-localization was obtained with the markers Rab5, TGN46 or LAMP1.

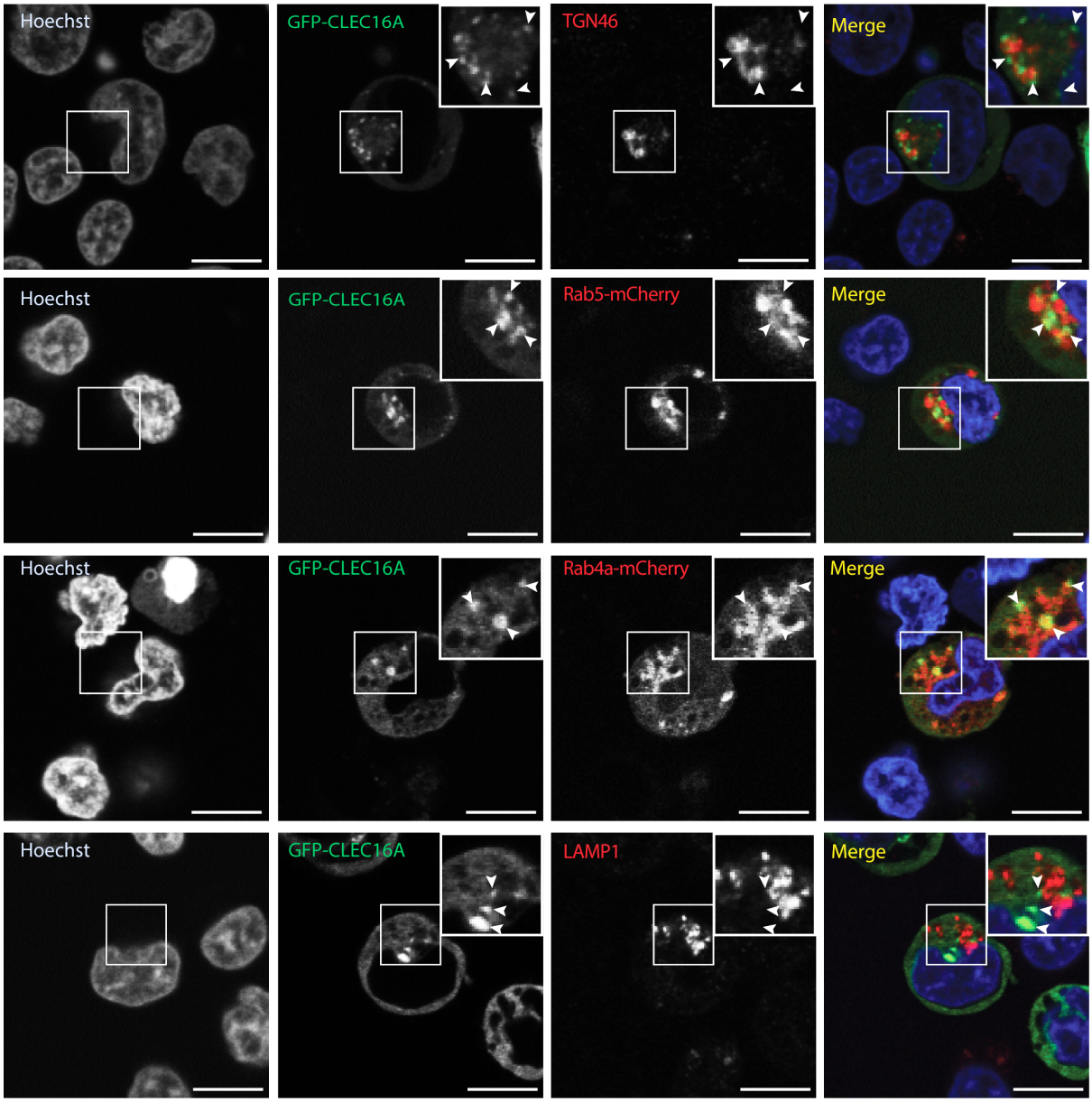

Figure 3.17. GFP_N-CLEC16A showed partly co-localization with Rab4a. Jurkat T cells were co-transfected with GFP_N-CLEC16A and the Rab-constructs indicated in the figure. The cells were stained with Hoechst, mounted on poly-L-lysine coated glass slides and fixed. Jurkat T cells transfected with only GFP_N-CLEC16A were treated as above, but also permeabilized and immunostained with anti-TGN46 or anti-LAMP1 and Alexa647-conjugated secondary antibody. The samples were analysed by confocal microscopy. Indicated areas are enlarged with arrowheads pointing at strong signals at the same place in all the images. In the merged image; Hoechst is indicated in blue, GFP_N-CLEC16A in green, the organelle marker is indicated in red and co-localized parts in yellow. Scale bars are 10 µm. One representative cell is shown from one experiment.

To summarize; CLEC16A-GFP_C was located in Rab4a-positive endosomes, meanwhile CLEC16A-MYC-DDK and GFP_N-CLEC16A were partially co-localized with the marker Rab4a. Additionally, CLEC16A-GFP_C as well as CLEC16A-MYC-DDK showed partially co-localization with the marker Rab5.

3.3 Distribution of endosomes

To investigate if CLEC16A has an effect on the distribution of endosomes in Jurkat T cells, cells were transfected with either CLEC16A-MYC-DDK or CLEC16A-siRNA and the corresponding controls, pCMV6-empty or control siRNA respectively. The markers that I managed to analyse to complete this thesis were the Rab4a (recycling endosomes), Rab5 (early endosomes) and LAMP1 (lysosomes). The samples were analysed by confocal microscopy and in parallel with Image Stream analyses (done by PhD student Ingvild Sørum Leikfoss). Confocal microscopy analyses generate high-resolution images, which will give a more detailed view of the cells compared to Image Stream. However, Image Stream is a powerful tool combining quantitative image analysis with flow cytometry that can verify and quantify statistically the results observed by confocal microscopy.

CLEC16A-MYC-DDK, CLEC16A-specific siRNA and controls, were either co-transfected with the Rab-construct or immunostained with anti-LAMP1. In all experiments, the transfection efficiency was measured by flow cytometry on Jurkat T cells transfected with pEGFP-N3. The knockdown and overexpression of CLEC16A was confirmed by Western blot or real-time quantitative PCR (qPCR). These verifications were done by PhD student Ingvild Sørum Leikfoss, whereas the sample preparation on glass slides for confocal microscopy was done by me.

3.3.1 Distribution of Rab4a-endosomes

The possible effect of CLEC16A on the distribution of Rab4a was investigated in Jurkat T cells. The cells were transfected with either CLEC16A-MYC-DDK or CLEC16A siRNA and the corresponding controls.

No obvious differences were detected in the Rab4a-positive endosomal distribution in Jurkat T cells overexpressing CLEC16A or in cells where CLEC16A were knocked down compared to their respective control (Figure 3.18). The Rab4a-marker used was expressed with a mCherry, which gave blurry images lacking clear cell structures, making it difficult to detect differences in endosomal distribution. However, the cells seemed to be larger for Jurkat T cells overexpressing CLEC16A compared to the other cells (see figure 3.18 B).

Preliminary results from Image Stream shows no obvious differences regarding the Rab4a-endosomal distribution in knocked down- or overexpressed CLEC16A Jurkat T cells.

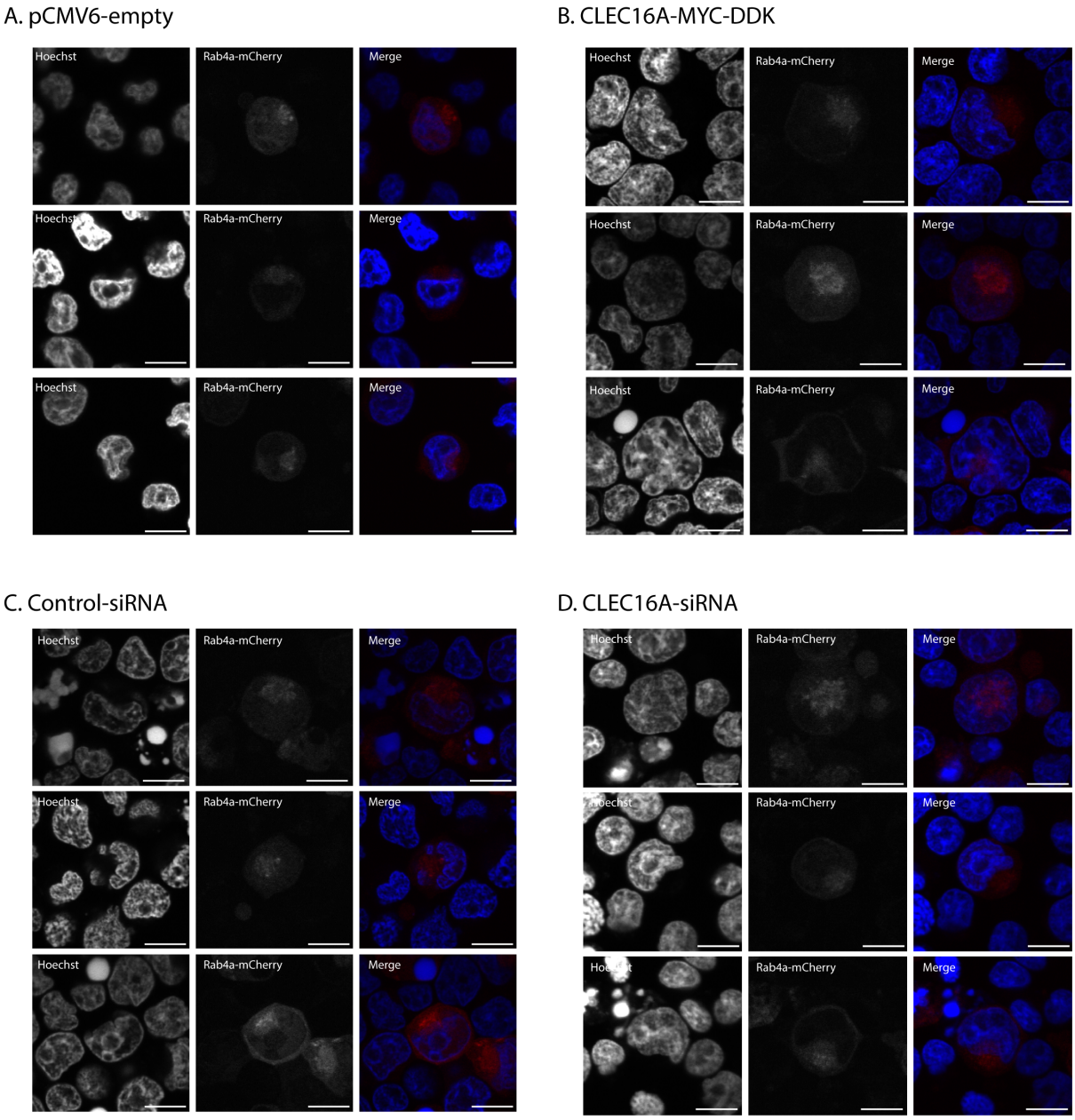

Figure 3.18. CLEC16A did not seem to affect the distribution of Rab4a-endosomes in Jurkat T cells. Jurkat T cells transfected with Rab4a-mCherry and **(A)** pCMV6-empty, **(B)** CLEC16A-MYC-DDK, **(C)** control siRNA or **(D)** CLEC16A-siRNA were stained with Hoechst, mounted on poly-L-lysine coated glass slides and fixed. The samples were analysed by confocal microscopy. In the merged image; Hoechst is indicated in blue and Rab4a-mCherry in red. Scale bars are 10 µm. Data shows three representative cells from each group from one experiment performed.

3.3.2 Distribution of Rab5-endosomes

To investigate the distribution of Rab5 endosomes, Jurkat T cells were transfected with either CLEC16A-MYC-DDK or CLEC16A siRNA and the corresponding controls. The samples were analysed by confocal microscopy (see figure 3.19).

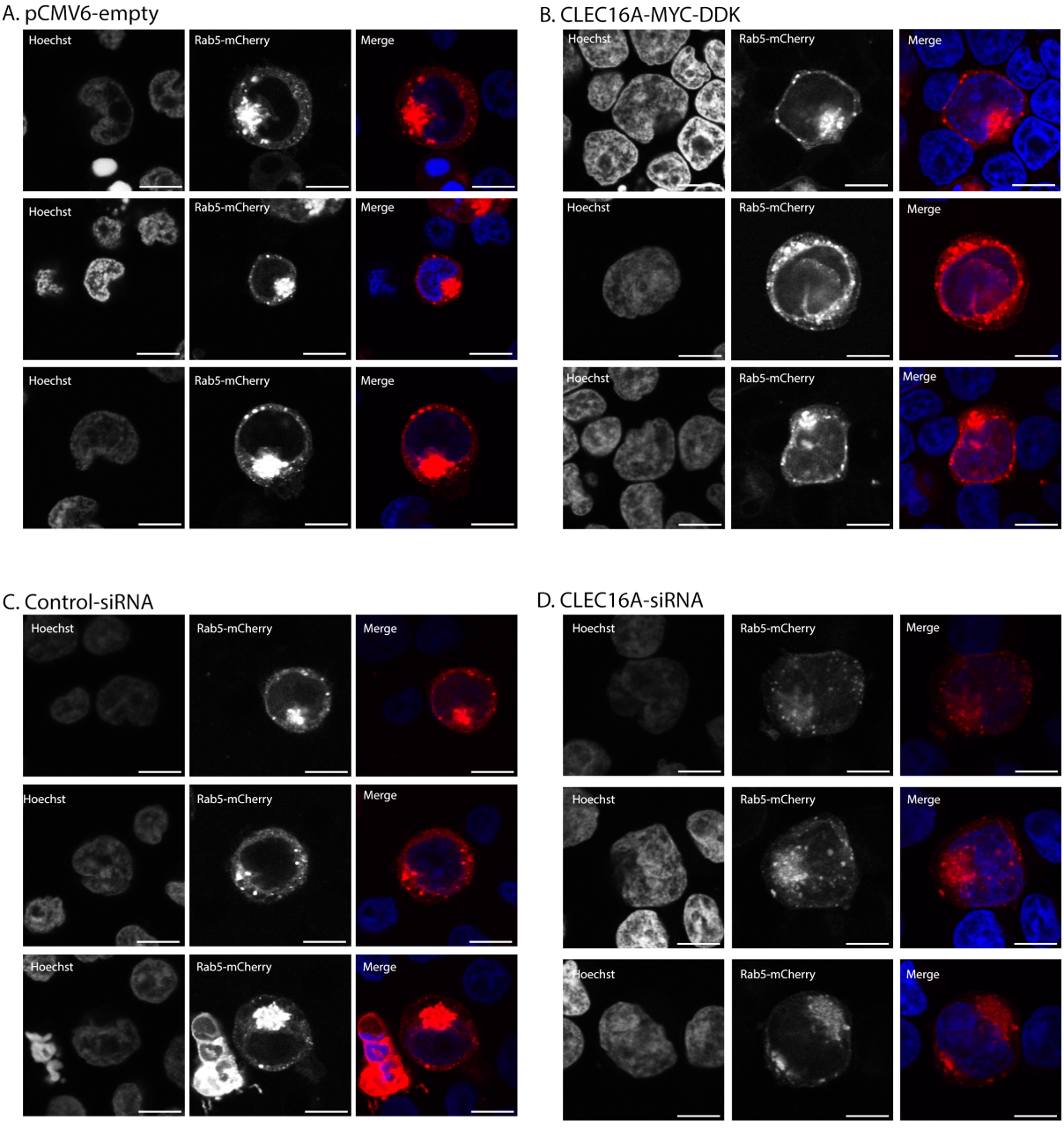

Figure 3.19. CLEC16A knockdown caused an increased number Rab5-endosomes in Jurkat T cells, which were more scattered throughout the interior of the cell. Jurkat T cells transfected with Rab5-mCherry and **(A)** pCMV6-empty, **(B)** CLEC16A-MYC-DDK, **(C)** control siRNA or **(D)** CLEC16A-siRNA**,** were stained with Hoechst, mounted on poly-L-lysine coated glass slides and fixed. The samples were analysed by confocal microscopy. In the merged image; Hoechst is indicated in blue and Rab5-mCherry in red. Scale bars are 10 µm. Three representative cells from each group from one experiment performed.

Jurkat T cells overexpressing CLEC16A resulted in evenly distributed Rab5-positive endosomes in close proximity to the plasma membrane (figure 3.19 B). For the corresponding control (see figure 3.19 A), the Rab5-positive endosomes were located in one intense spot in perinuclear area or distributed similar to the overexpressed cells. For the cells where CLEC16A was knocked down (see figure 3.19 D), there seemed to be an increased number of Rab5-positive endosomes compared to the corresponding control (see figure 3.19 C). The Rab5-positive endosomes seemed to be located in a larger area in the CLEC16A knocked down cells compared to the intense spot in the control. The knocked down CLEC16A cells also had an over-all weaker mCherry signal. Additionally, Jurkat T cells with CLEC16A overexpression were larger in size (same as for Rab4a, section 3.3.1) and less spherical compared to the other groups.

Image Stream analysis has not yet detected any major differences regarding the distribution of Rab5-positive endosomes in overexpression or knockdown of CLEC16A compared to controls (in Jurkat T cells). The Image stream analysis performed has been focusing on the distribution of the most intense mCherry signal in the cells relative to the plasma membrane and compared it between the different cell populations.

3.3.3 Distribution of LAMP1-endosomes

In this experiment, the cells transfected with CLEC16A-MYC-DDK was not included due to infection of the cell culture. Therefore it was only possible to analyse LAMP1 distribution in CLEC16A-specific siRNA transfected Jurkat T cells and corresponding control cells. Transfected Jurkat T cells were immunostained with anti-LAMP1 and analysed by confocal microscopy (figure 3.20).

Decreased amount of CLEC16A did not seem to influence the distribution of LAMP1-positive lysosomes. However, there were some indications that LAMP1 expression was higher in cells with CLEC16A knocked down.

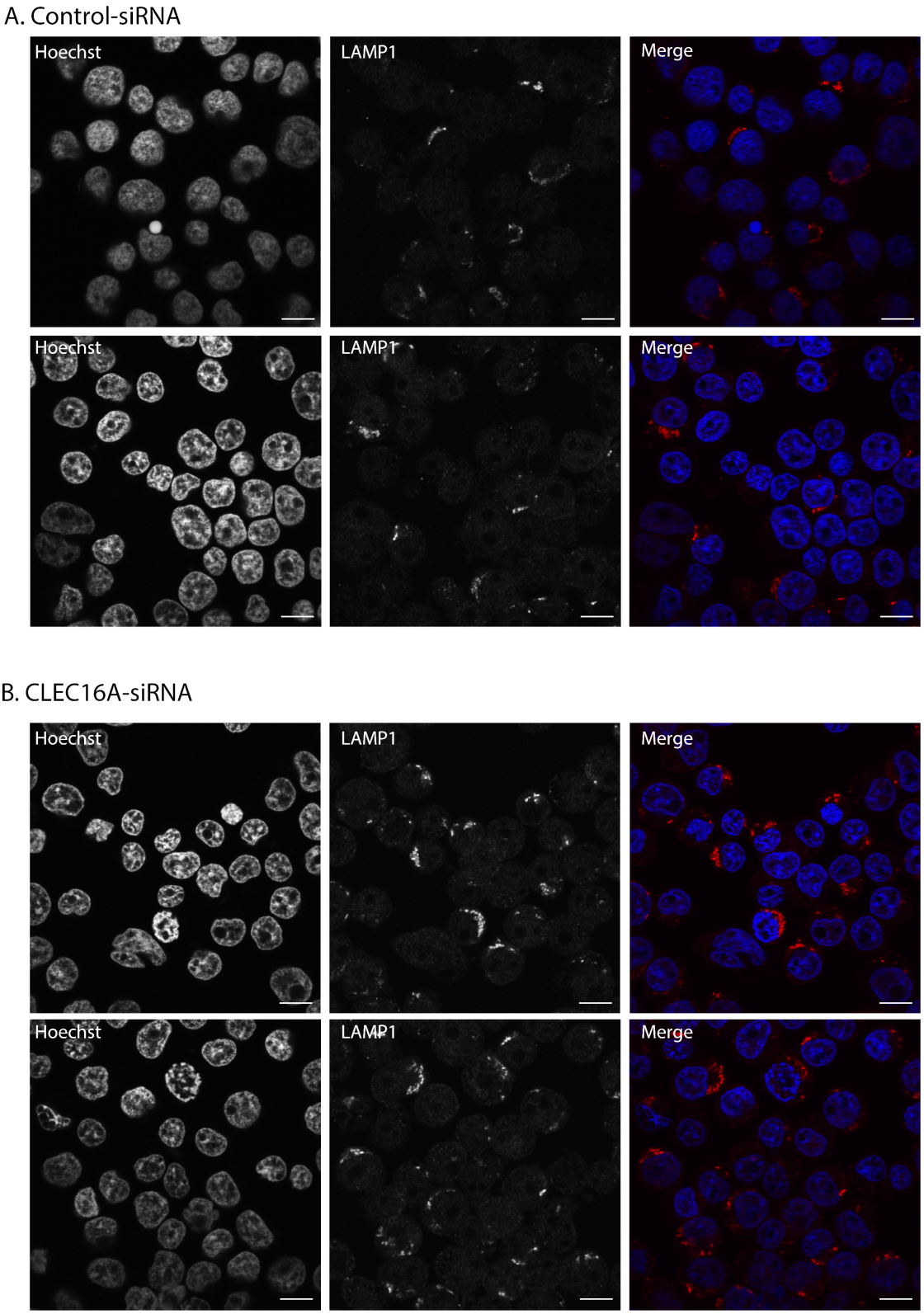

Figure 3.20. CLEC16A did not affect the distribution of LAMP1 lysosomes in Jurkat T cells. Jurkat T cells transfected with **(A)** control-siRNA or **(B)** CLEC16A-siRNA**,** were stained with Hoechst and mounted on poly-L-lysine coated glass slides, fixed and permeabilized before immunostaining with anti-LAMP1 and Alexa647-conjugated antibody. The samples were analysed by confocal microscopy. In the merged image; Hoechst is indicated in blue and LAMP1 in red. Data shows two representative sections from each sample, from one experiment performed. Scale bars are 10 μm.

4 Discussion

This thesis has two main aims (described in section 1.5) and the discussion will focus on the results regarding them. The background for this thesis is that the *CLEC16A* gene has been identified to associate with MS and by finding the subcellular localization of the protein encoded by this MS-associated gene, it will shed light on potential functions.

4.1 Comparison of the differently tagged CLEC16A proteins

Proteins are often dependent on sorting signals or specific interactions with other proteins for correct localization in the cells and tissues. By adding a tag to a protein the sorting processes can be disrupted and wrong localization may be obtained.

4.1.1 Endogenous staining

Since protein tags might affect the subcellular localization of proteins, the most accurate way to find the localization is by analysing the endogenous protein. When examining in confocal microscopy with immunostaining, the challenge is to find a working antibody for this purpose. The antibody needs to be both specific and sensitive. In the test we performed (figure 3.9) two antibodies were tested (Millipore, abcam). One of the antibodies (Millipore) did bind to CLEC16A when GFP-tagged CLEC16A was overexpressed in Jurkat T cells, as immunostaining signals from the CLEC16A antibody co-localized with the GFP signal (figure 3.9 A). However, the antibody was probably not sensitive enough to bind endogenous CLEC16A in Jurkat T cells, since no reduction could be detected when comparing staining in cells where CLEC16A was knocked down with control cells (see figure 3.9 B and C). The signals detected for the antibody are probably noise from high laser intensity and high voltage settings.

4.1.2 Comparison of localization of GFP and DDK-tagged CLEC16A

For the purpose of finding the localization of CLEC16A, N- and C-terminally GFP-tagged CLEC16A plasmids were created (section 3.1). The localization of both GFP-tagged CLEC16A proteins was compared to the localization of a C-terminally MYC-DDK-tagged CLEC16A (available in the lab). Since the MYC-DDK-tag is considerably smaller than the GFP tag, we would think that CLEC16A with the MYC-DDK-tag would localize more similar to endogenous CLEC16A compared to CLEC16A with a GFP-tag. The C-terminally

GFP-tagged CLEC16A did show partial co-localization with the MYC-DDK-tagged CLEC16A (figure 3.7). However, higher degree of co-localization was obtained between CLEC16A-MYC-DDK and N-terminally GFP-tagged CLEC16A (figure 3.8). The C-terminal side of CLEC16A is predicted to be unstructured (section 1.3.2), which means that it probably can move quite freely and might be important for interactions with other proteins that can influence its subcellular localization. These interactions can be disturbed when adding a large GFP tag. Since endogenous CLEC16A could not be detected in the fractions obtained from cellular fractionation, we could not compare the localization with the localizations from the tagged CLEC16A. However, since CLEC16A-MYC-DDK and GFP_N-CLEC16A is co-localized, it is more likely that they show the right localization for endogenous CLEC16A then CLEC16A-GFP_C.

When the expression of the N-terminally GFP-tagged CLEC16A in Jurkat T cells was investigated, the proteins were detected on Western blot with an antibody against GFP. In addition to the expected signal, there was one more protein detected by the GFP-antibody (figure 3.4). The signal corresponds to a protein slightly larger than GFP. This has been detected twice on Western blot, but the protein-lysate was from the same cells. The extra band can be an artefact from any of the treatments (transfection, making whole cell lysates or Western blot) prior to detection, and it is too early to conclude if this occurs routinely when overexpressing GFP_N-CLEC16A in Jurkat T cells. However, we must take into consideration that the GFP signal obtained in confocal microscopy and Image Stream for N-terminally GFP-tagged CLEC16A can be obtained from any of these two proteins. It can explain why a diffuse signal throughout the cell is detected when GFP_N-CLEC16A is expressed. If the band detected on Western blot is a protein obtained due to cleavage of the GFP_N-CLEC16A protein, the cause of the cleavage can be that the link created between GFP and CLEC16A is instable and may be processed by proteases, or if the cleavage is in the CLEC16A protein it could be a signal sequence, which is cleaved in the process. To further understand this, more studies are needed.

4.1 Do CLEC16A have different localization in different cells?

During the work on this thesis, two new studies have been published regarding the function of CLEC16A (68, 69). In those papers, CLEC16A shows various localizations in different cell-types, indicating that CLEC16A localization is tissue-dependent. It can also be dependent on which isoform of CLEC16A that has been studied, and that the various CLEC16A-isoforms (figure 1.7) are localized differently. Earlier work has shown that CLEC16A-isoform 1 (24 exons) is localized in ER in human erythroleukemia cell-line (K562 cells) (69), CLEC16A-isoform 2 (21 exons) is localized in lysosome/late endosome in pancreatic β-cells (Min6 β) (68) and Ema (CLEC16A ortholouge in *Drosophila melanogaster*) has been shown to localize in late endosomes in *Drosophila melanogaster* garland cells (71) and in Golgi in *Drosophila melanogaster* fat body cells (70). Here we identify CLEC16A-isoform 1 to be partially localized in Rab4a recycling endosomes in Jurkat T cells (figure 3.15, 3.16, 3.17). A lower degree of co-localization is also observed between CLEC16A and Rab5 (early endosome) however, no co-localization with Rab7 (late endosome), LAMP1 (lysosome) or TGN46 (Golgi) was observed in Jurkat T cells.

Furthermore, earlier studies have shown that CLEC16A is a membrane-associated protein, since it was detected in cellular fractions from both cytosol and membrane (68). When we performed cellular fractionation, we could exclude presence of CLEC16A in the cytosol in Jurkat T cells (figure 3.13), however, due to technical problems we were not able to identify whether CLEC16A was present in the membrane fraction also in T cells.

This together indicates that CLEC16A can be differently localized in various cells, but it cannot be excluded that the differences are seen due to overexpression of the proteins, since endogenous staining has not yet been performed in any of the studies. In addition, different CLEC16A isoforms could have different localizations within the cells.

4.2 Do CLEC16A have a role in endosomal trafficking?

Earlier studies have shown that CLEC16A has a role in endosomal trafficking and autophagy (68, 70, 71). We find that CLEC16A is partially localized in Rab4a recycling endosomes in Jurkat T cells, and when CLEC16A is knocked down the cells have characteristics indicating endosomal trafficking defects, as observed accumulations of early endosomes and lysosomes (figure 3.19 and 3.20).

4.2.1 CLEC16A is partially localized in Rab4a-recycling endosomes

To reveal the subcellular localization of CLEC16A, all three DDK/GFP-tagged CLEC16A proteins were analysed with intracellular markers in confocal microscopy (see figure 3.15, 3.16, 3.17). They all are partially co-localized with Rab4a-recycling endosome, CLEC16A-GFP_C more than the two other CLEC16A tagged proteins (figure 3.15, 3.16, 3.17). The Rab4a-positive recycling endosomes are thought to be responsible for rapid recycling between early endosomes (Rab5-positive) and the plasma membrane (11). Since CLEC16A is not detected on the plasma membrane, it is more likely that CLEC16A is resident in those endosomes than transported by them. The proteins that utilize this pathway are often cell surface receptors, like the transferrin receptor and TCR (14), but also tyrosine kinases, integrins (13) among others.

4.2.2 Do CLEC16A have a role in rapid recycling?

Previous studies have shown that Rab4-endosomal recycling is decreased in Rab4 mutant HeLa cells, leading to accumulation of early endosomes (Rab5-positive) in the perinuclear area (75). As in the Rab4 mutant cells, we observed an increased amount of Rab5 endosomes in CLEC16A siRNA transfected cells (see figure 3.19 D). This may indicate that CLEC16A has a role in the rapid recycling between Rab5 endosomes and the plasma membrane. A route that receptors like TCR is known to use (14) (described further in section 1.1.2).

An earlier CLEC16A study has shown that when CLEC16A is knocked down in B cells, there was no effect on the B cell´s ability to activate T cells, indicating that the MHC class II presentation was not dependent of CLEC16A in B cells (69). In contrast, a lower expression of HLA-II presented on the plasma membrane in monocyte derived dendritic cells has been observed when CLEC16A is knocked down compared to control (personal communication

Luijn) (more details in section 1.4.3). It remains to be studied whether the decreased HLA-II presentation in dendritic cells is affecting the T cell activation. In addition it remains to be analysed, whether the effect of CLEC16A knocked down in T cells has the same effect on TCR expression on the cell surface on T cells, as HLA-II in dendritic cells. A PhD student in our lab has analysed expression of T cell activation markers in Jurkat T cells, however, preliminary data does not indicate a change in their cell surface expression when CLEC16A is knocked down. The activation is performed with ionomycin and PMA, which do not require interactions with the TCR. There may be an effect on cell surface expression of activation markers if the T cell is activated through the TCR instead.

4.2.3 Do CLEC16A knockdown cause failure in endolysosomal trafficking?

In addition to the accumulated Rab5-endosomes (see figure 3.19 D) described above, there were indications that LAMP1 lysosomes accumulated in CLEC16A-knocked down cells (figure 3.20 B), which could indicate a trafficking problem in the endolysosomal trafficking. Ema mutant cells have shown defects in regulating the trafficking of cell membrane receptors, as has been observed for the bone morphogenetic protein signalling pathway receptors. In Ema mutant cells, the late endosomes can not be converted into degradative lysosomes (71). Additionally, for CLEC16A-knock out pancreatic β cells, defects in endolysosomal trafficking has been shown to have implications in autophagy, when autophagosomes not are able to fuse with lysosomes (68). If the result obtained from this thesis regarding the lysosomal accumulation is reproducible, CLEC16A could have a role in autophagy in immune cells as well as in pancreatic β cells as shown by (68).

As stated in the result part, preliminary results from Image Stream analyses have not identified any major differences in the endosomal distribution of the markers tested. However, with the more detailed images obtained by confocal microscopy, the analyses should be more specific against the accumulation of small Rab5 endosomes and the LAMP1-lysosome accumulation, instead of only analysing the distribution of the most intense spots during Image Stream analyses.

4.3 Methodological considerations

In this thesis, confocal microscopy has been a central part and Image Stream is going to be used to quantify the result seen in confocal microscopy. The considerations about the methods used are discussed here.

4.3.1 Overexpression of proteins

In the current study, we are analysing subcellular localization and endosomal distribution of proteins that mostly are overexpressed, i.e. for CLEC16A as well as for all markers, except LAMP1 and TGN46. By overexpressing proteins, they will not necessarily behave as endogenous proteins do and the result is more an indication of how it can be biological relevant. The best way for study a protein is when using antibodies, with high specificity and sensitivity, to be able to detect the endogenous protein.

4.3.2 Transient transfections

In this thesis, transient transfections are performed to introduce exogenous DNA/RNA. When performing transient transfection, all cells in a population are not being transfected. Additionally the transfected cells do express highly variable levels of the exogenous DNA. A more accurate way of analysing cells with introduced DNA/RNA, is to create stable cell-lines. All cells in a population will then contain the DNA of interest and express it, however, the levels are still probably higher than the endogenous levels.

4.3.3 Use of cell line

The cell model used to investigate CLEC16A in this thesis is the Jurkat TAg T cell line. This cell line is established from Jurkat E6.1, which is derived from peripheral blood of a patient with T cell leukemia (76) (more detail in section 2.2). Cell lines are very convenient to work with since the cells grow rapidly and the same cell batch can be used through several passages. However, it has some limitations. Since the cells are affected by cancer, the cells are not behaving in the same way, as primary T cells would do. The results need to be confirmed in primary cells.

4.4 Summary of findings

The aims for this thesis were to investigate the subcellular localization for CLEC16A, and to evaluate its role in endosomal distribution, both examined in T cells.

The main findings were:

4.4.1 Localization of CLEC16A:

Confocal microscopy shows that CLEC16A is partially co-localized with Rab4a, a marker for endosomes that rapidly recycle from early endosomes to the plasma membrane.

4.4.2 The role of CLEC16A in endosome distribution:

Confocal microscopy data shows accumulation of early endosomes and lysosomes in Jurkat T cells where CLEC16A has been knocked down, indicating a defect in endosomal trafficking.

The early endosomal accumulation observed in CLEC16A knocked down T cells together with the CLEC16A localization in recycling endosomes, indicate that CLEC16A have a role in recycling from early endosomes.

In addition, the lysosomal accumulation indicates that CLEC16A have a role in endolysosomal pathway, which has been observed for both Ema and CLEC16A earlier.

5 Future perspective

We are currently in the starting phase of revealing the function of CLEC16A and its possible effect on MS-disease, and still, little is known about the function of this protein. In a short-term perspective the localization studies and endosomal studies should be completed. In a longer perspective, the implications for these endosomal/lysosomal defects in CLEC16A knocked down T cells should be functionally followed up and identification of CLEC16A interaction partners could be mapped to identify pathways it is involved in. This will further identify underlying mechanisms in MS development.

5.1 Short term perspective

During the course of this thesis, I also made samples for Image stream analyses. A PhD student in the lab is now in the process of analysing these samples, and these data will quantify the degree of co-localization observed in the current thesis. In addition, endogenous staining of CLEC16A and the markers detected by overexpression (Rab4a, Rab5 and Rab7) should be performed to exclude that the co-localizations observed is artefacts from overexpressing the components analysed. For the endosomal distribution studies, the analyses of Image Stream data (already collected) should be guided by the conclusion from this study as explained in section 4.2.3.

5.2 Long term perspective

In a longer perspective the function of CLEC16A should be further evaluated both in context of autophagy and receptor trafficking. In addition, the interaction partners for CLEC16A and pathways they are involved in should be mapped to further find the underlying mechanisms for T cell activation and thereby MS development.

5.2.1 T cell activation and receptor trafficking

As discussed (in section 4.2) there are several lines of evidence indicating that CLEC16A is involved in receptor trafficking. This should be further evaluated for TCRs in T cells, to investigate whether CLEC16A is involved both in receptor trafficking and T cell activation. As discussed, one study has shown that CLEC16A is dispensable for MHC-II presentation in B cells (69), but in dendritic cells, CLEC16A seems to be important for HLA-II presentation

to the cell surface (Marvin Luijn, personal communication). The preliminary results from our lab indicate that CLEC16A is not necessary for T cells to become activated and to express activation markers such as CD25 and CD69 when being activated through PMA and ionomycin (Leikfoss, Berge unpublished). However, it remains to be investigated whether TCR expression is CLEC16A-dependent, and further if it affects T cell activation downstream of the TCR, for instance by using CD3/CD28 beads. A further investigation regarding the role of CLEC16A in TCR recycling, and possible T cell activation in CLEC16A-knockdown and overexpressed T cells would be of interest to study.

5.2.2 CLEC16A in autophagy

One cellular process involving membrane trafficking is autophagy, where defects can have disturbing effects on the cell. Earlier, it has been shown that when inducing autophagy in cells where CLEC16A is knocked out, the auotophagosomes are not being degraded (68). This indicates that the autophagosomes are not able to fuse with lysosomes. We observed increased expression of LAMP1 in CLEC16A knocked down cells (figure 3.20). A similar phenotype has earlier been observed in Ema-mutant cells and CLEC16A-knock-out cells. Ema affects the endosomal maturation between late endosome and lysosome (71), whereas CLEC16A affects the fusion between the autophoagosome and lysosome (68). In immune cells it would be interesting to further examine whether CLEC16A siRNA transfected cells display a defect in autophagy as has been observed for CLEC16A knockout in Min6 β cells. We did an attempt to examine this in T cells by staining the autophagosomes (anti-LC3) and lysosomes (LAMP1) to investigate whether there were any differences between controls and CLEC16A knocked down cells. However, the cells, in which autophagy was induced (by serum starvation) did not attach to the poly-L-lysine coated slides and could not be further analysed.

5.2.3 Structural mapping of CLEC16A and identification of protein interaction partners

To understand the role of CLEC16A-structural domains, different constructs expressing truncated or mutated version of CLEC16A can be generated. The phenotype can be investigated in transfected cells to find which structural domains are important to maintain the phenotype of wild-type CLEC16A and to identify the domains important for subcellular localization. In a longer perspective, the interaction partners of CLEC16A should further be

identified to better understand the pathways CLEC16A is involved in. Furthermore, it would be interesting to evaluate whether CLEC16A interacts with proteins encoded by other MS-associated genes. This opens the possibility for identifying underlying mechanisms in MS development.

References

1. Bretscher P, Cohn M. A theory of self-nonself discrimination. Science (New York, NY). 1970 Sep 11;169(3950):1042-9. PubMed PMID: 4194660. Epub 1970/09/11. eng.

2. Bretscher PA. A two-step, two-signal model for the primary activation of precursor helper T cells. Proceedings of the National Academy of Sciences of the United States of America. 1999 Jan 5;96(1):185-90. PubMed PMID: 9874793. Pubmed Central PMCID: PMC15114. Epub 1999/01/06. eng.

3. Chitnis T. The role of CD4 T cells in the pathogenesis of multiple sclerosis. International review of neurobiology. 2007;79:43-72. PubMed PMID: 17531837. Epub 2007/05/29. eng.

4. Gleeson PA. The role of endosomes in innate and adaptive immunity. Seminars in cell & developmental biology. 2014 Jul;31:64-72. PubMed PMID: 24631355. Epub 2014/03/19. eng.

5. Stenmark H. Rab GTPases as coordinators of vesicle traffic. Nature reviews Molecular cell biology. 2009 Aug;10(8):513-25. PubMed PMID: 19603039. Epub 2009/07/16. eng.

6. Scita G, Di Fiore PP. The endocytic matrix. Nature. 2010 Jan 28;463(7280):464-73. PubMed PMID: 20110990. Epub 2010/01/30. eng.

7. Zerial M, McBride H. Rab proteins as membrane organizers. Nature reviews Molecular cell biology. 2001 Feb;2(2):107-17. PubMed PMID: 11252952. Epub 2001/03/17. eng.

8. Sorkin A, von Zastrow M. Endocytosis and signalling: intertwining molecular networks. Nature reviews Molecular cell biology. 2009 Sep;10(9):609-22. PubMed PMID: 19696798. Pubmed Central PMCID: PMC2895425. Epub 2009/08/22. eng.

9. Huotari J, Helenius A. Endosome maturation. The EMBO journal. 2011 Aug 31;30(17):3481-500. PubMed PMID: 21878991. Pubmed Central PMCID: PMC3181477. Epub 2011/09/01. eng.

10. Mindell JA. Lysosomal acidification mechanisms. Annual review of physiology. 2012;74:69-86. PubMed PMID: 22335796. Epub 2012/02/18. eng.

11. Rzomp KA, Scholtes LD, Briggs BJ, Whittaker GR, Scidmore MA. Rab GTPases are recruited to chlamydial inclusions in both a species-dependent and species-independent manner. Infection and immunity. 2003 Oct;71(10):5855-70. PubMed PMID: 14500507. Pubmed Central PMCID: PMC201052. Epub 2003/09/23. eng.

12. Lazzarino DA, Blier P, Mellman I. The monomeric guanosine triphosphatase rab4 controls an essential step on the pathway of receptor-mediated antigen processing in B cells. The Journal of experimental medicine. 1998 Nov 16;188(10):1769-74. PubMed PMID: 9815254. Pubmed Central PMCID: PMC2212406. Epub 1998/11/17. eng.

13. Wandinger-Ness A, Zerial M. Rab Proteins and the Compartmentalization of the Endosomal System. Cold Spring Harbor perspectives in biology. 2014;6(11). PubMed PMID: 25341920. Epub 2014/10/25. Eng.

14. Finetti F, Patrussi L, Masi G, Onnis A, Galgano D, Lucherini OM, et al. Specific recycling receptors are targeted to the immune synapse by the intraflagellar transport system. Journal of cell science. 2014 May 1;127(Pt 9):1924-37. PubMed PMID: 24554435. Pubmed Central PMCID: PMC4004972. Epub 2014/02/21. eng.

15. Fooksman DR, Vardhana S, Vasiliver-Shamis G, Liese J, Blair DA, Waite J, et al. Functional anatomy of T cell activation and synapse formation. Annual review of immunology. 2010;28:79-105. PubMed PMID: 19968559. Pubmed Central PMCID: PMC2885351. Epub 2009/12/09. eng.

16. Das V, Nal B, Dujeancourt A, Thoulouze MI, Galli T, Roux P, et al. Activation-induced polarized recycling targets T cell antigen receptors to the immunological synapse; involvement of SNARE complexes. Immunity. 2004 May;20(5):577-88. PubMed PMID: 15142526. Epub 2004/05/15. eng.

17. Liu H, Rhodes M, Wiest DL, Vignali DA. On the dynamics of TCR:CD3 complex cell surface expression and downmodulation. Immunity. 2000 Nov;13(5):665-75. PubMed PMID: 11114379. Epub 2000/12/15. eng.

18. Finetti F, Onnis A, Baldari CT. Regulation of vesicular traffic at the T cell immune synapse: lessons from the primary cilium. Traffic (Copenhagen, Denmark). 2014 Nov 13. PubMed PMID: 25393976. Epub 2014/11/14. Eng.

19. Benzing C, Rossy J, Gaus K. Do signalling endosomes play a role in T cell activation? The FEBS journal. 2013 Nov;280(21):5164-76. PubMed PMID: 23834225. Epub 2013/07/10. eng.

20. D'Oro U, Munitic I, Chacko G, Karpova T, McNally J, Ashwell JD. Regulation of constitutive TCR internalization by the zeta-chain. Journal of immunology (Baltimore, Md : 1950). 2002 Dec 1;169(11):6269-78. PubMed PMID: 12444133. Epub 2002/11/22. eng.

21. Neefjes J, Jongsma ML, Paul P, Bakke O. Towards a systems understanding of MHC class I and MHC class II antigen presentation. Nature reviews Immunology. 2011 Dec;11(12):823-36. PubMed PMID: 22076556. Epub 2011/11/15. eng.

22. Moffat JM, Mintern JD, Villadangos JA. Control of MHC II antigen presentation by ubiquitination. Current opinion in immunology. 2013 Feb;25(1):109-14. PubMed PMID: 23183035. Epub 2012/11/28. eng.

23. Mizushima N, Yamamoto A, Matsui M, Yoshimori T, Ohsumi Y. In vivo analysis of autophagy in response to nutrient starvation using transgenic mice expressing a fluorescent autophagosome marker. Molecular biology of the cell. 2004 Mar;15(3):1101-11. PubMed PMID: 14699058. Pubmed Central PMCID: PMC363084. Epub 2003/12/31. eng.

24. Hara T, Nakamura K, Matsui M, Yamamoto A, Nakahara Y, Suzuki-Migishima R, et al. Suppression of basal autophagy in neural cells causes neurodegenerative disease in mice. Nature. 2006 Jun 15;441(7095):885-9. PubMed PMID: 16625204. Epub 2006/04/21. eng.

25. Komatsu M, Waguri S, Chiba T, Murata S, Iwata J, Tanida I, et al. Loss of autophagy in the central nervous system causes neurodegeneration in mice. Nature. 2006 Jun 15;441(7095):880-4. PubMed PMID: 16625205. Epub 2006/04/21. eng.

26. Hampe J, Franke A, Rosenstiel P, Till A, Teuber M, Huse K, et al. A genome-wide association scan of nonsynonymous SNPs identifies a susceptibility variant for Crohn disease in ATG16L1. Nature genetics. 2007 Feb;39(2):207-11. PubMed PMID: 17200669. Epub 2007/01/04. eng.

27. Rioux JD, Xavier RJ, Taylor KD, Silverberg MS, Goyette P, Huett A, et al. Genome-wide association study identifies new susceptibility loci for Crohn disease and implicates autophagy in disease pathogenesis. Nature genetics. 2007 May;39(5):596-604. PubMed PMID: 17435756. Pubmed Central PMCID: PMC2757939. Epub 2007/04/17. eng.

28. Marsh BJ, Soden C, Alarcon C, Wicksteed BL, Yaekura K, Costin AJ, et al. Regulated autophagy controls hormone content in secretory-deficient pancreatic endocrine beta-cells. Molecular endocrinology (Baltimore, Md). 2007 Sep;21(9):2255-69. PubMed PMID: 17579214. Epub 2007/06/21. eng.

29. Bronietzki AW, Schuster M, Schmitz I. Autophagy in T-cell development, activation and differentiation. Immunology and cell biology. 2014 Oct 7. PubMed PMID: 25287445. Epub 2014/10/08. Eng.

30. Shi CS, Kehrl JH. TRAF6 and A20 regulate lysine 63-linked ubiquitination of Beclin-1 to control TLR4-induced autophagy. Science signaling. 2010;3(123):ra42. PubMed PMID: 20501938. Epub 2010/05/27. eng.

31. Xu Y, Jagannath C, Liu XD, Sharafkhaneh A, Kolodziejska KE, Eissa NT. Toll-like receptor 4 is a sensor for autophagy associated with innate immunity. Immunity. 2007 Jul;27(1):135-44. PubMed PMID: 17658277. Pubmed Central PMCID: PMC2680670. Epub 2007/07/31. eng.

32. Sanjuan MA, Dillon CP, Tait SW, Moshiach S, Dorsey F, Connell S, et al. Toll-like receptor signalling in macrophages links the autophagy pathway to phagocytosis.

Nature. 2007 Dec 20;450(7173):1253-7. PubMed PMID: 18097414. Epub 2007/12/22. eng.

33. Delgado MA, Elmaoued RA, Davis AS, Kyei G, Deretic V. Toll-like receptors control autophagy. The EMBO journal. 2008 Apr 9;27(7):1110-21. PubMed PMID: 18337753. Pubmed Central PMCID: PMC2323261. Epub 2008/03/14. eng.

34. Pua HH, Dzhagalov I, Chuck M, Mizushima N, He YW. A critical role for the autophagy gene Atg5 in T cell survival and proliferation. The Journal of experimental medicine. 2007 Jan 22;204(1):25-31. PubMed PMID: 17190837. Pubmed Central PMCID: PMC2118420. Epub 2006/12/28. eng.

35. Miller BC, Zhao Z, Stephenson LM, Cadwell K, Pua HH, Lee HK, et al. The autophagy gene ATG5 plays an essential role in B lymphocyte development. Autophagy. 2008 Apr;4(3):309-14. PubMed PMID: 18188005. Epub 2008/01/12. eng.

36. Gerland LM, Genestier L, Peyrol S, Michallet MC, Hayette S, Urbanowicz I, et al. Autolysosomes accumulate during in vitro CD8+ T-lymphocyte aging and may participate in induced death sensitization of senescent cells. Experimental gerontology. 2004 May;39(5):789-800. PubMed PMID: 15130673. Epub 2004/05/08. eng.

37. Jia W, He YW. Temporal regulation of intracellular organelle homeostasis in T lymphocytes by autophagy. Journal of immunology (Baltimore, Md : 1950). 2011 May 1;186(9):5313-22. PubMed PMID: 21421856. Epub 2011/03/23. eng.

38. Hubbard VM, Valdor R, Patel B, Singh R, Cuervo AM, Macian F. Macroautophagy regulates energy metabolism during effector T cell activation. Journal of immunology (Baltimore, Md : 1950). 2010 Dec 15;185(12):7349-57. PubMed PMID: 21059894. Pubmed Central PMCID: PMC3046774. Epub 2010/11/10. eng.

39. Li C, Capan E, Zhao Y, Zhao J, Stolz D, Watkins SC, et al. Autophagy is induced in CD4+ T cells and important for the growth factor-withdrawal cell death. Journal of immunology (Baltimore, Md : 1950). 2006 Oct 15;177(8):5163-8. PubMed PMID: 17015701. Epub 2006/10/04. eng.

40. Nedjic J, Aichinger M, Emmerich J, Mizushima N, Klein L. Autophagy in thymic epithelium shapes the T-cell repertoire and is essential for tolerance. Nature. 2008 Sep 18;455(7211):396-400. PubMed PMID: 18701890. Epub 2008/08/15. eng.

41. Pua HH, Guo J, Komatsu M, He YW. Autophagy is essential for mitochondrial clearance in mature T lymphocytes. Journal of immunology (Baltimore, Md : 1950). 2009 Apr 1;182(7):4046-55. PubMed PMID: 19299702. Epub 2009/03/21. eng.

42. Willinger T, Flavell RA. Canonical autophagy dependent on the class III phosphoinositide-3 kinase Vps34 is required for naive T-cell homeostasis. Proceedings of the National Academy of Sciences of the United States of America. 2012 May 29;109(22):8670-5. PubMed PMID: 22592798. Pubmed Central PMCID: PMC3365213. Epub 2012/05/18. eng.

43. Parekh VV, Wu L, Boyd KL, Williams JA, Gaddy JA, Olivares-Villagomez D, et al. Impaired autophagy, defective T cell homeostasis, and a wasting syndrome in mice with a T cell-specific deletion of Vps34. Journal of immunology (Baltimore, Md : 1950). 2013 May 15;190(10):5086-101. PubMed PMID: 23596309. Pubmed Central PMCID: PMC3646937. Epub 2013/04/19. eng.

44. Compston A, Coles A. Multiple sclerosis. Lancet. 2008 Oct 25;372(9648):1502-17. PubMed PMID: 18970977. Epub 2008/10/31. eng.

45. Berg-Hansen P, Moen SM, Sandvik L, Harbo HF, Bakken IJ, Stoltenberg C, et al. Prevalence of multiple sclerosis among immigrants in Norway. Multiple sclerosis (Houndmills, Basingstoke, England). 2014 Oct 24. PubMed PMID: 25344371. Epub 2014/10/26. Eng.

46. Alonso A, Hernan MA. Temporal trends in the incidence of multiple sclerosis: a systematic review. Neurology. 2008 Jul 8;71(2):129-35. PubMed PMID: 18606967. Pubmed Central PMCID: PMC4109189. Epub 2008/07/09. eng.

47. Ben-Nun A, Wekerle H, Cohen IR. The rapid isolation of clonable antigen-specific T lymphocyte lines capable of mediating autoimmune encephalomyelitis. European journal of immunology. 1981 Mar;11(3):195-9. PubMed PMID: 6165588. Epub 1981/03/01. eng.

48. Vandenbark AA, Gill T, Offner H. A myelin basic protein-specific T lymphocyte line that mediates experimental autoimmune encephalomyelitis. Journal of immunology (Baltimore, Md : 1950). 1985 Jul;135(1):223-8. PubMed PMID: 2582032. Epub 1985/07/01. eng.

49. Pettinelli CB, McFarlin DE. Adoptive transfer of experimental allergic encephalomyelitis in SJL/J mice after in vitro activation of lymph node cells by myelin basic protein: requirement for Lyt 1+ 2- T lymphocytes. Journal of immunology (Baltimore, Md : 1950). 1981 Oct;127(4):1420-3. PubMed PMID: 6168690. Epub 1981/10/01. eng.

50. Zamvil SS, Steinman L. The T lymphocyte in experimental allergic encephalomyelitis. Annual review of immunology. 1990;8:579-621. PubMed PMID: 2188675. Epub 1990/01/01. eng.

51. Gay D, Esiri M. Blood-brain barrier damage in acute multiple sclerosis plaques. An immunocytological study. Brain : a journal of neurology. 1991 Feb;114 (Pt 1B):557-72. PubMed PMID: 2004256. Epub 1991/02/01. eng.

52. Vos CM, Geurts JJ, Montagne L, van Haastert ES, Bo L, van der Valk P, et al. Blood-brain barrier alterations in both focal and diffuse abnormalities on postmortem MRI in multiple sclerosis. Neurobiology of disease. 2005 Dec;20(3):953-60. PubMed PMID: 16039866. Epub 2005/07/26. eng.

53. Ascherio A, Munger KL, Lunemann JD. The initiation and prevention of multiple sclerosis. Nature reviews Neurology. 2012 Nov 5;8(11):602-12. PubMed PMID: 23045241. Epub 2012/10/10. eng.

54. Lill CM. Recent advances and future challenges in the genetics of multiple sclerosis. Frontiers in neurology. 2014;5:130. PubMed PMID: 25071715. Pubmed Central PMCID: PMC4094909. Epub 2014/07/30. eng.

55. Sawcer S. The complex genetics of multiple sclerosis: pitfalls and prospects. Brain : a journal of neurology. 2008 Dec;131(Pt 12):3118-31. PubMed PMID: 18490360. Pubmed Central PMCID: PMC2639203. Epub 2008/05/21. eng.

56. Sawcer S, Hellenthal G, Pirinen M, Spencer CC, Patsopoulos NA, Moutsianas L, et al. Genetic risk and a primary role for cell-mediated immune mechanisms in multiple sclerosis. Nature. 2011 Aug 11;476(7359):214-9. PubMed PMID: 21833088. Pubmed Central PMCID: PMC3182531. Epub 2011/08/13. eng.

57. Hafler DA, Compston A, Sawcer S, Lander ES, Daly MJ, De Jager PL, et al. Risk alleles for multiple sclerosis identified by a genomewide study. The New England journal of medicine. 2007 Aug 30;357(9):851-62. PubMed PMID: 17660530. Epub 2007/07/31. eng.

58. Sawcer S, Franklin RJ, Ban M. Multiple sclerosis genetics. Lancet neurology. 2014 Jul;13(7):700-9. PubMed PMID: 24852507. Epub 2014/05/24. Eng.

59. Beecham AH, Patsopoulos NA, Xifara DK, Davis MF, Kemppinen A, Cotsapas C, et al. Analysis of immune-related loci identifies 48 new susceptibility variants for multiple sclerosis. Nature genetics. 2013 Nov;45(11):1353-60. PubMed PMID: 24076602. Pubmed Central PMCID: PMC3832895. Epub 2013/10/01. eng.

60. Berge T, Leikfoss IS, Harbo HF. From Identification to Characterization of the Multiple Sclerosis Susceptibility Gene CLEC16A. International journal of molecular sciences. 2013;14(3):4476-97. PubMed PMID: 23439554. Pubmed Central PMCID: PMC3634488. Epub 2013/02/27. eng.

61. Choi NM, Majumder P, Boss JM. Regulation of major histocompatibility complex class II genes. Current opinion in immunology. 2011 Feb;23(1):81-7. PubMed PMID: 20970972. Pubmed Central PMCID: PMC3033992. Epub 2010/10/26. eng.

62. Fenner JE, Starr R, Cornish AL, Zhang JG, Metcalf D, Schreiber RD, et al. Suppressor of cytokine signaling 1 regulates the immune response to infection by a unique inhibition of type I interferon activity. Nature immunology. 2006 Jan;7(1):33-9. PubMed PMID: 16311601. Epub 2005/11/29. eng.

63. Romieu-Mourez R, Francois M, Boivin MN, Stagg J, Galipeau J. Regulation of MHC class II expression and antigen processing in murine and human mesenchymal stromal cells by IFN-gamma, TGF-beta, and cell density. Journal of immunology (Baltimore,

Md : 1950). 2007 Aug 1;179(3):1549-58. PubMed PMID: 17641021. Epub 2007/07/21. eng.

64. Geppert TD, Lipsky PE. Antigen presentation by interferon-gamma-treated endothelial cells and fibroblasts: differential ability to function as antigen-presenting cells despite comparable Ia expression. Journal of immunology (Baltimore, Md : 1950). 1985 Dec;135(6):3750-62. PubMed PMID: 3934267. Epub 1985/12/01. eng.

65. Mulder DJ, Pooni A, Mak N, Hurlbut DJ, Basta S, Justinich CJ. Antigen presentation and MHC class II expression by human esophageal epithelial cells: role in eosinophilic esophagitis. The American journal of pathology. 2011 Feb;178(2):744-53. PubMed PMID: 21281807. Pubmed Central PMCID: PMC3069880. Epub 2011/02/02. eng.

66. Schonefuss A, Wendt W, Schattling B, Schulten R, Hoffmann K, Stuecker M, et al. Upregulation of cathepsin S in psoriatic keratinocytes. Experimental dermatology. 2010 Aug;19(8):e80-8. PubMed PMID: 19849712. Epub 2009/10/24. eng.

67. McGreal EP, Martinez-Pomares L, Gordon S. Divergent roles for C-type lectins expressed by cells of the innate immune system. Molecular immunology. 2004 Nov;41(11):1109-21. PubMed PMID: 15476922. Epub 2004/10/13. eng.

68. Soleimanpour SA, Gupta A, Bakay M, Ferrari AM, Groff DN, Fadista J, et al. The diabetes susceptibility gene Clec16a regulates mitophagy. Cell. 2014 Jun 19;157(7):1577-90. PubMed PMID: 24949970. Epub 2014/06/21. eng.

69. Zouk H, D'Hennezel E, Du X, Ounissi-Benkalha H, Piccirillo CA, Polychronakos C. Functional evaluation of the role of C-type lectin domain family 16A at the chromosome 16p13 locus. Clinical and experimental immunology. 2014 Mar;175(3):485-97. PubMed PMID: 24237155. Pubmed Central PMCID: PMC3927909. Epub 2013/11/19. eng.

70. Kim S, Naylor SA, DiAntonio A. Drosophila Golgi membrane protein Ema promotes autophagosomal growth and function. Proceedings of the National Academy of Sciences of the United States of America. 2012 May 1;109(18):E1072-81. PubMed PMID: 22493244. Pubmed Central PMCID: PMC3344964. Epub 2012/04/12. eng.

71. Kim S, Wairkar YP, Daniels RW, DiAntonio A. The novel endosomal membrane protein Ema interacts with the class C Vps-HOPS complex to promote endosomal maturation. The Journal of cell biology. 2010 Mar 8;188(5):717-34. PubMed PMID: 20194640. Pubmed Central PMCID: PMC2835942. Epub 2010/03/03. eng.

72. Gostissa M, Hengstermann A, Fogal V, Sandy P, Schwarz SE, Scheffner M, et al. Activation of p53 by conjugation to the ubiquitin-like protein SUMO-1. The EMBO journal. 1999 Nov 15;18(22):6462-71. PubMed PMID: 10562558. Pubmed Central PMCID: PMC1171709. Epub 1999/11/24. eng.

73. Clipstone NA, Crabtree GR. Identification of calcineurin as a key signalling enzyme in T-lymphocyte activation. Nature. 1992 Jun 25;357(6380):695-7. PubMed PMID: 1377362. Epub 1992/06/25. eng.

74. Jensen EC. Types of imaging, Part 2: an overview of fluorescence microscopy. Anatomical record (Hoboken, NJ : 2007). 2012 Oct;295(10):1621-7. PubMed PMID: 22941879. Epub 2012/09/04. eng.

75. McCaffrey MW, Bielli A, Cantalupo G, Mora S, Roberti V, Santillo M, et al. Rab4 affects both recycling and degradative endosomal trafficking. FEBS letters. 2001 Apr 20;495(1-2):21-30. PubMed PMID: 11322941. Epub 2001/04/27. eng.

76. Schneider U, Schwenk HU, Bornkamm G. Characterization of EBV-genome negative "null" and "T" cell lines derived from children with acute lymphoblastic leukemia and leukemic transformed non-Hodgkin lymphoma. International journal of cancer Journal international du cancer. 1977 May 15;19(5):621-6. PubMed PMID: 68013. Epub 1977/05/15. eng.

Appendix 1: Abbrevations

AA	-	Alopecia areata
APC	-	Antigen-presenting cell
BSA	-	Bovine serum albumin
CD	-	Cluster of differentiation
CD	-	Crohn´s disease
cDNA	-	Complementary DNA
CIITA	-	MHC class II transactivator
CLEC16A	-	C-type lectin-like domain family 16A
CLIP	-	Class II-associated invariant chain peptide
CNS	-	Central nervous system
CTLD	-	C-type lectin-like domain
DEXI	-	Dexamethasone-induced
dH_2O	-	Distilled water
DNA	-	Deoxyribonucleic acid
dNTP	-	Deoxynucleotide
E.Coli	-	Escherichia coli
EAE	-	Experimental autoimmune encephalomyelitis
ECL	-	Enhanced chemiluminescence
EGFR	-	Epidermal growth factor receptor
FBS	-	Fetal bovine serum
FSC	-	Forward scatter
GAPDH	-	Glyceraldehyde 3-phosphate dehydrogenase
GFP	-	Green fluorescent protein
GWAS	-	Genome-wide association study
GYT	-	Glycerol-yeast extract-tryptone
HC	-	Healthy controls
HLA	-	Human leukocyte antigen
HRP	-	Horseradish peroxidase
HV	-	High voltage
IFNγ	-	Interferon gamma
IMSGC	-	International MS Genetics Consortium
ITAM	-	Immunoreceptor tyrosine-based activation motif
JIA	-	Juvenile idiopathic arthritis
kb	-	Kilo bases
kDa	-	Kilo Daltons
LAMP1	-	Lysosomal-associated membrane protein 1
LB	-	Lysogeny broth
Lck	-	Lymphocyte-specific protein tyrosine kinase
LCL	-	Lymphoblastoid cell line
MCS	-	Multiple cloning sites
MHC	-	Major histocompatibility complex
MIIC	-	MHC class II compartment
Mq		Milli-Q
mRNA	-	messenger RNA
MS	-	Multiple Sclerosis
ng		Nano gram

nm		Nano meter
OD	-	Optical density
PAGE	-	Polyacrylamide gel electrophoresis
PAI	-	Primary adrenal insuffienciey
PBC	-	Primary biliary cirrhosis
PBS	-	Phosphate buffered saline
PCR	-	Polymerase chain reaction
PEG	-	Polyethylene glycol
pfa	-	Paraformalaldehyd
PIC	-	Protease inhibitor cocktail
PMA	-	Phorbol 12-myristate 13-acetate
PVDF	-	Polyvinylidene fluoride
qPCR	-	quantitative PCR
RA	-	Rheumatoid arthritis
RIPA	-	Radioimmunoprecipitation assay buffer
RNA	-	Ribonucleic acid
RNaseP	-	Ribonuclease P
RPMI	-	Roswell Park Memorial Institute
RT	-	Room temperature
SDS	-	Sodium dodecyl sulphate
SDS-PAGE	-	Sodium dodecyl sulphate polyacrylamide gel electrophoresis
siRNA	-	small interfering RNA
SNP	-	Single nucleotide polymorphism
SOC	-	Super Optimal broth with catabolite Repression
SOCS1	-	Suppressor of cytokine signalling 1
SSC	-	Side scatted
SUMO	-	Small Ubiquitin-like Modifier
T1D	-	Type I diabetes
TAE	-	Tris-acetate-EDTA
TBS	-	Tris-Buffered Saline
TBS/T	-	Tris-Buffered Saline with Tween 20
TCR	-	T cell receptor
TE	-	Tris-EDTA
TGN	-	Trans-golgi network
TID	-	type I diabetes
TM	-	Trans membrane
TPB	-	TATA-box binding protein
UV	-	Ultraviolet light
WTCCC2	-	Wellcome Trust Case Control Consortium

Appendix 2: Materials

Material	Producer	Catalog number
Enzymes		
FastAP Thermosensitve Alkaline Phosphatase	Thermo Scientific	EF0654
FastDigest BamHI	Thermo Scientific	FD0054
FastDigest EcoRI	Thermo Scientific	FD0274
FastDigest NotI	Thermo Scientific	FD0593
FastDigest SmaI	Thermo Scientific	FD0663
FastDigest XbaI	Thermo Scientific	FD0684
Klenow Fragment	Thermo Scientific	EP0054
pfu Turbo DNA Polymerase	Agilent Technologies	600250
PmeI	Thermo Scientific	ER1341
T4 DNA ligase	Thermo Scientific	EL0014
Buffers		
20x PBS	Ullevål substrate division	
FastAP Thermosensitve Alkaline Phosphatase Reaction buffer	Thermo Scientific	Supplied
FastDigest reaction buffer	Thermo Scientific	Supplied
Klenow Fragment reaction buffer	Thermo Scientific	Supplied
pfu Turbo DNA Polymerase Reaction buffer	Agilent Technologies	Supplied
T4 DNA ligase reaction buffer	Thermo Scientific	Supplied
Ladders		
1 kb plus DNA ladder	Invitrogen	10787-018
Precision Plus Protein™ Standard	Bio-Rad	161-0374
Components for enzymes		
dNTP Mix 100mM	Life technologies	362271
PEG 4000	Thermo Scientific	Supplied
Gel electrophores		
6X loading dye	Thermo Scientific	R0611
Ethidium Bromide	MP Biomedical	190202
Seakem® LE Agarose	Lonza	50004
TAE Buffer (50X)	G-Bioscience	R023

Antibiotics

Kanamycin	Sigma Aldrich	K4000-5G
Ampicillin	Sigma Aldrich	A9393

Protein work

Quick Start™ Bradford 1x Dye Reagent	Bio-Rad	500-0105
Quick Start™ Bradford protein assay kit 1	Bio-Rad	500-0201
RIPA	Thermo Scientific	11542461

Primary antibodies

Anti TGN46 rabbit	AbB serotec	AHP1588
Anti-CLEC16A polyclonal antibody	Millipore	ABN167
Anti-DDK monoclonal antibody	Origene technologies	TA50011-100
Anti-LAMP1 antibody	Abcam®	ab62562
Anti-vimentin antibody	Abcam®	EPR3776
EGFR (1005) rabbit polyclonal IgG	Santa Cruz biotechnology	sc-03
GAPDH (6C5) mouse monoclonal	Santa Cruz biotechnology	SC-32233
GFP(FL) polyclonal antibody	Santa Cruz biotechnology	SC-8334
Rb pAb to lamin B1	Abcam®	Ab16048

HRP-conjugated secondary antibodies

Perioxidase-conjugated AffiniPure Goat Anti-Mouse IgG	Jackson ImmunoResearch	115-035-146
Perioxidase-conjugated AffiniPure Goat Anti-rabbit IgG	Jackson ImmunoResearch	111-001-003
Perioxidase-conjugated AffiniPure Mouse Anti-Goat IgG	Jackson ImmunoResearch	205-035-108

Alexa-conjugated secondary antibodies

Alexa Fluor® 555 $F(ab)_2$ Fragment of Goat Anti Mouse IgG (H+L)	Molecular Probes ® by Life technologies	A21425
Alexa Fluor® 647 Goat Anti-Rabbit IgG	Molecular Probes ® by Life technologies	A21245
Alexa Fluor® 647 Rabbit Anti-Mouse IgG (H+L)	Molecular Probes ® by Life technologies	A21239

Cell culture

2-mercaptoethanol	Sigma Aldrich	M3148-100ML
Counting Slides dual chamber for cell count	Bio-Rad	145-0011
Electroporation Cuvettes 4mm Gap	VWR®	732-1137
Fetal Bovine Serum	HyClone® Thermo Scientific	SV30160.03
MEM NEAA (100X)	Gibco® by Life technologies	11140-035
Pen Strep	Gibco® by Life technologies	15140-122
RPMI medium 1640 (1X)	Gibco® by Life technologies	21875-034
RPMI medium 1640 (1X)	Gibco® by Life technologies	21875-034
Sodium Pyruvate 100mM (100X)	Gibco® by Life technologies	11360-039
Trypan Blue solution 0,4%	Sigma Aldrich	T8154

Immunostaining

Cover glass thickness no 1	VWR®	631-0146
Hoechst 33342	Molecular Probes® by Life technologies	H1299
Polysine™ microscope slides	VWR®	631-0107
Rinderalbumin 30%	Bio-Rad	805095
Saponin from quilaja bark	Sigma Aldrich	S7900
SlowFade® Gold antifade reagent	invitrogen	S36936
Sodium Azide 0,1M	Sigma Aldrich	08591-1ML-F

SDS PAGE and WB

10% Criterion™ Tris-HCl Gel	Bio-Rad	345-0009
4–20% Criterion™ Tris-HCl Gel	Bio-Rad	345-0032
7.5% Criterion™ Tris-HCl Gel	Bio-Rad	345-0005
Extra thick blot paper filter paper	Bio-Rad	1703967
Hypercasette™	Amersham Bioscience	11642
Hyperfilm™ ECL	GE healthcare-Amersham	28906837
Immuno-Blot PVDF membrane	Bio-Rad	162-0177
Methanol	Sigma Aldrich	32213-5L
Restore Western Blot Sripping Buffer	Thermo Scientific	21062
Skim milk powder	Sigma Aldrich	70166-5006
SuperSignal ® West pica Chemiluminescent substrate	Thermo Scientific	34080
Tween® 20	Sigma Aldrich	P1379

Buffers for Attune Acoustic focusing cytometer

Attune® Focusing Fluid	Life technologies	4449790
Attune® Performance Tracking Beads	Life technologies	4449754
Attune® Shutdown Solution	Life technologies	4454955
Attune® Wash Solution	Life technologies	A-24974

Commercial kits

Compartmental Protein Extraction kit	Millipore	2145
Endofree® Plasmid maxi kit (10)	Qiagen	12362
QiAprep® spin miniprep kit (50)	Qiagen	27104
Wizard® SV Gel and PCR clean-up system	Promega	A9281

Plasmids and siRNA

Dharmacon On-target plus Non-targeting Pool	Dharmacon	D-001810-10-20
Dharmacon On-target plus SMART Pool CLEC16AsiRNA	Dharmacon	L-022485-02-0020
pCMV6-CLEC16A-MYC-DDK	Origene	RC214696
pEGFP-C1-SUMO	Gift from Odd Stokke Gabrielsen´s group	
pEGFP-N1	Gift from Anne Spurkland´s group	
Rab4a-mCherry	Gift from Anne Spurkland´s group	
Rab5-mCherry	Gift from Anne Spurkland´s group	
Rab7-GFP	Gift from Anne Simonsen´s group	

Machines and Equipment

Amersham ECL Semi-Dry Blotters TE 77 PWR	Amersham Bioscience
Attune acoustic focusing cytometer	Applied Biosystem by Life Technologies
Centrifuge 5810R	Eppendorf
Criterion™ cell	Bio-Rad
Curix 60	AGFA HealthCare
ECM 399 electroporation system BTX®	Harvard Apparatus
ECM 830 Electro Square Porator™ BTX	Harvard Apparatus
GeneGenius Gel Light Imaging System	Syngene
GeneGenius Gel Light Imaging System	Syngene
Heracell 150i CO_2 incubator	Thermo Scientific
Innova 4000 Incubator shaker	The New Brunswick
MJ research PTC-200 thermal cycler	GMI
Nanodrop 2000 c spectrophometer	Thermo scientific
Nanodrop 2000 C spectrophometer	Thermo Scientific
Olympus FluoView™ FV1000 BX61 confocal	Olympus

microscope	
PLAPO 60X	Olympus
SCANLAF MARS Bio Safety Cabinet Class 2	Labotal Scientific Equipment
Sorvakk Lynx 6000 centrifuge	Thermo Scientific
TC20™ Automated Cell Counter	Bio-Rad
Ultraspec 2100 pro	Amersham Bioscience
UPLSAPO 60X	Olympus

Software

FLUOVIEW FV1000	Olympus
Geneious 6.1.6	www.geneious.com
Illustrator® CC Tryout	Adobe
ImageJ64	http://imagej.nih.gov/ij/
NanoDrop 2000	Thermo Scientific
Photoshop® CC Tryout	Adobe

Appendix 3: Recipes

For Western blot analysis:

10x Tris/Glycin/SDS running buffer (5 litre):
(0,25 M Tris, 1,92 M glycin, 1 % SDS)

Tris base (Mm = 121,14 g/ml)	150g
Glycin (Mm = 75.0666 g/mol)	720g
20 % SDS (v/w)	250 ml
dH_2O	up to 5 litre

Transfer buffer til 1 hr semi-dry (10 litre)
(25 mM Tris, 192 mM glycin, 10 % methanol)

Tris base (Mm = 121,14 g/ml)	30 g
Glycin (Mm = 75.0666 g/mol)	144 g
Metanol	1,0 litre
dH_2O	up to 10 litre

10xTBS, ph 7.6 (5 litre)
(100 mM Tris, 1,5 M NaCl)

Tris base (Mm = 121,14)	60,6 g
NaCl (Mm = 58.44)	432,8 g
dH_2O	up to approximatly 4,5 litre

1 x TBS-T (3 litre)
(10 mM Tris, 150 mM NaCl)

10x TBS, pH 7,6	300 ml
Tween 20	3 ml
dH_2O	2,7 litre

6x Sample treatment buffer (SDS-PAGE)
(350 mM Tris-HCl pH 6.8, 10 % SDS, 30 % glycerol, 0,175 mM Bromophenolblue)

1,5 M Tris-HCl, pH 6.8	5,8 ml
SDS (Mw = 288,4 g/mol)	2,5 g
Glycerol	7,5 ml
Bromophenolblue (Mm = 691.9 g/mol)	3 mg
β-Mercaptoethanol	830 µl

Bacteria work:

LB medium (1 litre):

Bacto yeast extract	5g
Bacto tryptone	10g
NaCl	10g
MQ-H_2O	up to 1 litre

LB agar (1 litre):

LB medium	1 litre
Bacto agar	15g

Gyt medium (20 ml):

Glycerol	2 ml
Bacto yeast extract	25 mg
Bacto tryptone	50 mg
MQ-H_2O	up to 20 ml

SOC medium (100ml):

Bacto Tryptone	2 g
Bacto yeast extract	0,5 g
NaCl	0,06 g
$MgSO_4$*7H_2O	0,25 g
$MgCl_2$	0,20 g

10% Glycerine (100ml):

Glycerol	10 ml
MQ-H_2O	90 ml

Cell-work:

8% PFA:

PFA	16g
dH_2O	100 ml
NaOH	2 ml
10x PBS	20 ml
HCl, 1 M pH 7,4	1,5 ml

10% Saponin:

PBS	2 ml
Saponin	200 mg

Appendix 4: Primer sequences

Primers for generating inserts in sub cloning:

Primer	**Sequence (5´→3)**
EGFP_NotI_Frw	TATTGCGGCCGCTAGTGAGCAAGGGCGAGGAG
EGFPstop_Rev	GCTTTACTTGTACAGCTCGTCCA
EGFP_NotI_Rev	GAGTCGCGGCCGCTTTAC

Primer	**Sequence (5´→3´)**
3012F	CGAATCGCTGACCCTTGTCC
VPI:5	GGACTTTCCAAATGTCG
XL39R	ATTAGGACAAGGCTGGTGGG
EGFR_F	GTACATCAATGGGCGTGGATAG

CLEC16A-siRNA pool	**RNA sequences**
J-022485-25	CUGCACUACAUCCGAGAUA
J-022485-24	UCACAGAACAGAACCGGAA
J-022485-23	GCGGCAUGGUCCAGCGAUU
J-022485-22	UGUCUGAGAUGUACGCUAA

For subcloning section 3.1.1:

Primer combination 1: EGFP_NotI_Frw and EGFPstop_Rev.

Primer combination 2: EGFP_NotI_Frw and EGFP_NotI_Rev